GAS CONDENSATE WELL TEST ANALYSIS

A REPORT
SUBMITTED TO THE DEPARTMENT OF PETROLEUM ENGINEERING
OF STANFORD UNIVERSITY
IN PARTIAL FULFILLMENT OF THE REQUIREMENTS
FOR THE DEGREE OF
MASTER OF SCIENCE

By
Bruno Roussennac
June 2001

I certify that I have read this report and that in my opinion it is fully adequate, in scope and in quality, as partial fulfillment of the degree of Master of Science in Petroleum Engineering.

Roland N. Horne
(Principal advisor)

Abstract

Multiphase flow and mixture composition change in the reservoir make the interpretation of well tests in gas condensate reservoirs a real challenge. In this report, the different techniques to analyze gas condensate well tests using single-phase pseudopressure and two-phase pseudopressure are reviewed. The "steady-state" and more recent "three-zone" method to compute the two-phase pseudopressure are presented. The calculation of the two-phase pseudopressure requires the knowledge *a priori* of a pressure-saturaton relationship during the test. The steady-state method assumes the same pressure-saturation relationship during the test as during a hypothetical steady-state flow, which ignores any composition change in the reservoir. The three-zone method accounts for the composition change in the reservoir and is based on modeling the depletion by three main flow regions:

- A near wellbore region (Region 1) where the oil saturation is important allowing both phase, vapor and liquid to be mobile.
- Region 2 where condensate and gas are present but only the gas is mobile. In Region 2, the condensate builds up and the composition of the flowing mixture is changing.
- An outer Region 3 exists when the reservoir pressure is greater than the initial gas dew point and contains only gas.

Sensitivities of the "steady-state" and "three-zone" methods to various parameters (skin, relative permeability curves, flow rate, initial pressure, initial fluid richness) are studied using compositional flow simulations for drawdown tests. The three-zone

method gives accurate results for the estimated permeability and the estimated skin for all the tested cases. The steady-state method considerably underestimates the skin, the permeabilty being slightly overestimated.

Uncertainty due to errors (measurements or nonrepresentativity) in the relative permeability curves, the gas-oil ratio and the fluid characterization (sampling) is also considered here. Both the steady-state and the three-zone methods were found to be very sensitive even to small errors in the relative permeability curves, the gas-oil ratio and the fluid sampling. The methods are so sensitive to the relative permeability curves, which are typically not known accurately that their use for well test interpretation seems difficult if we want to determine precisely parameters as kh and skin. In addition, the gas-oil ratio and the fluid sampling are also uncertain. However, the proposed methods may be used for well deliverability and inflow performance calculation with more success for sensitivity studies.

Acknowledgments

I would like to thank my research advisor Professor Roland N. Horne for his support and guidance during the course of this study. Professor Roland N. Horne has always been available to answer my questions.

I wish to thanks Denis Gommard and Jean-Luc Boutaud de la Combe, my advisors in Elf Exploration Production who suggested this research. Valuable discussions with Denis Gommard allowed me to achieve my research.

I am very grateful to the staff of the Department of Petroleum Engineering, who are always available for questions and discussions which helped me a lot for this research.

Thanks to Robert Bissell and Pierre Samier from Elf Exploration Production who helped me solving a problem with numerical simulations.

Sincere thanks are due to my friends in Stanford, they made my stay in Stanford very fun. I would like to express my special appreciation to Cristina, Alex, Baris, Christian, Helene and Per.

Financial support from Elf Exploration Production and the members of the SUPRI-D Research Consortium on Innovation in Well Testing is gratefully acknowledged.

Contents

List of Tables

List of Figures

Chapter 1

Introduction

Gas condensate reservoirs differ essentially in their behavior from conventional gas reservoirs, and the optimization of hydrocarbon recovery needs careful reservoir analysis, planning and management.

At the time of discovery, gas condensates are often found as single-phase gas in the reservoir. As the reservoir is being produced, the pressure decreases from the reservoir to the wells and to the surface installations, leading to condensation of liquids out of the gas. This isothermal condensation as the pressure drops below the dew point pressure of the original fluid is known as retrograde condensation.

Due to lower permeability to liquid and a high liquid-to-gas viscosity ratio, most of the condensed liquid in the reservoir is unrecoverable and constitutes the "condensate loss". Condensate loss is one of the greatest economical concerns since the condensate contains valuable intermediate and heavier components of the original fluid now trapped in the reservoir.

Characterization of gas condensate reservoirs is a difficult task, since multiphase flow in the reservoir and change of the mixture composition as fluid flows towards the well complicates the interpretation of well tests considerably. Gas condensate-related topics (well deliverability, well test interpretation, flow in reservoir in general) have

been long-standing problems.

O'Dell and Miller (1967) presented the first gas rate equation using a pseudopressure function to describe the effect of condensate blockage. Fussel (1973) showed that the productivity of a gas condensate well is much higher than the productivity predicted by the O'Dell and Miller (1967) theory, which is unable to predict the saturation profile in the two-phase region correctly. Using compositional simulations, Fussel (1973) concluded that the O'Dell and Miller (1967) theory may be used to predict the sandface saturation, provided that the gas in the single-phase region is identical to the initial composition of the fluid.

Boe et al. (1981) suggested techniques to determine sandface saturations during the drawdown and buildup periods for solution-gas-drive systems. The Boe et al. (1981) techniques require that the saturation and pressure profile may be expressed as a single-valued function of r^2/t. Unfortunately, for gas-condensate systems with nonzero skin, pressure and saturation cannot be put in the form $f(r^2/t)$. Jones and Raghavan (1988) showed that drawdown pressure responses from retrograde gas condensate systems could be correlated with the classical liquid solution, if the pressures were transformed to appropriate two-phase "reservoir" pseudopressure. However, since the construction of the reservoir integral requires knowledge of the reservoir saturation and pressure profiles in advance, the reservoir integral (although a useful theoretical tool) cannot be used for analysis. Jones and Raghavan (1988) also showed that a "steady-state" two-phase pseudopressure can be used to estimate the reservoir flow capacity (kh) and to give a lower bound for the skin. Jones and Raghavan (1989) developed the same results for buildup tests. Raghavan et al. (1995) analyzed several field and simulated cases using the "steady-state" pseudopressure, and concluded that their method works best when the reservoir pressure is much higher than the dew point pressure and the well bottomhole pressure is much lower. The Raghavan et al. (1995) results comes from the fact that the "steady-state" method neglects any oil saturation transition zone. Jatmiko et al. (1997) described an iterative technique to compute the sandface saturation that also assumes steady-state flow

of initial components, this approach gives similar results as the Jones and Raghavan (1988) "steady-state" pseudopressure. The "steady-state" method models the flow in the reservoir into two regions with no transition zone in the oil saturation profile. The two regions are: a near-wellbore region where oil and gas are present and mobile (oil saturation is greater than the critical oil saturation) and an outer region containing single-phase gas only (oil saturation is zero).

Fevang (1995) accounted for the existence of a transition zone, where both oil and gas are present but only the gas is moving, in his well deliverability study. Fevang (1995) developed two-phase pseudopressure using a pressure-saturation relationship computed separately in each of the three regions. Xu and Lee (1999b) applied the Fevang (1995) "three-zone" concept to gas condensate well test analysis, showing that the three-zone method is more accurate than the "steady-state" method for estimating skin and reservoir flow capacity. The two-phase pseudopressure assumes *a priori* knowledge of the relative permeability curves as a function of saturation and the correct fluid characterization, in addition the "three-zone" requires a correct measure of the producing gas-oil ratio. However Xu and Lee (1999b) did not consider the impact of errors (in the relative permeability curve for example) to the "three-zone" pseudopressure.

In practice, most field engineers attempt to analyze pressure transient data from gas condensate reservoirs using real gas pseudopressure. Thompson et al. (1993) examined the information available from the real pseudopressure type of analysis by developing a modified single-phase pseudopressure. Xu and Lee (1999a) showed that even the simple real gas pseudopressure can be used to give estimates of the flow capacity.

In this study, the concept of "steady-state" and "three-zone" model are reviewed. The use of a single-phase pseudopressure in a radially composite reservoir model is outlined. Sensitivities to various parameters are considered for the two-phase pseudopressure methods (steady-state and three-zone) in drawdown tests. The robustness

of the method to errors or nonrepresentativity in the relative permeability curves, in the fluid characterization and in the gas-oil ratio are examined in this report.

Chapter 2 discusses the flow behavior in gas condensate systems. Both drawdown tests (primary depletion) and buildup tests are examined. The effect of skin and production data is explained. A review of well test analysis and pseudopressure concept is presented in Chapter 3. The steady-state and the three-zone method for two-phase pseudopressure calculation are detailed. Sensitivities and robustness of the two two-phase pseudopressure methods are performed in Chapter 4 for drawdown tests. A radial one-dimensional fully compositional model is used to simulate the well response in a gas condensate system. The effect of a zone of altered permeability around the well is considered (skin). The reservoir is homogeneous and is divided into radial grids, the gravity and capillary forces are not considered. The model contains no water or only at the connate water saturation. The effect of velocity-dependent relative permeability is not considered here.

Chapter 2

Gas Condensate Flow Behavior

2.1 Gas Condensate Characterization

Hydrocarbon reservoir fluids range continuously from dry gases containing almost no condensible liquid to solid tars and bitumin. Those hydrocarbons are classified in arbitrary divisions based on their color, density and gas-oil ratio (Gravier, 1986). Although some gases have their source in carbonaceous rocks, most hydrocarbon accumulations originate from organic rich shales. The degree of degradation of complex organic molecules increases with the temperature and pressure to which the organic matter has been subjected. As a consequence, the deeper the source rock the more likely the resulting hydrocarbon mixture is to be a gas or a gas condensate. Gas condensates are indeed found in deep reservoirs. The classical categories of hydrocarbons are in decreasing order of volatility:

- Gases
- Gas condensates
- Volatile oils
- Black oils
- Heavy oils

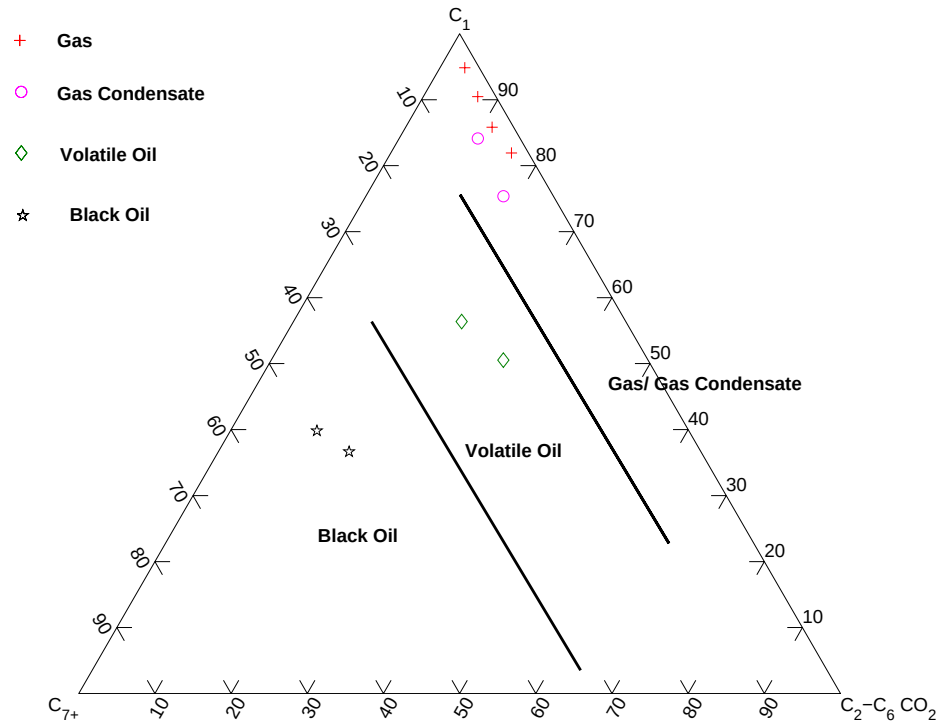

Figure 2.1: Ternary Visualization of Hydrocarbon Classification

- Oil sand oils
- Asphalts/bitumens

The category in which a given fluid falls depends on both its composition and the reservoir conditions (pressure and temperature). For a given composition, the same mixture can fall in different category for different reservoir pressure and temperature. Figure 2.1 shows an approximate classification of reservoir fluids as a function of their composition (for a given pressure and temperature). Typical compositions for the fluid categories are given in the Table 2.1. A gas condensate will generally yield from about 30 to 300 barrels of liquid per million standard cubic feet of gas. Most known retrograde gas-condensate reservoirs are in the range of 5000 to 10000 ft deep, at 3000 psi to 8000 psi and a temperature from 200°F to 400°F. These pressure and temperature ranges, together with wide composition ranges lead to gas condensate

Table 2.1: Typical Composition and Characteristics of Three Fluid Types from Wall (1982)

Component	Black Oil	Volatile Oil	Condensate	Gas
Methane	48.83	64.36	87.07	95.85
Ethane	2.75	7.52	4.39	2.67
Propane	1.93	4.74	2.29	0.34
Butane	1.60	4.12	1.74	0.52
Pentane	1.15	2.97	0.83	0.08
Hexanes	1.59	1.38	0.60	0.12
C_7+	42.15	14.91	3.80	0.42
Molecular wt C_7+	225	181	112	157
Gas-Oil Ratio SCF/Bbl	625	2000	182000	105000
Liquid-Gas Ratio Bbl/MMSCF	1600	500	55	9.5
Tank oil gravity API	34.3	50.1	60.8	54.7
Color	Green/black	Pale red/brown	Straw	White

fluids that have very different physical behavior (Moses and Donohoe, 1962)

2.2 Flow Behavior

2.2.1 Phase and Equilibrium Behavior

The reservoir behavior of a gas condensate system will depend on both the phase envelope of the fluid and the conditions of the reservoir. A typical phase envelope (P-T diagram) is shown in Figure 2.2. This phase envelope consists of a bubble point line (under which the first bubble of gas vaporizes from the liquid) and a dew point line (under which the first droplet of liquid condenses from the vapor) meeting at the critical point. For pressure above the cricondenbar pressure or for temperature above the cricondentherm temperature, two phases cannot co-exist. At the critical point the properties of the liquid and vapor phase cannot be distinguished anymore. With increasing molecular weight the critical point tends to move clockwise round

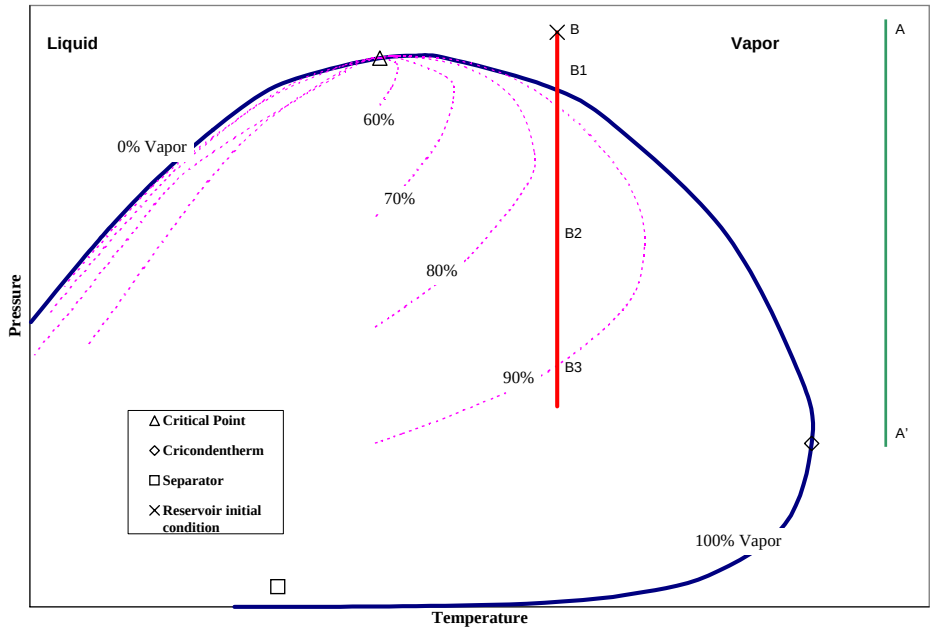

Figure 2.2: Typical Gas Condensate Phase Envelope

the phase envelope, and the phase envelopes itself tends to move to lower pressure and to higher temperature (Wall, 1982). The phase envelope (Figure 2.2) correspond to a given mixture composition, depending on the reservoir conditions, the retrograde condensation will or will not occur. Reservoir depletion is an isothermal expansion, represented by a vertical line on the P-T diagram. Gas and gas condensate reservoirs can be distinguished depending on the initial reservoir conditions:

- Gas reservoirs

  If the reservoir initial conditions are at point A, the path A-A' of Figure 2.2 will never enter the two-phase region, and the reservoir fluid will be a gas. No liquid will condense from the gas phase and the effluent composition will remain constant.

- Gas condensate reservoirs

  However, for reservoir temperatures between the critical and the cricondentherm temperature and if the initial pressure is close to the phase envelope (point B

of Figure 2.2) retrograde condensation will occur in the reservoir. Between B and B1, the fluid will remain single phase gas and the effluent mixture will be the original fluid. As the reservoir is being more and more depleted, the pressure will drop below the dew point pressure of the original fluid (point B1) and liquid will condense in the reservoir. This condensate phase has a much lower mobility than the associated gas phase. At low condensate saturations, the mobility is almost zero: only the gas will flow, dropping the intermediate and heavier components in the condensate phase. Consequently, the composition of the fluid is changing. This composition change can be interpreted by a shift of the phase envelope as shown in Figure 2.3. As the pressure decreases in the reservoir, more and more oil will drop out until the pressure reaches B'_2 where the oil saturation is maximum for a given position in the reservoir. If the production is continued further, the oil will redissolve in the vapor phase and eventually a second dew point may be encountered.

It is important to note that point B'_2 does not correspond to the maximum liquid drop-out in a constant composition expansion (point B_2 in Figure 2.2 and Figure 2.3) because the phase envelope is shifting during the depletion. Point B'_2 will correspond to a higher oil saturation than point B_2. The isothermal path BB_3 can therefore be described by a constant composition expansion (CCE) from B to B_1 and then a constant volume depletion (CVD) after B_1 (please refer to Appendix A for descriptions of CCE and CVD). However the CVD experiment is a good representation of the reservoir depletion only if the condensate phase is immobile which is not true for high liquid saturation, further explanation on reservoir depletion will be discussed in Section 2.2.3.

2.2.2 Difference between Static Values and Flowing Values

Before explaining the flow behavior of gas condensate through porous media in detail, it is important to state the difference of static values and flowing values (value is referred to as any properties, oil saturation for example). In one hand, the static

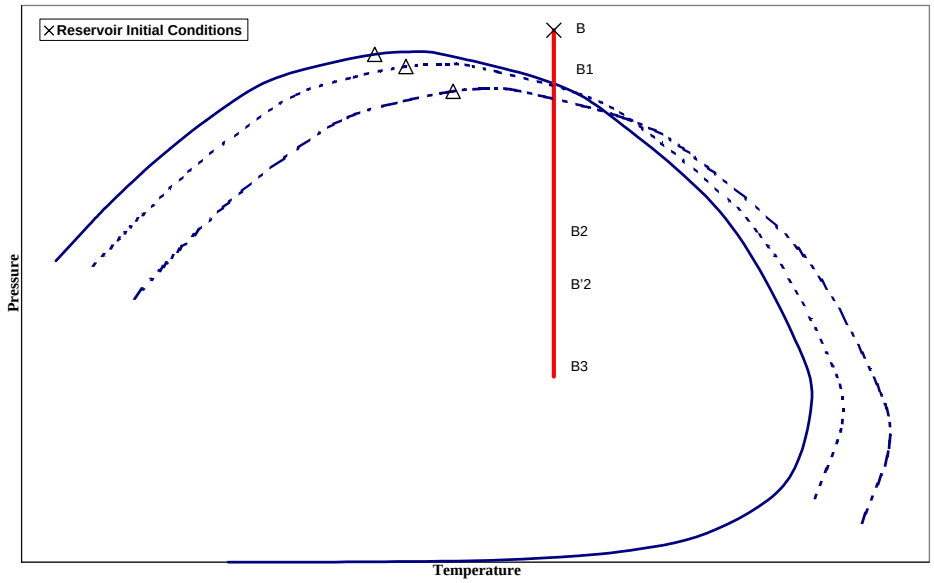

Figure 2.3: Shift of Phase Envelope with Composition Change on Depletion

values are the value at a given location in the reservoir, the value describing the state of the fluids at this given location and a given time. From a numerical simulation perspective this will be referred to as block value, for instance the oil saturation of a given block at a given time. On the other hand, the flowing value corresponds to a value of a fluid that is flowing through the media or from one grid block to another.

Figure 2.4 illustrates the difference between flowing and static values of oil saturation and overall mixture composition. The rectangles referred to as "cells" on the top part of the figure represent the volume fraction of oil and gas in the mixture, and the cells on the bottom part, the overall (vapor and liquid phase together) composition in the three components C_1, C_2 and C_3 that make the mixture. We are considering the flow of a mixture from cell 1 to cell 2 which could be two adjacent grid blocks in a flow simulator. The cells represented in the middle of the Figure 2.4 do not correspond to a physical location but just represent the liquid fraction or the composition of the flowing mixture that is going from cell 1 to cell 2. The block oil saturation at a given time in cell 1 is the volumetric fraction of oil phase that exists in cell 1. The overall

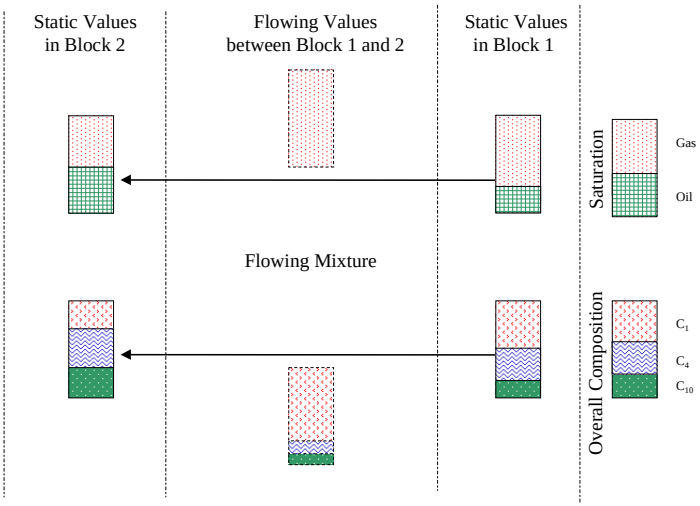

Figure 2.4: Difference between Static Values and Flowing Values

mixture in this cell has an overall composition shown in the lower right cell. However the mixture flowing from cell 1 to cell 2 will be mostly gas because gas mobility is much higher than oil mobility, therefore the fraction of oil phase in the flowing mixture will be almost zero (only gas is flowing here). The oil saturation in the block 2 will be higher due to the pressure drop (needed for the mixture to flow from 1 to 2). The overall composition of the flowing mixture will also be different than either of the block overall composition. In the same manner all subsequent properties such as density, viscosity will be different if they refer to a mixture at a grid block or a flowing mixture. The well producing gas-oil ratio (GOR) is an important measured value that can be related to the flowing composition.

2.2.3 Drawdown Behavior

Fluid flow towards the well in a gas condensate reservoir during depletion can be divided into three concentric main flow regions, from the wellbore to the reservoir (Fevang, 1995):

- Near-wellbore Region 1:
  Around the wellbore, region with high condensate saturation where both gas

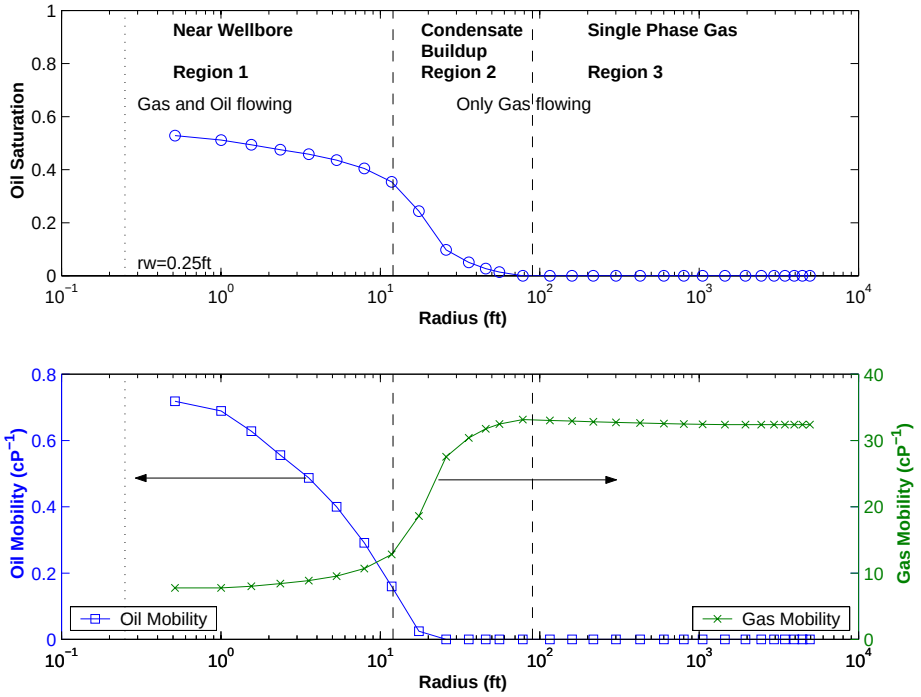

Figure 2.5: Flow Regimes During a Drawdown Test in a Gas Condensate Reservoir (MIX2, skin=2, case R21112)

and condensate are flowing simultaneously.

- Condensate buildup Region 2:
  Region where the condensate is dropping out of the gas. The condensate phase is immobile and only gas is flowing.

- Single phase gas Region 3:
  Region containing only the original reservoir gas.

Depending on the production and reservoir conditions, one, two or three regions will develop in the reservoir. The flow regions are illustrated for a special case (R21112: MIX2 skin=2, description of cases is given in Appendix B) in Figure 2.5. Figure 2.6 shows a schematic representation of gas condensate flow during production.

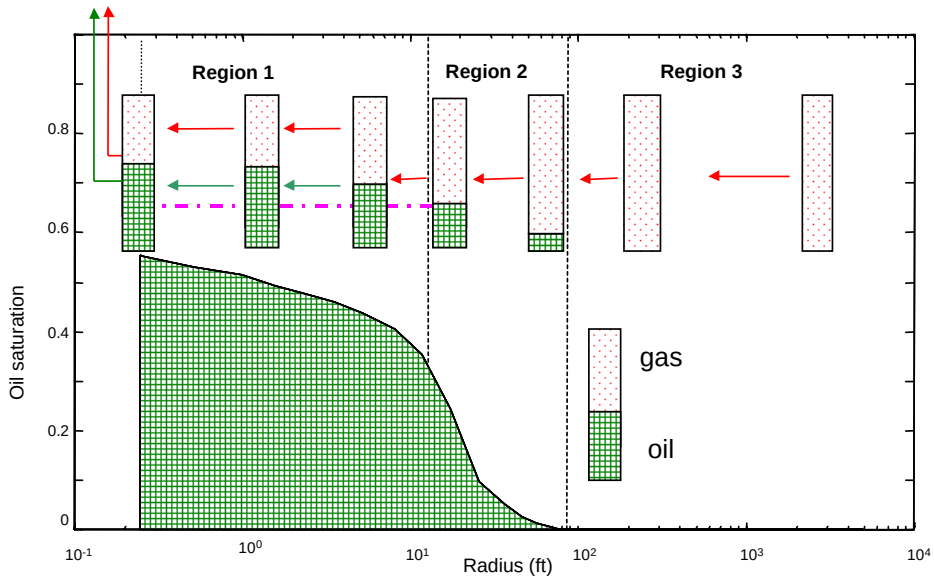

Figure 2.6: Schematic Gas Condensate Flow Behavior

Near-Wellbore Region 1: The oil saturation in this region is high enough to allow the condensate to flow. The flowing composition (GOR) is almost constant throughout Region 1. This means that the overall composition of the flowing mixture is constant in Region 1 and equal to the composition of the single-phase gas at the limit between Region 2 and Region 1. Consequently, the composition of the producing wellstream is the composition of the single phase gas leaving Region 2. Furthermore, the dew point pressure of the producing wellstream is equal to the pressure at the boundary between Region 2 and Region 1. The oil saturation increases in the reservoir as the mixture flows towards the well because the pressure decreases (Figure 2.5). Since the composition of the flowing mixture is constant throughout Region 1, the liquid saturation could be calculated by a constant composition expansion of the producing mixture. The amount of oil dropped out in Region 1 depends primarily on the PVT properties of the original mixture and the production rate. Figure 2.7 shows the pressure, saturation and mobility profiles for MIX2 at different time. The oil saturation is greter closer to the wellbore. For a given radial distance to the well, the amount of condensate flowing in Region 1 is equal to the difference in solution Oil

Gas Ratio (OGR or r_s) Δr_s between the gas leaving Region 2 and entering Region 1 and the gas flowing at this given distance. Since the OGR (Figure B.7) decreases with pressure, the condensate saturation increases towards the wellbore.

Because of the high oil saturation in Region 1, the actual two-phase, compressible flow will defer essentially from the single-phase gas flow.

Condensate Buildup Region 2: The condensate is dropping out of the gas but it has zero or very low mobility (Figure 2.5). At the outer edge of Region 2 the first droplets of liquid condense from the original gas, therefore the pressure at the outer edge of Region 2 (at the boundary with Region 3) equals the dew point pressure of the original reservoir gas.

The buildup of condensate is due to the pressure drop below the dew point pressure. As the gas flows towards the well in Region 2, the pressure drops as two origins: (1) the pressure decline in the bulk of the reservoir, (2) the pressure gradient imposed on the flowing reservoir gas. As shown by Whitson and Torp (1983), the condensate drop out due to the pressure decline in the reservoir can be computed from the CVD experiment, corrected for water saturation. For well test analysis, the second contribution to condensate saturation can be neglected.

Since only the gas is flowing in Region 2, leaving behind the heavier and intermediate components in the oil phase, the composition of the flowing gas is changing becoming leaner and leaner. Figure 2.12 presents the composition profiles at different times, the two lower plots shows the composition in the vapor phase: the fraction of C_4 (and C_{10} not shown on the plot) decreases as we go towards the well.

At a given radial distance from the well in Region 2, the pressure is decreasing and the oil saturation is increasing until it becomes so high that the oil can move towards the well as shown in Figure 2.7. This given radius now becomes the new boundary between Region 1 and Region 2. Region 2 develops after the bottomhole flowing

pressure (BHFP) has dropped below the dew point pressure, as the drawdown test continues, the outer boundary of Region 2 moves away from the well and the oil saturation in the vicinity of the well increases. Once the condensate saturation around the well allows oil mobility, Region 1 develops from the well. Therefore Region 2 first expands from the well outwards and then moves away from the well. From all the cases we tested, the size of Region 2 is maximum when the BHFP just equals the dew-point pressure and then decreases with time leading to sharper saturation profiles, however it is hard to observe from Figure 2.7. Region 2 is greater for leaner gas (see Section 4.2.3).

The average oil saturation in Region 2 is much less than the average oil saturation in Region 1, therefore the deviation from the single-phase gas flow will be much less. However the existence of Region 2 has a very important consequence on fluids and flow behavior during the test. For instance, the observed wellstream producing GOR is leaner than calculated by a simple volumetric material balance (CCE experiments). The (incorrect) material balance using CCE experiment implies that Region 2 does not exist (only Region 1 and Region 3 exist). The CCE material balance will overestimate the flow resistance in Region 1 considerably, especially just after the BHFP drops below the dew point. This point will be discussed in more details in Section 3.4.7.

Single-Phase Gas Region 3: The pressure is greater than the dew point pressure of the original gas in the entire region 3. Consequently, only original gas is present.

Coexistence of Flow Regions: Region 1 exists only if the BHFP is below the dewpoint pressure of the original reservoir gas (p_{dew}). When BHFP$<p_{dew}$, Region 1 forms after a short transition zone, but will always exist (if the test is long enough, practically more than 1 hour). Region 2 always exists together with Region 1 (if the $BHFP < p_{dew}$). If the boundaries are reached during the test and the reservoir pressure drops below p_{dew} , Region 3 will disappear. Region 2 may become negligible for very rich gas condensate. For near-critical gas condensate, Region 2 is very small and

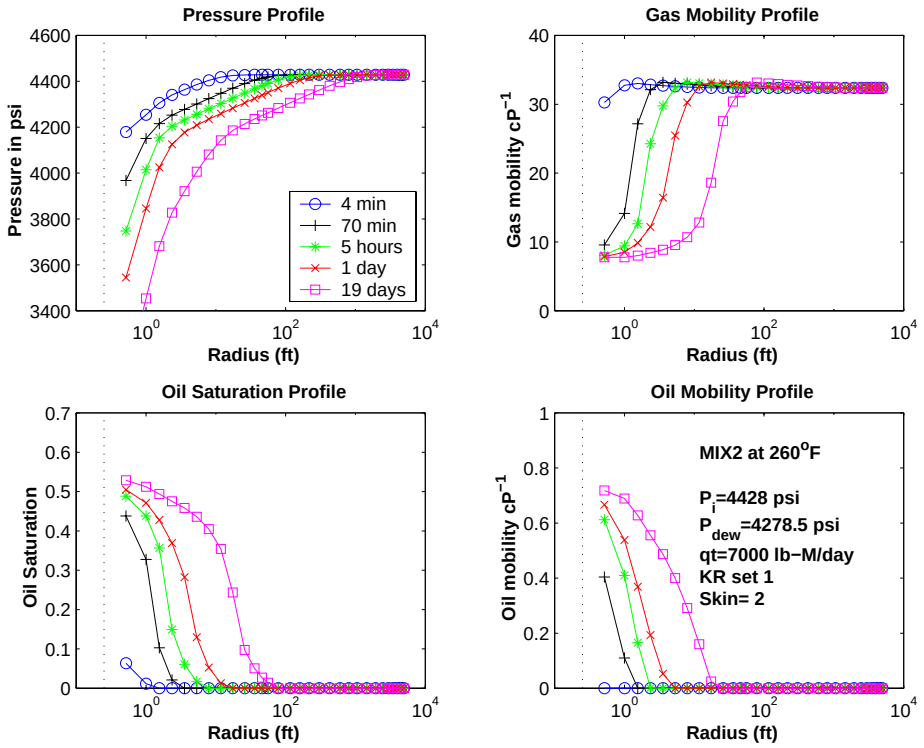

Figure 2.7: Pressure, Saturation and Mobility Profiles for MIX2 (case R21112)

	Region 1	**Region 2**	**Region 3**
p_{wf} >p_{dew}			X
P$_r$<p_{dew}	X	(X)	
p_{wf} <p_{dew} and P$_r$ > p_{dew}	X	(X)	X
X exists (X) may exist			

Table 2.2: Coexistence of Flow Regions from Fevang (1995)

Region 1 will exist alone if the reservoir pressure drops below p_{dew}. The coexistence of flow regions is summarized in Table 2.2.

Flow Regions on History Plots: We discussed the three main flow regions and how they appear on profiles in the reservoir. If we now consider production data plots (at the wellbore), the three main flow behaviors will be observed in reverse order on any history plot (say well block saturation versus time). Figure 2.8 identifies the three regions on a well block oil saturation, the producing GOR and flowing composition history.

Figure 2.8 shows the regions boundary on history plots of the well block saturation, the producing gas-oil ratio and the overall C_4 composition of the mixture flowing from the weel block to the wellbore. Each region corresponds to a characteristic pressure range. Since the well block saturation is related to the well block pressure, the regions boundary occur at the same times on the well block saturation history plot as on the wel block pressure history plot, but not at the same times as on a well pressure history plot.

The producing GOR becomes constant once the well block pressure p_{wb} drops below a calculated p^*. The well block saturation at the wellbore for the pressure p^* is higher than the critical oil saturation specified in the relative permeability curves allowing both oil and gas phase to be mobile. ($S_{oc} = 0.1$ and $S_o^{wellblock} = 0.18$ when $p_{wf} = p^*$ for the case shown in Figure 2.8). The composition of intermediate component (C_4) in the flowing mixture exhibits the same behavior as the GOR. In Region 3 (early times) only gas exists and its composition is constant. Then in Region 2 only gas is flowing; the flowing gas gets leaner and loses intermediate and heavy components. When finally, Region 1 develops at the well, the composition of the flowing mixture (both gas and oil are flowing) becomes constant again at a lower value (leaner producing wellstream).

2.2.4 Effect of Skin

The effect of a non-zero skin factor is studied in this section. The skin is modeled by a radial zone of lower permeability around the well. As has been shown in Section 3.4.2,

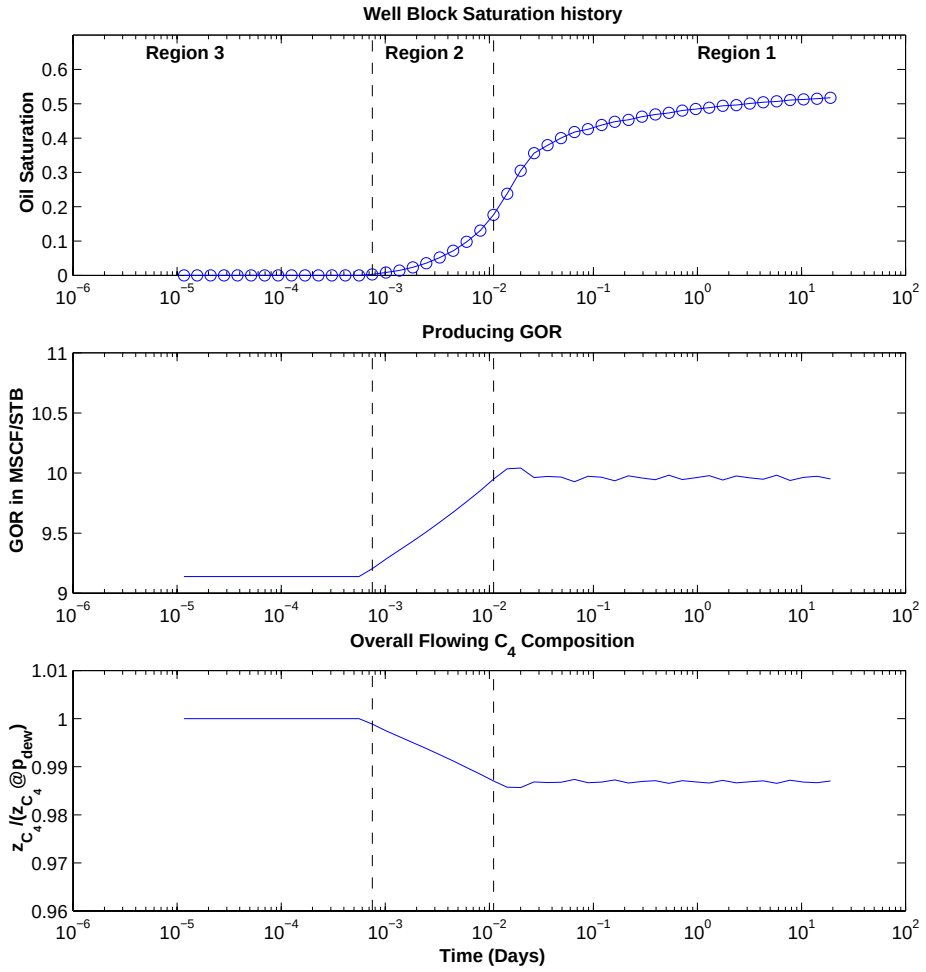

Figure 2.8: The Three Main Flow Regions identified on History Plots (MIX2, skin=0, case R21111.

pressure and saturation profiles cannot be expressed as a single valued function of r^2/t as soon as the skin factor is not zero.

A skin zone extending three feet from the well with half-permeability ($k_s = 1/2k$ is considered here. The inclusion of a skin zone affects the pressure profile which becomes sharper around the well but no noticeable effect is observed on the saturation profile as shown in Figure 2.9. However the observations made on history plots of

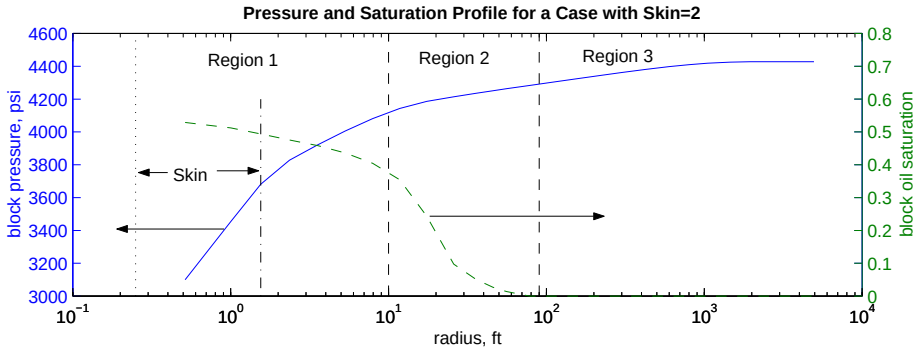

Figure 2.9: Pressure and Saturation Profile for a Case with Skin, s=2 (case R21112)

flowing values (such as producing gas-oil ratio, producing wellstream composition) differ from the case with no skin. Figure 2.10 displays the oil saturation at the well block, the producing gas-oil ratio and the composition in C_4 of the producing mixture. At early time, the original gas is produced and the gas-oil ratio is constant (Region 3). After the well pressure drops below the dew point of the original mixture (at $t = 10^{-4}$ days), condensate drops out of the gas in the reservoir and are not being produced, therefore, the produced mixture (single phase gas) becomes leaner and the gas-oil ratio increases. Finally, when the pressure at the sandface reaches a critical value, the oil saturation at the sandface becomes large enough to allow the oil phase to move, this corresponds to the beginning of Region 1.

If the skin was zero the gas-oil ratio will stabilized directly after Region 2 (see Figure 2.8), in the present case, the gas-oil ratio first decreases to stabilized at the same value (10 Mscf/bbl) that for the case skin=0.

These flow behaviors are not described in the literature and are based on simulation results, therefore it is not proven that this actually represents the true mechanism.

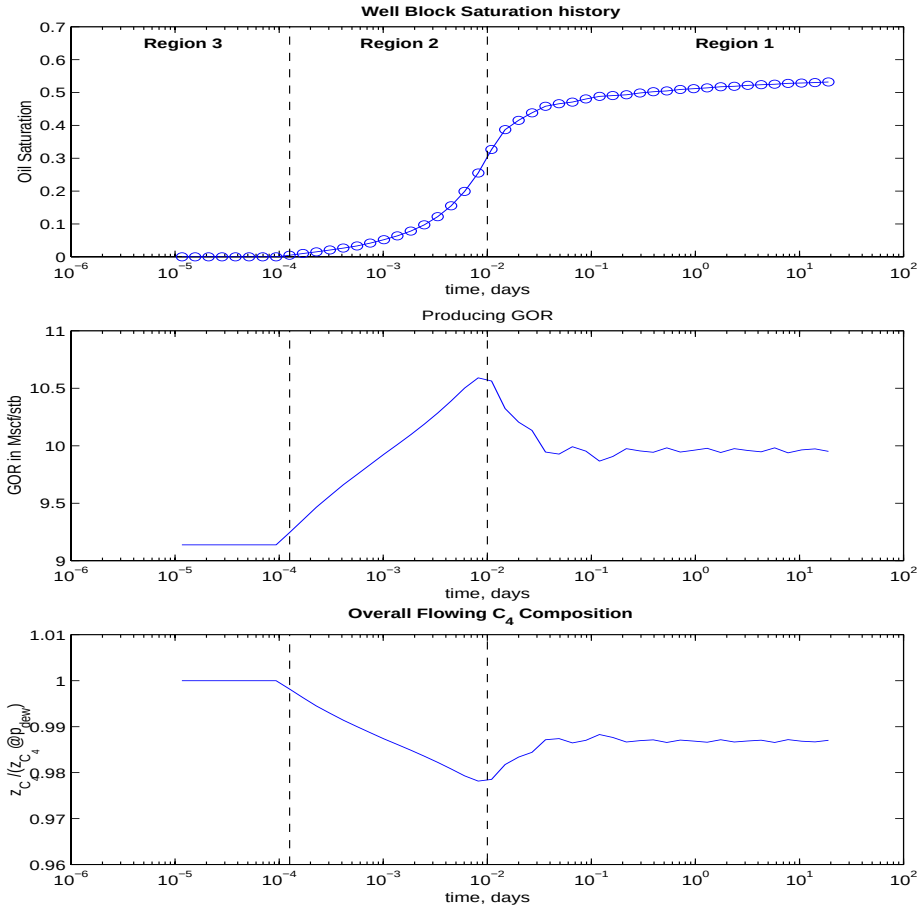

Figure 2.10: Effect of Non-Zero Skin on Production Response

2.2.5 Condensate Blockage

As the mixture flows towards the well (Figure 2.5), the gas mobility increases slightly in Region 3 (gas viscosity is a slightly increasing function of pressure above the dew point), decreases significantly as the condensate builds up in Region 3 and stays at a lower value in Region 1 where the condensate begins to flow. Even if the condensate production at the well can be neglected, the mobility of gas and thus the well deliverability has decreased significantly. This phenomenon is referred to as "condensate blockage".

Region 1 constitutes the main resistance to gas flow, and the blockage effect will depend mainly on the gas relative permeability and the size of Region 1. The flow resistance in Region 2 is much less than in Region 1. Fevang (1995) studied well deliverability and the blockage effect of condensate.

2.2.6 Hydrocarbon Recovery and Composition Change

As the original gas flows through Region 2 in the reservoir, its composition changes; the flowing gas becomes leaner and leaner, dropping the intermediate and heavy components (C_4 and C_{10}) in the reservoir. Consequently, the oil in Regions 1 and 2 becomes heavier as the pressure decreases. In Figure 2.11, this implies that the overall mixture (gas and oil) anywhere in Region 1 or 2 will become heavier as the pressure decreases below p_{dew} . For example, if we pick a time after the beginning of the production, say 1 day, the profile of concentration is drawn in diagonal crosses in Figure 2.12. The overall C_1 composition profile for t=1 day decreases towards the well bore, indicating that the mixture becomes heavier. On the other hand, the vapor phase becomes leaner as we approach the well bore. This behavior is illustrated in Figure 2.11. At the scale of production times, Region 1 will quickly develop at the well bore, and therefore the producing wellstream composition will be constant (Figure 2.8) and leaner than the original reservoir gas, the intermediate and heavier components being left in the reservoir in Region 1 and Region 2.

2.2.7 Buildup Behavior

The flow behavior after the well has been shut-in is very dependent on the pressure, saturation and composition profiles at the moment of shut-in. During the drawdown period preceding the buildup test, the overall composition of the mixture is changing in the reservoir, therefore the associated critical properties and phase envelope are also changing.

The phase envelope associated with the mixture present in the well block during the drawdown is shown Figure 2.13 for different production time. The thicker line in

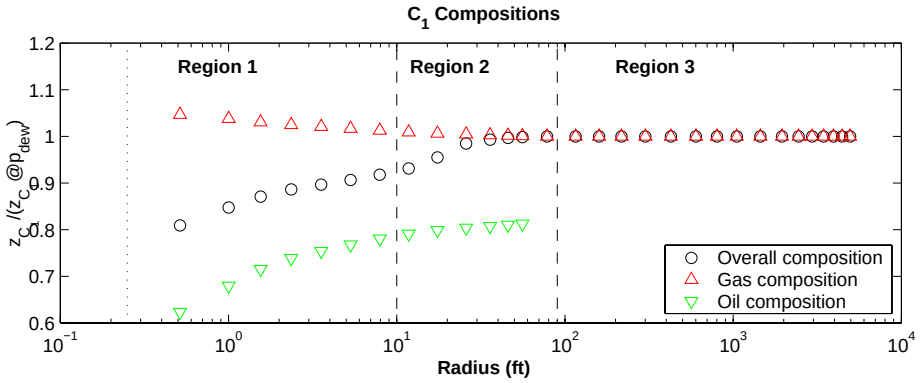

Figure 2.11: Compositions Profiles at t=19 days for MIX2, skin=2 (case R21112)

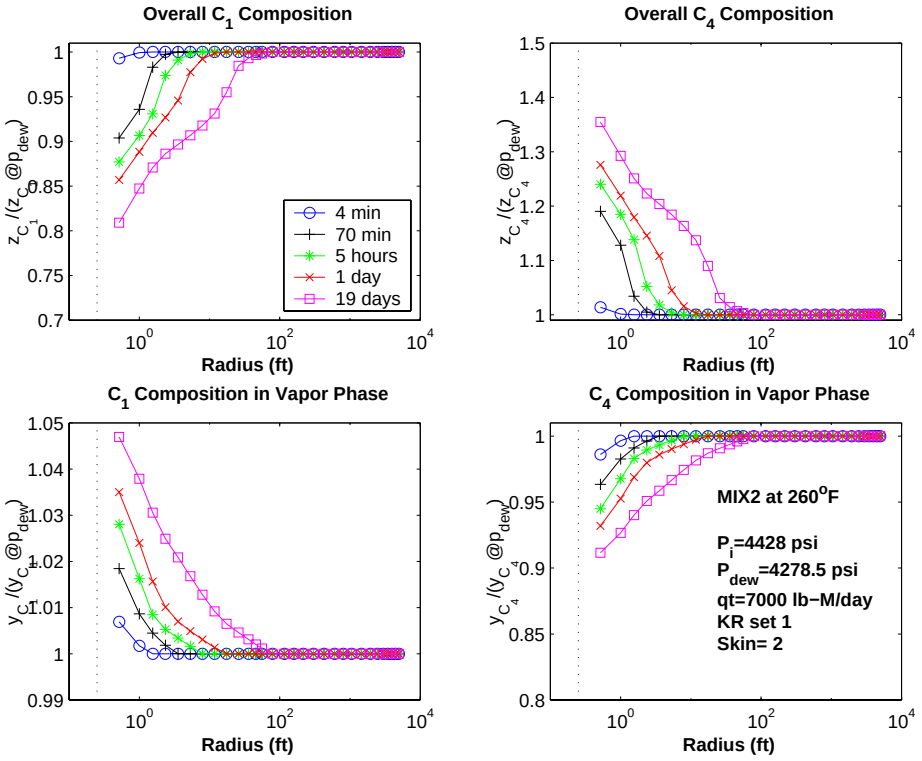

Figure 2.12: Compositions Profiles for MIX2, skin=2 (case R21112)

Figure 2.13 represents the locus of the critical point associated with the well block mixture at different time. The initial reservoir pressure is 4428 psia and the reservoir temperature is 720°R (260°F). The critical point of the initial mixture ($p_c = 4091$ psia and $t_c = 461.7$°R) lies to the left of the trajectory followed by the reservoir pressure (at $t = 720$°R). Hence the model behaves like a gas condensate initially.

During the drawdown period, oil condenses in the well grid cell and the overall mixture in that cell (oil and gas together) becomes richer in heavy components. After 19 days of production, the composition in the well grid cell leads to the phase envelope shown as a broken line in Figure 2.13. The critical point now lies to the right of the trajectory followed by the reservoir pressure. Thus the fluid now behaves like a dissolved gas reservoir.

During the buildup period, the pressure increases and we would expect the oil to revaporize. However if the production time is greater than a certain threshold (specific to the case considered), the fluid near the wellbore behaves like a dissolved gas and the oil saturation increases near the wellbore during the buildup. Figure 2.14 shows the well block oil saturation during the buildup period that follows a production period of 11.7 min and 38.8 min. After 11.7 min (left plot in Figure 2.14), the fluid near the wellbore still behaves like a gas condensate and the oil saturation decreases as the pressure increases. For production time of 38.8 min (right plot), the well block fluid behaves like a volatile oil and the oil saturation increases.

For the case shown in Figure 2.13, the fluid in the well grid cell switches from a gas condensate behavior to a dissolve gas behavior only after approximately 15 min of production. However the fluid in the outer cell may still behave like a gas condensate. Figure 2.15 shows the phase envelopes associated with the mixture present at every given radius in the reservoir after 19 days of production. After 19 days of production, the reservoir pressure is below the dew point pressure (p_{dew} of the original gas) up to a radius r_{dew} of 116 ft, for greater radius, the reservoir pressure is still above p_{dew} and the fluid is the original single-phase gas. For radius lesser than r_{dew},

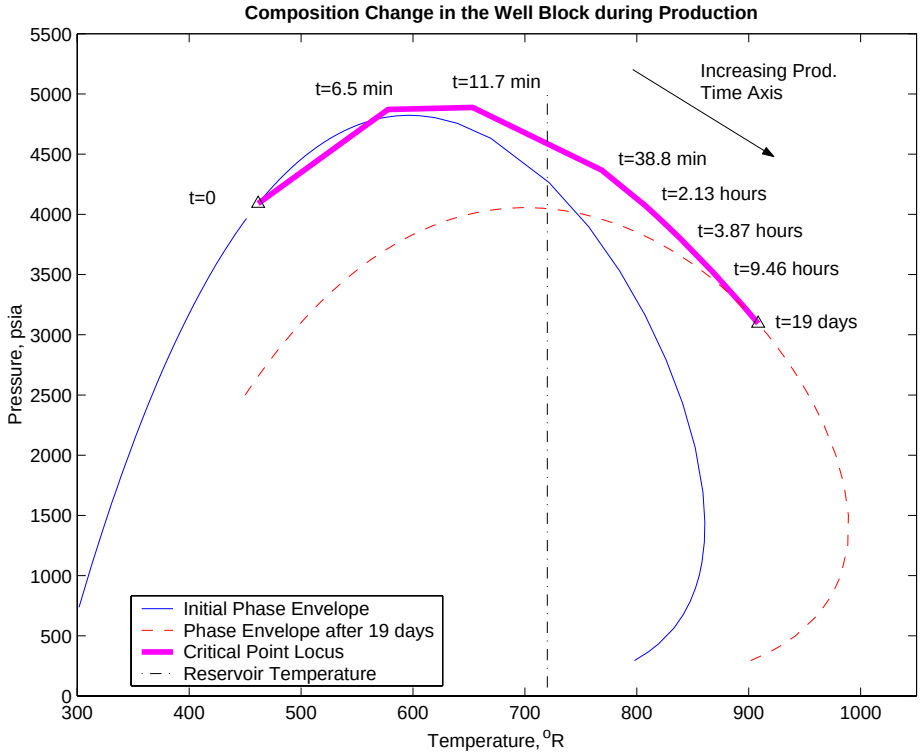

Figure 2.13: Well Block Composition Change during Drawdown Shown with Envelope Diagram

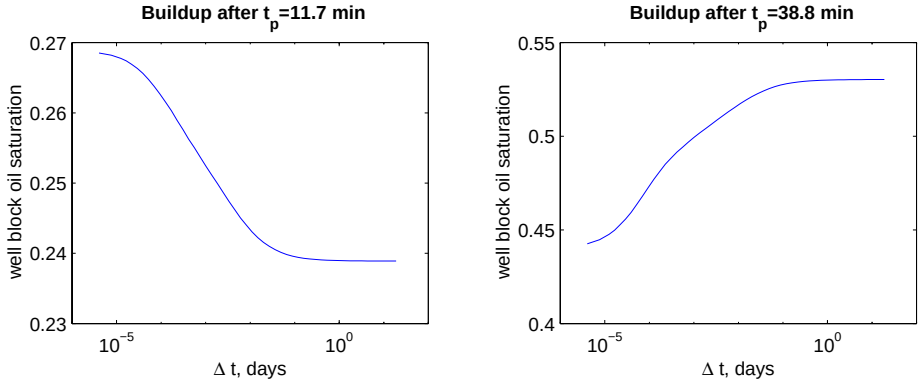

Figure 2.14: Well Block Oil Saturation during Buildup Period after Different Production Time

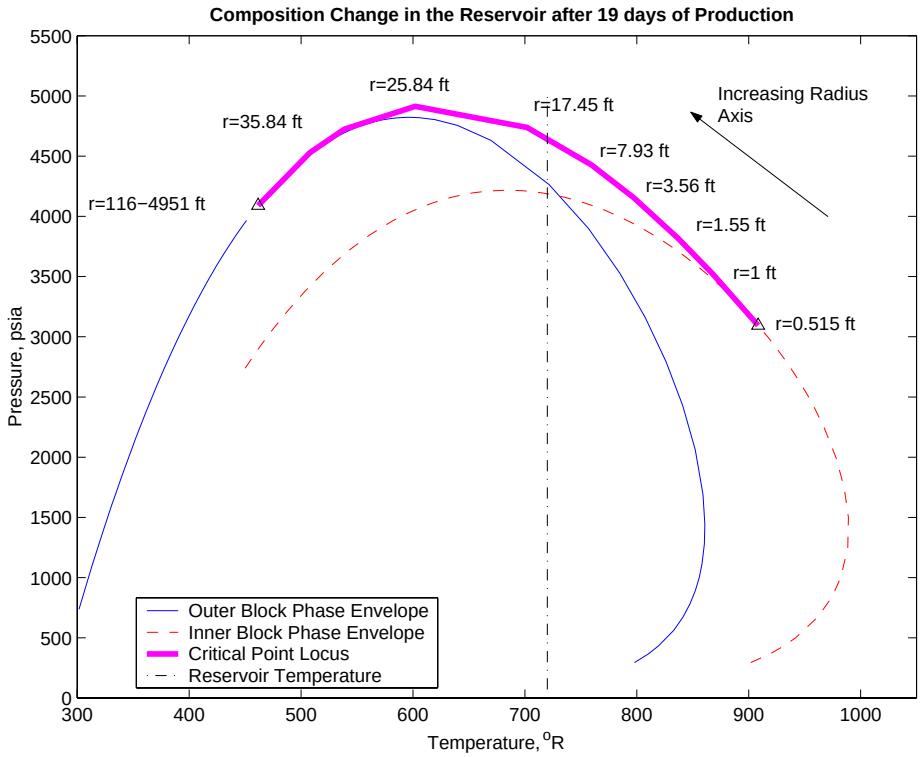

Figure 2.15: Composition Change in the Reservoir after 19 days of Production

the phase envelope differs more and more from the original phase envelope as we go towards the well. For the case considered in Figure 2.15, the fluid will behave as a volatile oil for radius less than approximately 10 ft.

Figure 2.16 shows the oil saturation during the buildup period following 2.13 hours of production at different radius from the well. As explained earlier, the fluid behavior gradually changes from gas condensate behavior away from the well (bottom right plot in Figure 2.16) to volatile oil behavior near the well (top row of plots). At $r = 1.55ft$ (bottom left plot in Figure 2.16), the oil saturation first increases (until $\Delta t = 10^{-3}$ days) and then decreases, this shows that the mixture at this radius gets richer in light components during the buildup.

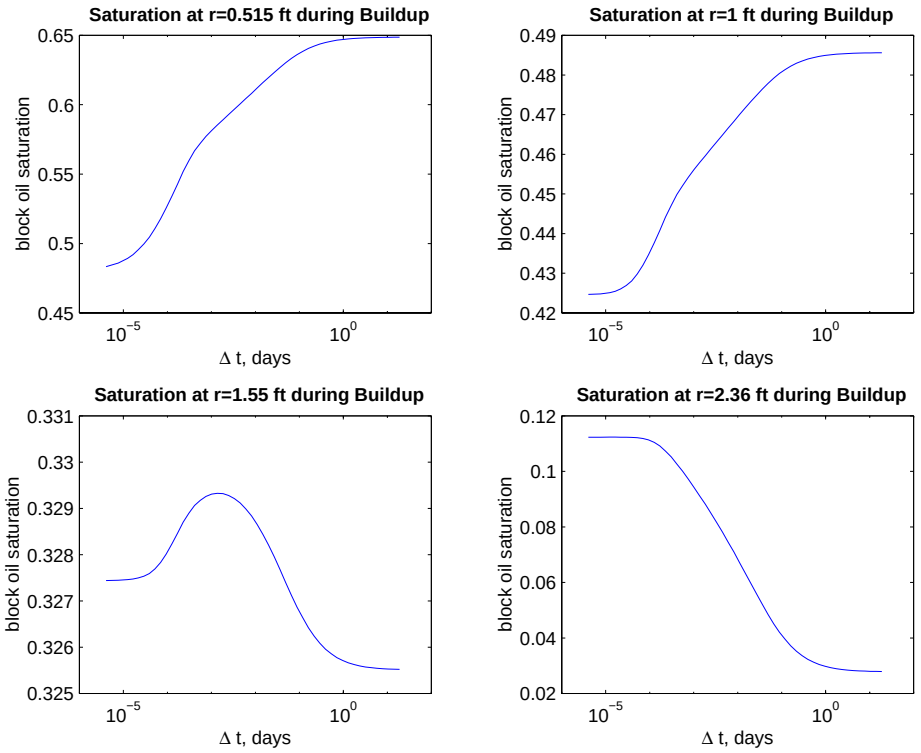

Figure 2.16: Block Oil Saturation during Buildup Period after t_p=2.13 hours at Different Radii in the Reservoir

Chapter 3

Well Test Analysis

3.1 Introduction

All direct interpretations of pressure transient from a well test are based on the linear diffusion equation:

$$\nabla^2 p - \frac{\phi \mu c_t}{k} \frac{\partial p}{\partial t} = 0 \tag{3.1}$$

This equation is derived under the following assumptions (Horne, 1995):

1. Darcy's Law applies,
2. Single-phase flow,
3. Porosity, permeabilities, viscosity and compressibility are constant,
4. Fluid compressibility is small,
5. Pressure gradients in the reservoir are small,
6. Gravity and thermal effects are negligible.

Hence the equation (Equ. 3.1) applies essentially to a single-phase slightly compressible oil reservoir (i.e. with $p_r > p_{bubble}$). However for other fluids those assumptions are rarely met:

- For gas reservoirs, the fluid properties such as compressibility and viscosity are strong functions of pressure. The pressure gradient in the near wellbore region can be high and Darcy's Law may not apply.
- In an oil field in which the reservoir pressure is close to the bubble point, gas may vaporize and multiphase flow may occur in the formation.
- For gas condensate reservoirs, liquid may condense in the reservoir where gas and condensate will be present together. Not only are the fluid properties strong functions of pressure but multiphase flow may also occur in the reservoir.

As a consequence the flow equations that can be derived for such fluids in porous media are strongly nonlinear and Eq. 3.1 is not valid anymore. A classical method to handle such deviation from the single-phase slightly compressible condition is to define a variable $m(p)$ named pseudopressure such that the equation governing pressure transmission becomes of the form:

$$\nabla^2 m(p) - \frac{1}{\eta}\frac{\partial m(p)}{\partial t} = 0 \tag{3.2}$$

Ideally, η would not be dependent on pressure or time, but usually the reservoir hydraulic diffusivity η is a function of pressure and thus time. The equation can be linearized further by the introduction of a pseudotime. If such a pseudopressure and pseudotime can be defined and computed almost all solutions developed for standard well test analysis can be used simply by the use of pseudopressure and pseudotime instead of pressure and time. However in the case of multiphase well tests (volatile oil and gas condensate), the pseudopressure must take into account the relative permeability data at reservoir conditions, which can be very difficult to obtain.

3.2 Liquid Flow Equation

Liquid Solution: Under the conditions listed in Section 3.1, the flow equation can be written as Eq. 3.1. This equation can be written in a dimensionless form as:

$$\nabla^2 p_D - \frac{\partial p_D}{\partial t_D} = 0 \tag{3.3}$$

Using the dimensionless pressure p_D and the dimensionless time t_D:

$$p_D(t_D) = \frac{kh}{141.2qB\mu}(p_i - p) \tag{3.4}$$

$$t_D = \frac{0.000264kt}{\phi c_t \mu r_w^2} \tag{3.5}$$

For a well in an infinite homogeneous reservoir the diffusivity equation Eq. 3.3 has the following solution (drawdown tests):

$$p_{wD}(t_D) = \frac{1}{2}(\ln t_D + 0.8091) + s \tag{3.6}$$

The skin factor, s, is defined by the Hawkins formula Hawkins (1966):

$$s = (\frac{k}{k_s} - 1) \ln \frac{r_s}{r_w} \tag{3.7}$$

where k_s is the permeability of the damaged zone which extends from the wellbore to a radius r_s.

Analysis on a Semilog Plot: On a semilog plot of p_D vs. $\log t_D$, the liquid solution is represented by a straight line of slope $\frac{\ln 10}{2} = 1.1513$ and which equals approximately $s + 0.4$ at $t_D = 1$. Hence if a pseudopressure is the right liquid analog, its semilog representation m_D vs. t_D should give exactly the same straight line. The deviation in the slope between the pseudopressure and the liquid solution measures the error in the permeability estimation using the pseudopressure and the vertical shift measures the error in the skin estimation. Figure 3.1 summarizes the permeability and skin estimation by pseudopressure using a semilog plot.

3.3 Single-Phase Pseudopressure

3.3.1 Real Gas Formulation

1. Gas without retrograde condensation:

   In the case of a gas reservoir without retrograde condensation, Al Hussainy and Ramey (1966) and Al Hussainy et al. (1966) showed for a gas obeying the real

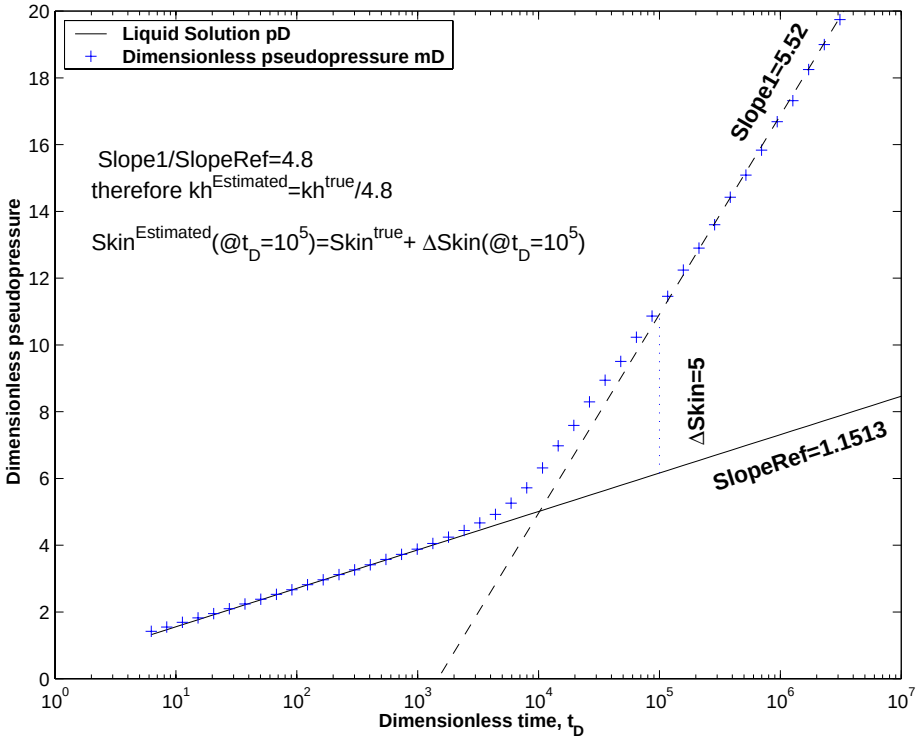

Figure 3.1: Semilog Analysis Using Pseudopressure (for Drawdown Test)

gas equation:

$$pv = ZRT \tag{3.8}$$

that the flow equation can be linearized using the real gas pseudopressure:

$$m(p) = 2\int_{p_0}^{p} \frac{p'}{\mu Z} dp' \tag{3.9}$$

Or equivalently, we will use the following pseudopressure referred to as the gas pseudopressure:

$$m^{gas}(p) = \int_{p_0}^{p} \frac{\rho_g}{\mu_g} dp' \tag{3.10}$$

where $\rho_g = \frac{1}{v_g}$ is the molar density of the gas (from Eq. 3.8, $m(p) = 2RTm^{gas}(p)$). The dimensionless pseudopressure is given by:

$$m_D^{gas}(p) = \frac{2\pi C_1 kh}{q_t}\Big[m^{gas}(p_{init}) - m^{gas}(p)\Big] \tag{3.11}$$

The dimensionless time t_D is defined the same as for liquid wells (Eq. 3.5) $c_t\mu$ evaluated at initial reservoir pressure.

$$t_D = \frac{0.000264kt}{\phi(c_t\mu)_i r_w^2} \tag{3.12}$$

For example, during a drawdown test in a homogeneous gas reservoir the infinite acting radial flow will be represented by the pseudopressure equation:

$$m_D^{gas} = \frac{1}{2}(\ln t_D + 0.8091) + s \tag{3.13}$$

2. Gas Condensate:

   The gas pseudopressure (Eq. 3.10) can be calculated for a gas condensate well test using the viscosity and the molar density from laboratory (or Equation of State based) experiments, either Constant Composition Expansion (CCE) or Constant Volume Depletion (CVD).

   Two gas condensate drawdown tests (corresponding to the cases R21111 and R21112) interpreted using the real gas pseudopressure are shown in Figure 3.2. The real gas pseudopressures (cross) are compared to the liquid solution given by Eq. 3.5 (unbroken lines) which are straight lines on a semilog plot. At early times, the bottom hole flowing pressure (BHFP) is greater than the dew point pressure of the original reservoir gas (p_{dew}), therefore only gas is present in the reservoir and the real gas pseudopressure matches the liquid solution. When skin is included in the model, the real gas pseudopressure first shows a transition region until the compressible zone goes beyond the damaged zone. As soon as the BHFP drops below p_{dew}, the gas relative permeability (given in Appendix B in Figure B.2) drops below unity and the crosses deviate from their corresponding liquid solution. The deviation is more pronounced for a positive skin.

   In reference Jones and Raghavan (1988), their conclusions on real gas pseudopressure seem to differ: *"At early times, we obtain excellent agreement with*

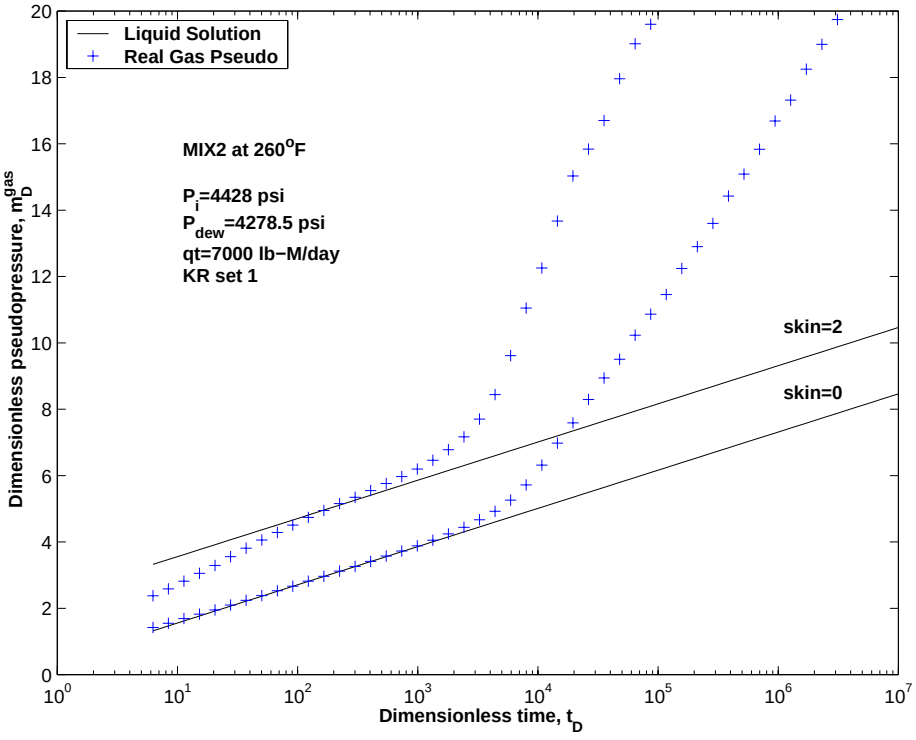

Figure 3.2: Drawdown Response Interpreted with the Classical Real Gas Pseudopressure

the liquid-flow solution; however, once the oil saturation at the sandface becomes large enough for the liquid phase to be mobile, significant deviations from the liquid-flow solution are evident", whereas we observed here that the deviation occurs as soon as oil saturation is larger than zero (even if oil is not moving). In fact, the difference comes from the choice of relative permeability curves, our curves (Figure B.2 in Appendix B) were chosen such that k_{rg} drops below unity as soon as oil is present (k_{ro} still being zero), Jones and Raghavan (1988) chose k_{rg} to drop below unity only when the oil becomes mobile for saturations greater than a critical oil saturation. Finally, our conclusions agree that the real gas pseudopressure deviates from the liquid-flow solution as soon as the permeability to gas decreases.

3.3.2 Single-Phase Gas Analogy in Radially Composite Model

In practice, most gas condensate buildup tests are interpreted using the single-phase real gas pseudopressure in a radially composite reservoir model available in standard well test analysis software. Yadavalli and Jones (1996) used a radially composite model to interpret transient pressure data from hydraulically fractured gas condensate wells with a single-phase analogy. Xu and Lee (1999a) showed that a single-phase analogy coupled with radial composite model can be used to estimate successfully flow capacity from buildup tests in homogeneous reservoirs with a skin zone.

The reservoir model to be used in well test analysis software is a two-zone radial composite reservoir including an inner altered permeability zone (skin zone) as shown in Figure 3.3. The estimated total skin s_t will then account for both the mechanical skin s_m and the skin due to the condensate bank s_{2p}. If oil saturation in the condensate bank is assumed constant, the total skin is given by (Xu and Lee, 1999a):

$$s_t = \frac{s_m}{k_{rg}} + s_{2p} \tag{3.14}$$

After interpretation of simulated buildup tests, Xu and Lee (1999a) classified the pressure buildup response into two types, depending on the position of the condensate bank at time of shut-in with respect to the altered permeability zone. Type I, which is caused by a small condensate bank, has two horizontal straight lines in the derivative of the pseudopressure. Type II corresponds to a large condensate bank which extends further than the skin zone as shown in Figure 3.4 and is characterized by three horizontal lines on the pseudopressure derivative plot.

3.4 Two-Phase Pseudopressure

3.4.1 Introduction

The real gas pseudopressure only integrates deviation from the liquid solution due to the high compressibility of the fluid in comparison with slightly compressible liquid. The real gas pseudopressure does not consider the decrease in permeability to gas

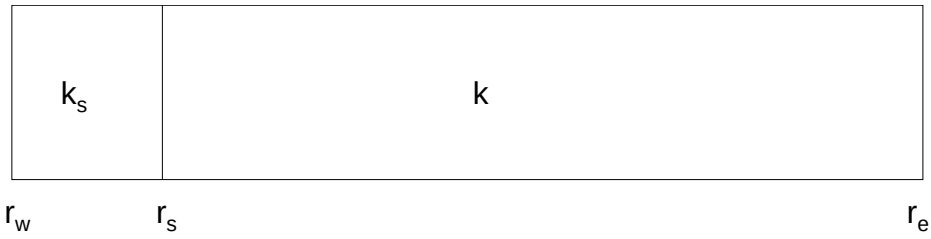

Figure 3.3: Well Test Analysis Reservoir Model

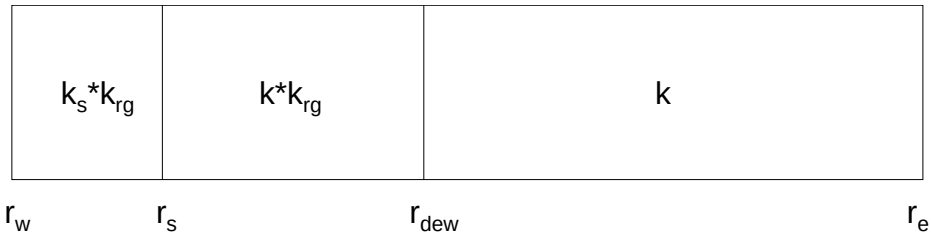

Figure 3.4: Radially Composite Reservoir Model, Type II

due to the presence of condensate phase, therefore it is not the right liquid analog to interpret gas condensate well test response. A natural definition for a two phase pseudopressure will then be for drawdown:

$$m(p) = \int_{p_0}^{p} \frac{\rho_g k_{rg}}{\mu_g} + \frac{\rho_o k_{ro}}{\mu_o} dp' \tag{3.15}$$

which considers the compressibility of the fluids ρ as well as relative permeability effects due to multiphase flow.

Rigorously, the density and viscosity of a mixture are functions of both the pressure and the composition (for a fixed temperature). However, the density and the viscosity are not strong functions of composition over the range of composition changes observed in well tests. Xu and Lee (1999b) showed that the fluid PVT properties such as viscosity and density in both lab CCE and CVD processes are essentially the same and are good approximations of the actual reservoir viscosity and density.

For buildup tests, the pseudopressure will be defined as (Jones and Raghavan, 1989):

$$m_(p) = \int_{p_{wf,s}}^{p_{ws}} \frac{\rho_g k_{rg}}{\mu_g} + \frac{\rho_o k_{ro}}{\mu_o} dp' \tag{3.16}$$

Relative permeabilities are very difficult properties to measure at reservoir scale. Assuming that the correct relative permeabilities have been measured, they are known as functions of saturation only. Therefore we need a relationship between reservoir saturation and pressure to compute the integral in Eq. 3.15. For a given reservoir fluid characterization and given set of relative permeability curves, the two-phase pseudopressure in Eq. 3.15 is determined completely by the relationship of pressure-saturation that we need to infer from production measurements (GOR, well pressure, well rate...).

Methods for calculating two-phase pseudopressure differ essentially in the model being used to infer the actual reservoir pressure-saturation relationship. Gas condensate well tests seem to be very similar to volatile oil well tests, unfortunately, methods to compute volatile oil pseudopressure are not appropriate for gas condensate cases as we will discuss in the following Section 3.4.2.

The sandface integral and the reservoir integral introduced by Jones (1985) are theoretical pseudopressures in the sense that they can only be computed if the reservoir properties and fluid properties are known at any time and any location in advance. Those two integrals provide a theoretical background to understand how the flow equations are being linearized.

Fussel (1973) modified the O'Dell and Miller (1967) method to compute an approximate pressure-saturation relationship based on steady-state assumptions. The resulting pseudopressure will be referred to as the "steady-state" pseudopressure. Jones and Raghavan examined the effect of liquid condensation on the well response using the two "theoretical" integrals and the "steady-state" pseudopressure for drawdown tests (Jones and Raghavan, 1988) and buildup tests (Jones and Raghavan, 1989).

First introduced by Fevang (1995) for well deliverability calculations, the concept of three main flow regions in the reservoir has been applied by Xu and Lee (1999b) to well test analysis. The general form of the two-phase pseudopressure is common to both "steady-state" and "three-zone" methods and is given by Equ. 3.17 for drawdowns and Equ. 3.18 for buildups (in dimensionless form):

$$m_D(p_{wf}) = \frac{2\pi C_1 kh}{q_t} \int_{p_i}^{p_{wf}} \frac{\rho_g k_{rg}}{\mu_g} + \frac{\rho_o k_{ro}}{\mu_o} dp' \tag{3.17}$$

$$m_D(p_{ws}) = \frac{2\pi C_1 kh}{q_t} \int_{p_{wf,s}}^{p_{ws}} \frac{\rho_g k_{rg}}{\mu_g} + \frac{\rho_o k_{ro}}{\mu_o} dp' \tag{3.18}$$

The different methods to compute the pseudopressure are shown here, their use for analyzing well test response will be illustrated through many different numerical simulations in Section 4.2 and finally Section 4.3 will investigate the robustness of the methods if uncertainties are introduced. All methods using two-phase pseudopressure require the knowledge of the following:

1. Measurements of the well pressure during the test.
2. Standard requirements for well tests (flow rate, production time, average porosity).
3. Representative original reservoir gas characterization (tuned equation of state together with gas composition).
4. Representative relative permeability curves.

3.4.2 Similarity and Difference with Volatile Oil Case

Both volatile oil and gas condensate reservoirs experience multiphase flow in the reservoir once the well flowing pressure drops below the bubble point for volatile oil and the dew point for gas condensate.

Boe et al. (1981) proposes a technique to determine saturations in the vicinity of the well for the drawdown and buildup periods for solution-gas-drive systems. Their

theory is based on the assumption that saturations and pressures for two-phase flow systems depend only on the ratio r^2/t. If this assumption is true, then the flow equation can be derived using the Boltzmann variable ($\frac{\phi r^2}{4kt}$). (Other prerequisites for the validity of the Boltzmann transform are that the reservoir is infinite, the well is a line source and that the boundary conditions can be expressed in terms of the Boltzmann variable). Under those assumptions, Boe et al. (1981) showed that it is possible to predict the saturation variable with time around the well from pressure, PVT and relative permeability data. Then the relationship between well pressure and oil saturation around the well is used to compute pseudopressure. Numerical simulations showed that this procedure can be used to analyze drawdown tests, provided that the influence of the boundaries during the test period is negligible.

Unfortunately the Boe et al. (1981) method cannot be used for gas condensate well tests because saturations cannot always be expressed as a single-valued function of $\frac{\phi r^2}{4kt}$. In fact, if the skin is zero then saturations (and pressures) can be expressed as a function $\frac{\phi r^2}{4kt}$, however this is not valid when skin is not zero or even for small values of the skin. Figure 3.5 shows two plots of the saturations plotted versus the Boltzmann variable corresponding to a case with skin=0 and skin=2. The squares represent the oil saturation at the first block close to the well (at r=0.515 ft) plotted versus $\frac{\phi(0.515)^2}{4kt}$; the circles the oil saturation in the reservoir at a time t=19 days.

3.4.3 Steady-State Pseudopressure for Drawdown Tests

Fussel (1973) examined the performance of a well in a gas condensate reservoir, and found that the productivity predicted by the O'Dell and Miller (1967) theory was underpredicting the well productivity, because the O'Dell and Miller (1967) theory was unable to predict the saturation profile in Region 1. Fussel (1973) concluded that the O'Dell theory can be used to predict saturation around the well only if the composition of the fluids in Region 1 is the same as the original reservoir gas, or equivalently that Region 2 does not exist. Finally, the saturation-pressure relationship as predicted by Fussel (1973) and O'Dell and Miller (1967) equations is exactly

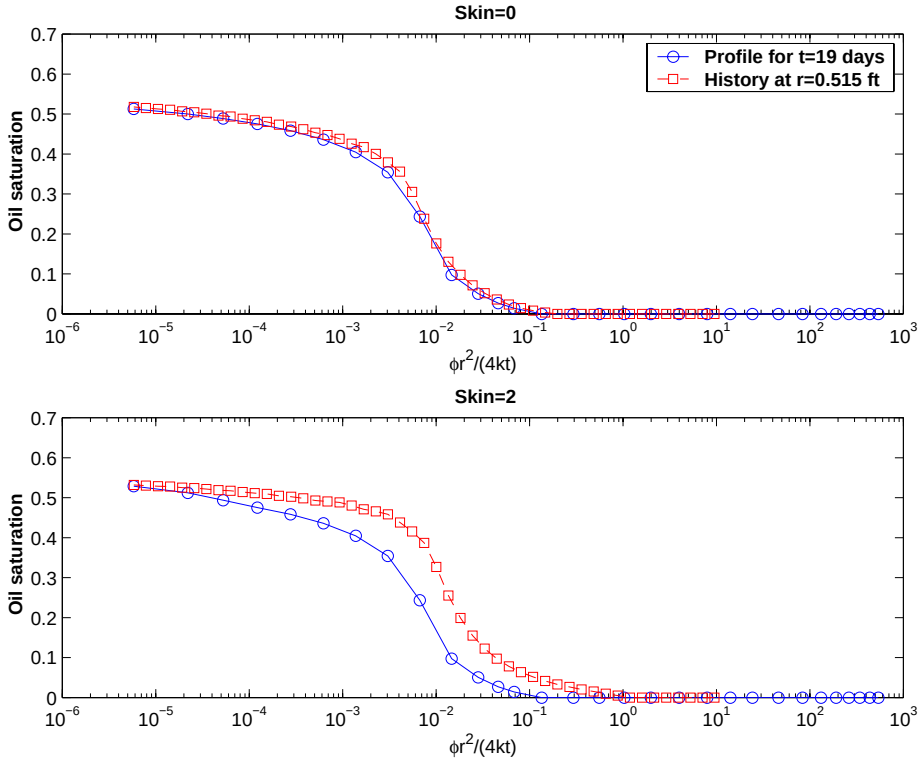

Figure 3.5: Oil Saturation in Gas Condensate Well Test Plotted vs. the Boltzmann Variable $\frac{\phi r^2}{4kt}$

the saturation-pressure relationship corresponding to the steady-state flow shown by Chopra and Carter (1985) and also Jones and Raghavan (1988). This theory states that the saturation pressure relationship for steady state flow is given by:

$$\frac{k_{ro}}{k_{rg}} = \frac{\rho_g L \mu_o}{\rho_o V \mu_g} \tag{3.19}$$

where L and V are the molar fraction of liquid and vapor calculated from flash equations. The left hand side of Eq. 3.19 is a function of saturation only and the right hand side is given by a CCE experiment and is only function of pressure. Jones and Raghavan (1988) proved that steady-state flow implies:

1. The overall composition of the flowing mixture at any location r in the reservoir is the composition of the original reservoir gas. This implies that Region 2

where compositions of the flowing mixture are changing does not exist and only Regions 1 and 3 coexist.

2. The vapor composition and the liquid composition, along with L and V can be calculated directly from a CCE (flash equations).

3. The pseudopressure as expressed by Eq. 3.17 is the right liquid analog, which means that the pressure distribution in the reservoir expressed in terms of pseudopressure satisfies the classical liquid equation for steady-state flow.

4. When two phases are in equilibrium, both are mobile. Therefore there is a discontinuity in the saturation from zero to a saturation higher than the critical oil saturation at the radius r_{dew} where the pressure equals p_{dew} .

5. Under steady flow, liquid and vapor do not flow at equal velocities.

The pseudopressure computed from the steady-state method will be referred to as steady-state pseudopressure and denoted m_D^{SS}. Figure 3.6 illustrates the use of the steady-state pseudopressure to interpret a drawdown well test and Figure 3.7 shows the pressure-saturation relationship used to compute the pseudopressure. At early times, the steady-state pseudopressure is in good agreement, the pseudopressure deviates from the liquid flow solution when k_{rg} begins to decrease. Fortunately, after a transition period (of about 1.5 log cycle) the pseudopressure follows a straight line essentially parallel to the liquid-flow solution. If the test lasts long enough to reach the second straight line, the formation flow capacity kh can be estimated accurately, however the skin will be underestimated.

3.4.4 Steady-State Pseudopressure for Buildup Tests

If the steady-state theory applies, then the "steady-state" pressure-saturation relationship can be used to compute the two-phase dimensionless pseudopressure given in Equ. 3.18. The viscosity and density will be approximated by a constant composition expansion of the original mixture.

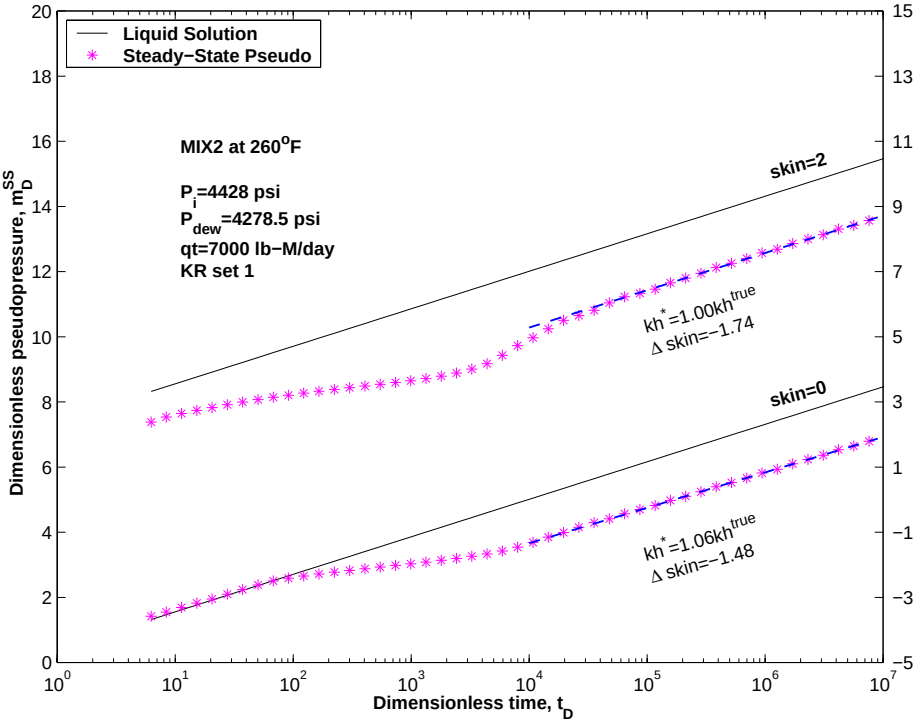

Figure 3.6: Drawdown Response Interpreted with the Steady-State Pseudopressure

3.4.5 Three-Zone Pseudopressure for Drawdown Tests

Drawdown Analysis

In addition to the previously cited requirements (see Section 3.4.1) the three-zone method needs:

1. A correct measure of the producing GOR (R_p).

2. Black-oil representation of the reservoir fluid. (This can be deduced directly from the reservoir fluid composition and a tuned equation of state).

We have seen earlier that the gas condensate flow towards the well can be divided into three main flow Regions (see Section 2.2.3), recalling:

- **Region 1:** Near-wellbore region where two phases are mobile, the condensate saturation is high and the composition of the flowing mixture is constant. Once

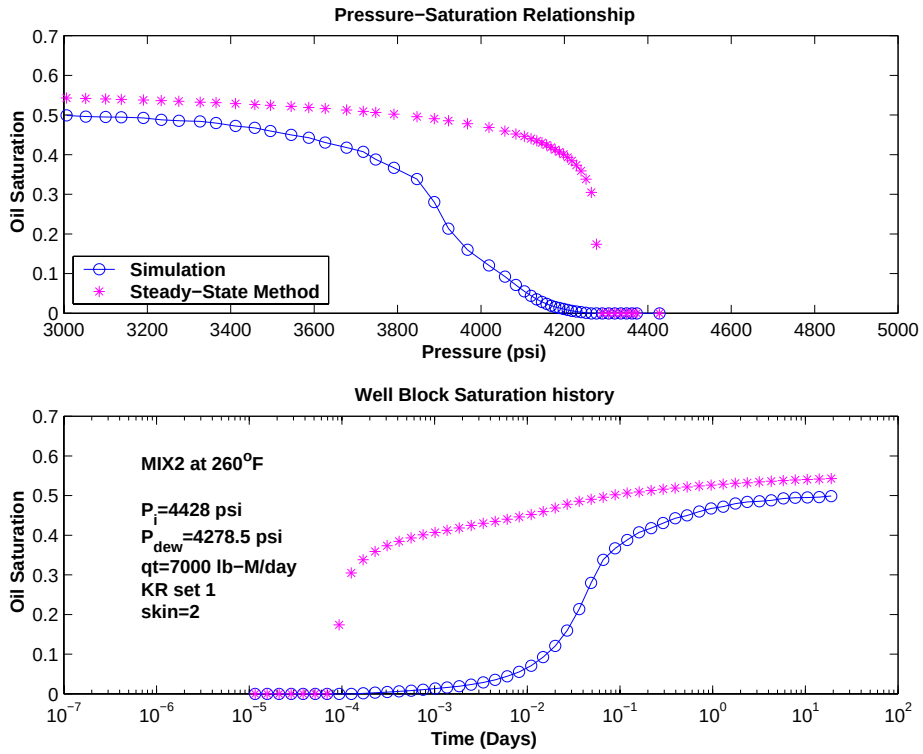

Figure 3.7: Comparison of the Well Block Oil Saturation from the Simulation and as Predicted by Steady-State Method

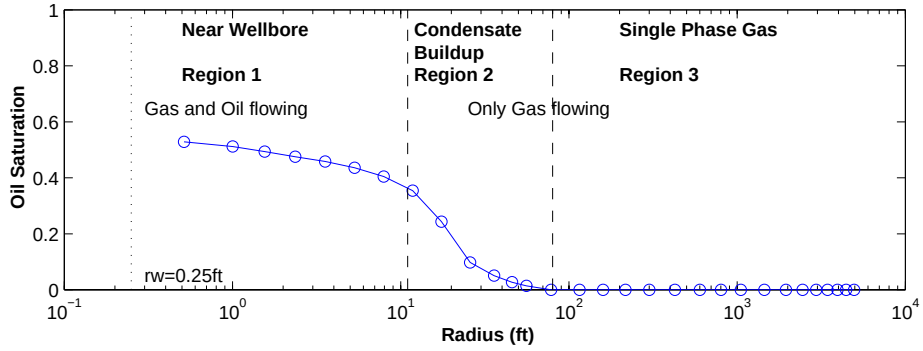

Figure 3.8: The Three Main Flow Regions During a Drawdown Test

region 1 develop at the wellbore, the producing GOR is constant. The pressure range corresponding to that region goes from the wellbore flowing pressure p_{wf} to a pressure p^*.

- **Region 2:** Condensate buildup region where the condensate saturation is low enough so that the oil phase is immobile and only the gas is flowing. The composition of the mixture is changing. While Region 2 is developing at the wellbore, the produced gas becomes leaner and the GOR is increasing. The inner boundary pressure is p^* and the outer boundary is p_{dew} the dew point pressure of the original reservoir gas
- **Region 3** contains only single-phase original gas.

The pseudopressure integral is computed from Eq. 3.20. The density and viscosity are computed for a given pressure from either a CCE or CVD experiment. The pressure-saturation relationship is constructed differently for each pressure range corresponding to the different flow regions.

$$\begin{aligned}
\text{Total} \qquad m^{3Z}(p_{wf}) &= \int_{p_{wf}}^{p_r} (\rho_o \frac{k_{ro}}{\mu_o} + \rho_g \frac{k_{rg}}{\mu_g}) dp \\
\text{Region 1} &= \int_{p_{wf}}^{p^*} (\rho_o \frac{k_{ro}}{\mu_o} + \rho_g \frac{k_{rg}}{\mu_g}) dp \\
\text{Region 2} &+ \int_{p^*}^{p_{dew}} (\rho_o \frac{k_{ro}}{\mu_o} + \rho_g \frac{k_{rg}}{\mu_g}) dp \\
\text{Region 3} &+ k_{rg}(S_{wi}) \int_{p_{dew}}^{p_r} \frac{\rho_g}{\mu_g} dp
\end{aligned} \tag{3.20}$$

Region 1 Pressure Limits: Region 1 only develops after the well flowing pressure p_{wf} drop sufficiently below the dew-point pressure p_{dew} so that the oil phase is mobile, we will call this pressure p^*. Therefore, for well flowing pressure less than p^*, the pressure limits of Region 1 are p_{wf} and p^*. If $p_{wf} < p^*$ then Region 1 has not developed

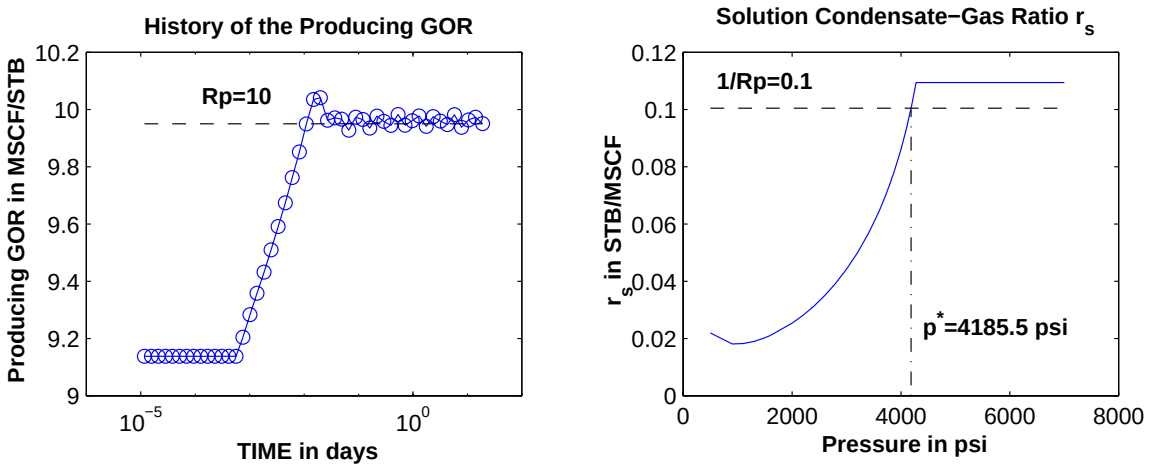

Figure 3.9: Determination of p^*, Boundary Pressure between Region 1 and Region 2

yet and the corresponding saturation will be computed using the method described for Region 2. Since only single-phase gas is flowing from Region 2 into Region 1, the dew-point pressure of the gas entering Region 1 must equal p^*. Furthermore, p^* must be equal to the dew-point of the producing wellstream, since the flowing mixture composition and the producing GOR is constant in Region 1 and equal to R_p. Alternatively, we can use the black-oil PVT characterization (see Appendix A) of our gas condensate with the solution oil gas ratio r_s known as a function of pressure: p^* will be the pressure where $r_s = 1/R_p$. Figure 3.9 illustrates the determination of p^*.

Region 2 Pressure Limits: The previously calculated pressure p^* is the lower pressure limit of Region 2. At the outer boundary of Region 2 the pressure equals the dew-point pressure of the original reservoir gas. The upper limit of the pressure range is equal to the initial dew-point pressure p_{dew} if $p_r > p_{dew}$ or it equals the average reservoir pressure p_r if $p_r < p_{dew}$.

Region 3 Pressure Limits: Region 3 exists only if $p_r > p_{dew}$, in which case the lower limit is p_{dew} and the upper limit is p_r.

Region 1 Pressure-Saturation Relationship: The pressure-saturation relationship corresponding to this pressure range is solved using a modified Evinger and Muskat (1942) approach as proposed by Fevang (1995). For a system with known producing GOR R_p, black oil properties can be related to R_p as shown by Fetkovich et al. (1986):

$$R_p = R_s + \frac{k_{rg}}{k_{ro}} \frac{\mu_o B_o}{\mu_g B_{gd}} (1 - r_s R_p) \tag{3.21}$$

Solving for k_{rg}/k_{ro} we obtain:

$$\frac{k_{rg}}{k_{ro}}(p) = (\frac{R_p - R_s}{1 - r_s R_p}) \frac{\mu_g B_{gd}}{\mu_o B_o} \tag{3.22}$$

The black oil PVT properties (R_s, B_o, r_s, B_{gd}, μ_o and μ_g) are simulated using the technique of Whitson and Torp (1983) and are functions of pressure only (even if this is an approximation, see Appendix A). The producing GOR R_p is constant when Region 1 develops from the well, which will happen a short time after well opening depending on the initial conditions, the reservoir and the fluid characteristics. Hence, the right hand side of Eq. 3.22 is a known function of pressure only. Since k_{rg}/k_{ro} is known as a function of saturation, the pressure can be related to the saturation using Eq. 3.22.

Eq. 3.22 is equivalent to the following formulation:

$$\frac{k_{rg}}{k_{ro}}(p) = \frac{\rho_g L \mu_o}{\rho_o V \mu_g} \tag{3.23}$$

where L and V are the liquid and vapor molar fraction of the producing wellstream and instead of the original reservoir mixture. Relative permeabilities k_{rg} and k_{ro} can be expressed as a function of the ratio k_{rg}/k_{ro} when both phases are mobile (Evinger and Muskat, 1942). Finally, for a given R_p and for the pressure range $[p_{wf}, p^*]$, k_{rg} and k_{ro} can be expressed directly as a function of pressure $k_{rg}(p) = f[k_{rg}/k_{ro}(p)]$ and $k_{ro}(p) = g[k_{rg}/k_{ro}(p)]$, using Eq. 3.22. The integral for Region 1 is then easy to compute since all terms are pressure-dependent only. For a given gas condensate reservoir, the pressure-saturation relationship computed in Region 1 depends only on the value of R_p.

Region 2 Pressure-Saturation Relationship: The oil saturation in Region 2, for the pressure range $[p^*, p_{dew}]$, equals the oil saturation as calculated in a CVD experiment corrected for initial water saturation:

$$S_o(p) = (1 - S_{wi})S_{oCVD} \tag{3.24}$$

Region 3 Pressure-Saturation Relationship: For pressure greater than the initial dew-point pressure (p_{dew}) the oil saturation is zero. Only PVT properties have to be integrated, the traditional real gas pseudopressure is used here.

The pseudopressure computed from the three-zone method will be referred to as three-zone pseudopressure and denoted m_D^{3Z}. The resulting pressure-saturation relationship is shown in Figure 3.10. Figure 3.11 illustrates the use of the three-zone pseudopressure to interpret a drawdown well test. The three-zone pseudopressure always matches almost exactly the liquid flow solution at later time. When the skin is nonzero, there could be two transition zones, the earlier one corresponding to the single-phase gas flow through the unaltered zone and the later one to the condensate flow through the altered zone. Both the skin and the formation flow capacity kh are estimated correctly (the maximum deviation for all our cases is less than 15% for kh, the mean eror being 1%) and the error on the skin is less than ± 1.5 (the mean value is $+0.11$), the full distributions of error are given later in Figure 4.19.

Pseudopressure Calculation using Black-Oil Data Only: The three-zone pseudopressure can be computed from the black-oil data only, the integral in Eq. 3.15 will now be written as:

$$m^{3Z}(p_r) - m^{3Z}(p_{wf}) = \int_{p_{wf}}^{p_r} (\frac{k_{rg}}{B_{gd}\mu_g} + R_s\frac{k_{ro}}{B_o\mu_o})dp \tag{3.25}$$

The pressure-saturation relationship is computed in the same way as previously in Region 1 and Region 3. In Region 2, the CVD saturation can be computed from black oil properties as described by Fevang (1995).

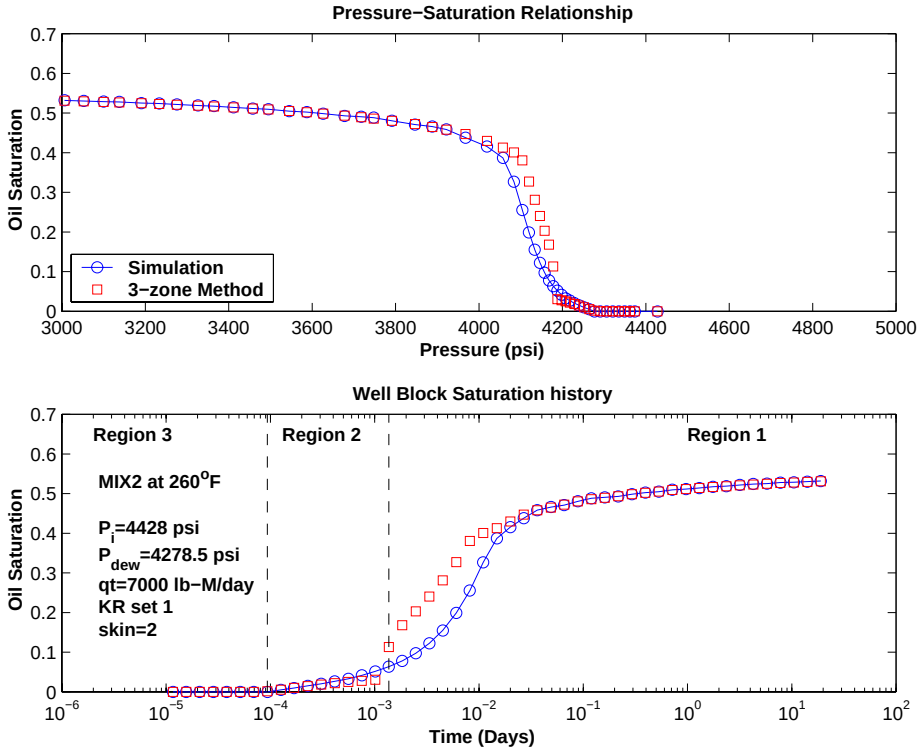

Figure 3.10: Comparison of the Well Block Oil Saturation from the Simulation and as Predicted by Three-Zone Method

3.4.6 Three-Zone Pseudopressure for Buildup Tests

Just as in drawdown cases, the integral 3.20 is broken into three parts corresponding to the three regions pressure ranges.

$$\begin{aligned}
\text{Total} \qquad m^{3Z}(p_{ws}) &= \int_{p_{wf,s}}^{p_{ws}} (\rho_o \frac{k_{ro}}{\mu_o} + \rho_g \frac{k_{rg}}{\mu_g}) dp \\
\text{Region 1} \qquad &= \int_{p_{wf,s}}^{p^*} (\rho_o \frac{k_{ro}}{\mu_o} + \rho_g \frac{k_{rg}}{\mu_g}) dp \\
\text{Region 2} \qquad &+ \int_{p^*}^{p_{dew}} (\rho_o \frac{k_{ro}}{\mu_o} + \rho_g \frac{k_{rg}}{\mu_g}) dp \\
\text{Region 3} \qquad &+ k_{rg}(S_{wi}) \int_{p_{dew}}^{p_{ws}} \frac{\rho_g}{\mu_g} dp
\end{aligned} \tag{3.26}$$

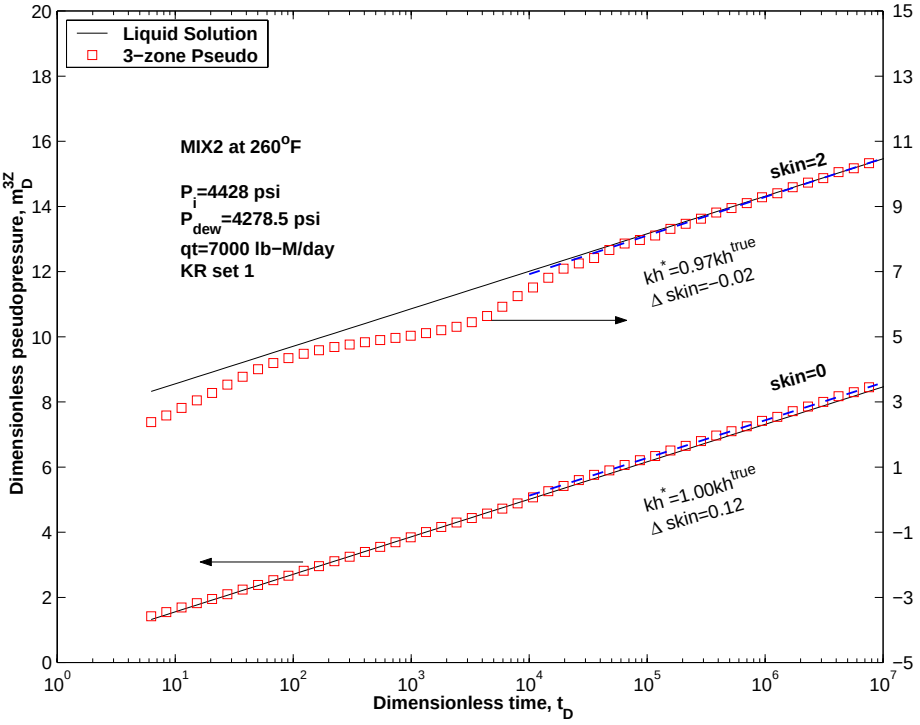

Figure 3.11: Drawdown Response Interpreted with the Three-Zone Pseudopressure

Each part of the integral is computed using a specific pressure-saturation relationship as described in Section 3.4.5. The densities and the viscosities are approximated using constant composition expansion data.

3.4.7 Pseudopressure Comparison and Discussion

By ignoring the existence of Region 2 where the flowing gas becomes leaner, the steady-state method predicts a much higher oil saturation than the simulation and thus underestimates the skin, however the formation flow capacity kh is well reproduced. The three-zone method will handle the change in composition in the reservoir by taking information from the stabilized producing GOR.

However, the contribution to the three-zone integral of Region 2 ($\int_{p^*}^{p_{dew}} (\rho_o \frac{k_{ro}}{\mu_o} + \rho_g \frac{k_{rg}}{\mu_g}) dp$)

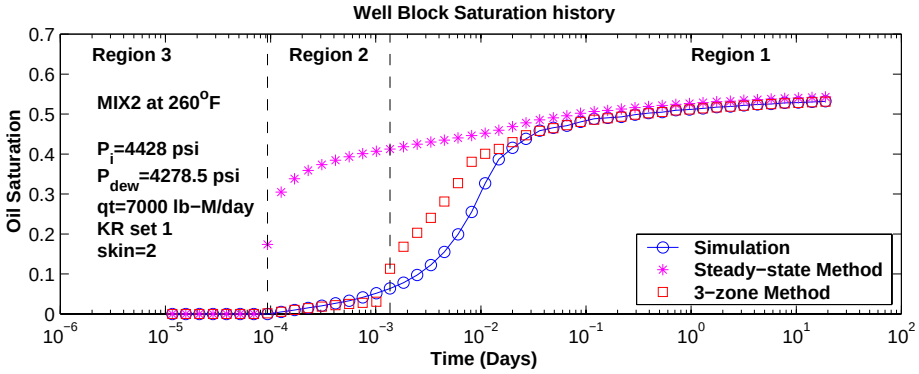

Figure 3.12: Comparison of the Well Block Oil Saturation from the Simulation, as Predicted by Steady-State Method and by Three-Zone Method

is negligible against the contribution corresponding to Region 1 because the oil saturation in Region 2 is always much less than in Region 1. Furthermore, the contribution of the condensate part of the integral $\rho_o \frac{k_{ro}}{\mu_o}$ is negligible against the contribution of the gas $\rho_g \frac{k_{rg}}{\mu_g}$, except for near-critical gas condensate. The oil saturations as predicted by each method are compared in Figure 3.12.

Chapter 4

Sensitivities and Robustness

In order to test the efficiency of the "steady-state" and the "three-zone" pseudopressure, several well tests are simulated using the commercial compositional simulator *Eclipse 300*. Laboratory experiments (CCE and CVD) are simulated using the Peng-Robinson equation of state.

4.1 Gas Condensate Well Test Simulation

4.1.1 Compositional vs. Black Oil PVT Formulation

Coats (1988) showed that a modified black-oil PVT formulation gives the same results as a fully compositional Equation of State (EOS) PVT formulation where the EOS fluid characterization uses only one C_{7+} fraction. However Fevang (1995) showed that if the C_{7+} had been split, significant differences would have been observed on the oil viscosity and in the well deliverability. Fully compositional simulations are therefore used for this study.

4.1.2 Grid Size Distribution Effects

Numerical simulation of well tests in gas condensate reservoirs is not an easy task. The pressure transient information occurs during the first hours of the test, and the near wellbore region is of great interest. The numerical simulation should therefore

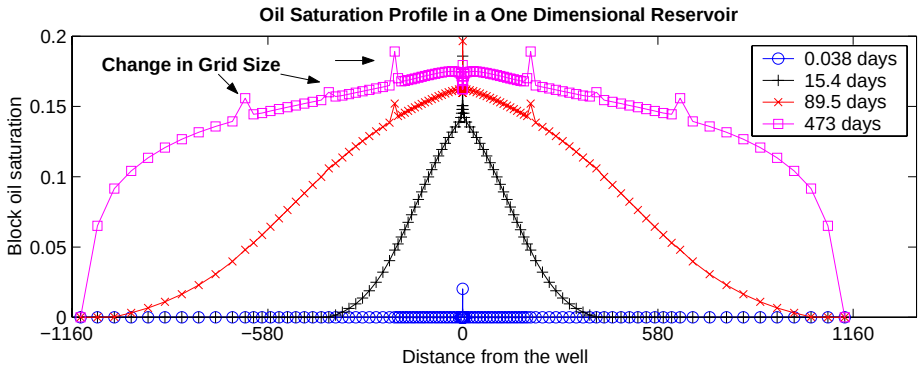

Figure 4.1: Effect of Grid Size Change in a One Dimensional Reservoir

be performed on very small grid blocks around the well using very small time steps. However, since the reservoir volume to be simulated is very large, a distribution of grid cell size has to be chosen (usually radial grid using logarithmic size distribution). The change of size between two adjacent cells can create numerical instability even with an implicit formulation. The choice of the grid size distribution has to be such that these instabilities are minimized. Figure 4.1 shows saturation profiles at different times in a one-dimensional reservoir. The well is located at the center of the reservoir and produces at constant total molar rate, the outer boundary is at constant pressure. There are discontinuities in the saturation profile at the locations where the grid size is changing.

In a radial case, the grid size change cannot be avoided when a large volume has to be simulated with a small number of blocks and more details are needed near the well. The grid size distribution could be set up by matching single-phase simulations to analytical solutions in which the well bottom-hole pressure is above the dew point. However, in some cases, this approach is not enough and instabilities are still observed when simulating two-phase flow cases. We used the two-phase reservoir pseudopressure as introduced by Jones and Raghavan (1988) to check the validity of our simulations. Jones and Raghavan (1988) showed that the transient pressure

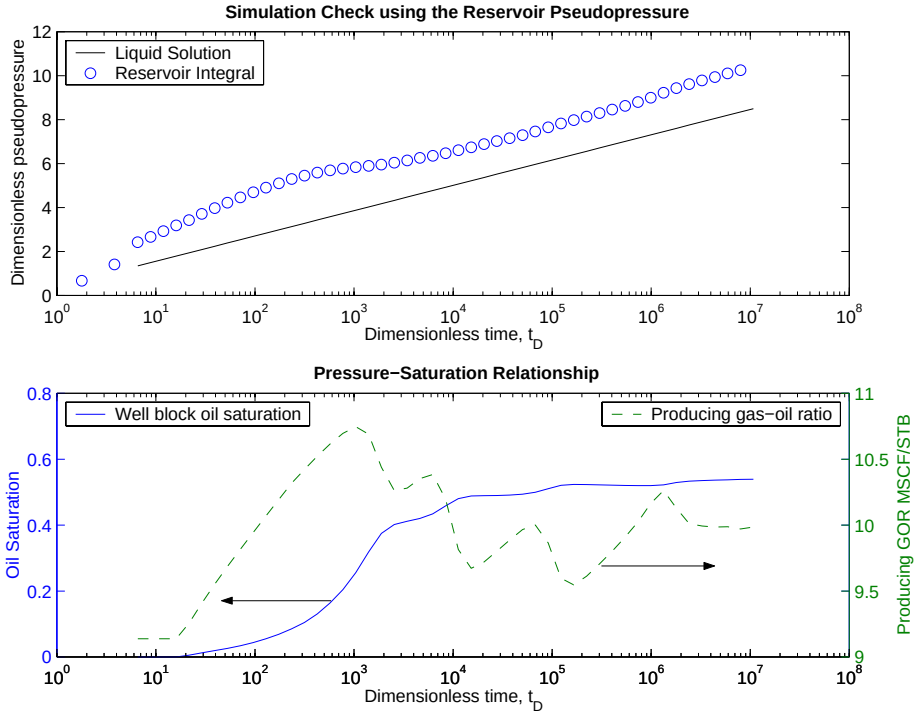

Figure 4.2: Radial Grid Size Distribution with Nonsmooth Changes

response from retrograde gas condensate systems could be correlated with the classical liquid solutions, if the pressure were transformed to a reservoir pseudopressure. The reservoir pseudopressure calculation requires the pressure and saturation profiles obtained from the simulator and therefore cannot be used for analysis. For all our simulations, the grid size and the time steps were adjusted such that the reservoir pseudopressure matches the liquid solution. Nevertheless, the check with the reservoir pseudopressure does not ensure that production data (such as producing gas-oil ratio) does not oscillate and further tuning has to be made. Figure 4.2 shows the results of a gas condensate drawdown simulation using nonsmoothly varying grid size. Oscillations in the gas-oil ratio and in the oil saturation are large, the resulting reservoir pseudopressure does not match the liquid solution, indicating that the numerical simulation is wrong. After tuning of the grid size, the oscillations can be minimized and the reservoir pseudopressure matches the liquid solution as shown in Figure 4.3.

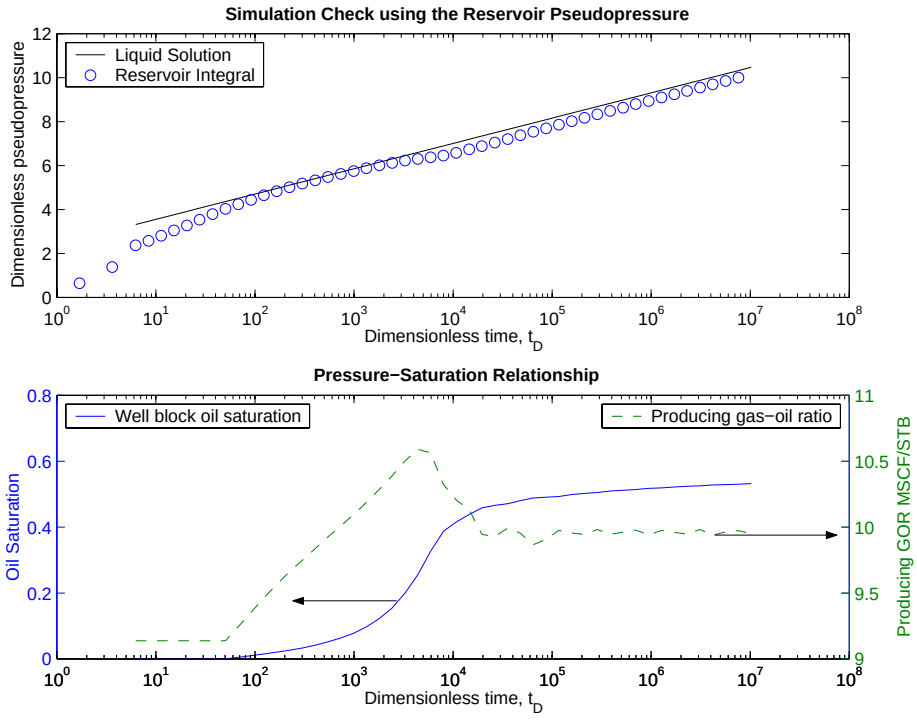

Figure 4.3: Final Radial Grid Size Distribution with Smooth Size Changes

Rigorously, this grid size tuning should be done for each of the particular considered cases. However, we only use one grid for all our cases and then checked if the reservoir pseudopressure agreed with the liquid solution. For all our cases, oscillations are small and the reservoir pseudopressure reproduces the liquid solution.

4.2 Sensitivity Study

The two methods for computing the two-phase pseudopressure (steady-state and three-zone) are tested on a large variety of cases considering, nonzero skin, fluids of different richness in condensate, different relative permeability curves, different reservoir initial conditions and different flow rate. 67 cases are studied, they are identified using an specific name (for example “R21112”) where each number stands for a value

of a specific parameter. The identifier specification is explain fully in Appendix B.1, the results of the interpretation of each case are tabulated in Appendix D.

4.2.1 Brief Description of the Cases Studied

This section gives a brief description of the cases under consideration, a complete description is given in Appendix B.

- **Reservoir Mixture:** Four simple methane-butane-decane mixtures ($C_1 - C_4 - C_{10}$) were considered for demonstration purposes. The mixtures have different composition and behave as retrograde gas condensate systems at the associated reservoir temperature and pressure range. Their compositions have been chosen such that MIX1 corresponds to a very lean gas-condensate system and MIX4 to a very rich system, MIX2 and MIX3 are intermediate. Figure 4.4 shows the liquid drop-out during a constant composition experiment (CCE) and the solution condensate-gas ratio r_s of the four mixtures. A richer system has a higher liquid drop-out in a CCE and a higher condensate-gas ratio at dew point. The characteristics of these four mixtures are given in more detail in Appendix B.4.

- **Skin:** Three different values for skin are considered: 0, 2 and 4.6, the corresponding extents of the skin zone are tabulated in Table 4.1.

- **Relative Permeability Curves:** Three sets of relative permeability curves as shown in Figure 4.5 are considered.

- **Flow Rate:** Three total molar flow rates are considered: 5000, 7000 and 10000 $lb - M/d$.

- **Initial Pressure Difference ($p_i - p_{dew}$):** Four different initial pressure difference $p_i - p_{dew}$ are tested: 50, 100, 150 and 400 psi.

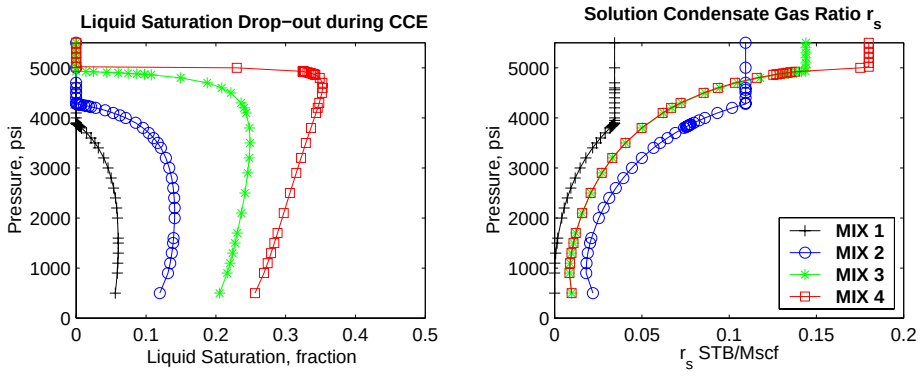

Figure 4.4: Characteristics of the Four Mixtures Considered in this Study

Table 4.1: Values Considered for the Skin

skin	Extend of the skin zone, feet	Ratio of Permeability k_s/k
0	0.0	1.0
2	1.9	0.5
4.6	4.3	0.5

4.2.2 Effect of Skin

As described in Section 2.2.4, the skin has an effect on producing wellstream properties (gas-oil ratio, wellstream mixture composition). The skin has been modeled by a zone of altered permeability k_s extending to a radius r_{skin} from the well. In the case with zero skin, the gas-oil ratio increases in Region 2 to reach a maximum and stabilized value in Region 1 (see Figure 2.10). When an altered zone is introduced around the well (positive skin), the gas-oil ratio reaches a maximum at the end of Region 2 and then decreases in Region 1 to finally stabilized at the same value (10 Mscf/stb) as in the corresponding zero skin case as shown in Figure 2.10. The stabilized value of the gas-oil ratio (10 Mscf/stb for the case shown in Figure 2.10) is being used for R_p to compute the three-zone pseudopressure.

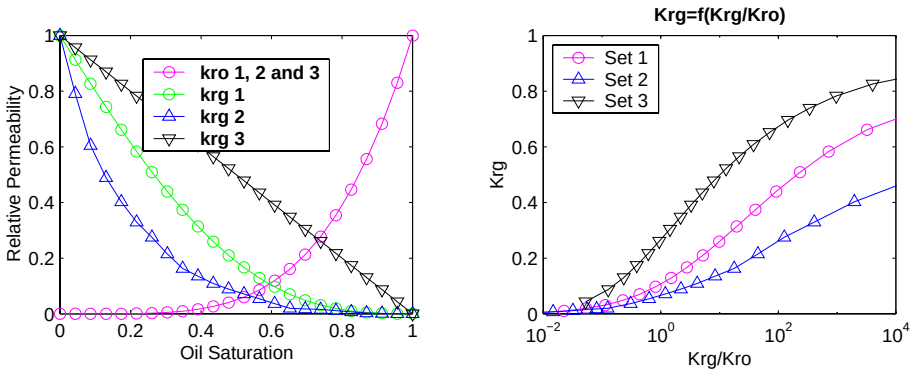

Figure 4.5: Relative Permeability Curves Considered for the Sensitivity Study

The skin delays the stabilization of the pseudopressures (both for the steady-state and the three-zone method) as shown in Figure 3.6 and Figure 3.11. However the efficiency of the method is still the same in that the steady-state method still underestimates the skin, gives a good estimate of the flow capacity and the three-zone method still leads to an accurate skin and flow capacity.

Because R_p was chosen to be the stabilized GOR value (10 Mscf/stb), the three-zone method locates the boundary between Region 2 and Region 1 at the pressure p^* corresponding to the first time the gas-oil ratio equals 10 Mscf/stb (at $t = 550$ days), this boundary is represented by the dashed line on Figure 2.10. The oil becomes mobile only later, at a pressure corresponding to the maximum in the GOR (at $t = 4500$ days).

If the maximum value of the gas-oil ratio (10.6 Mscf/stb) instead of the stabilized value (10 Mscf/stb) is used for R_p, the predicted pressure boundary p^* between Region 2 and Region 1 will be lower (see Section 3.4.5). Hence the boundary will occur later on history plots, and the actual true boundary is better predicted as shown in Figure 4.7. However, the saturation in Region 1 at late time becomes less accurately approximated and consequently, the skin is overestimated. Except if stated so, for now the three-zone pseudopressure will always be computed using the stabilized

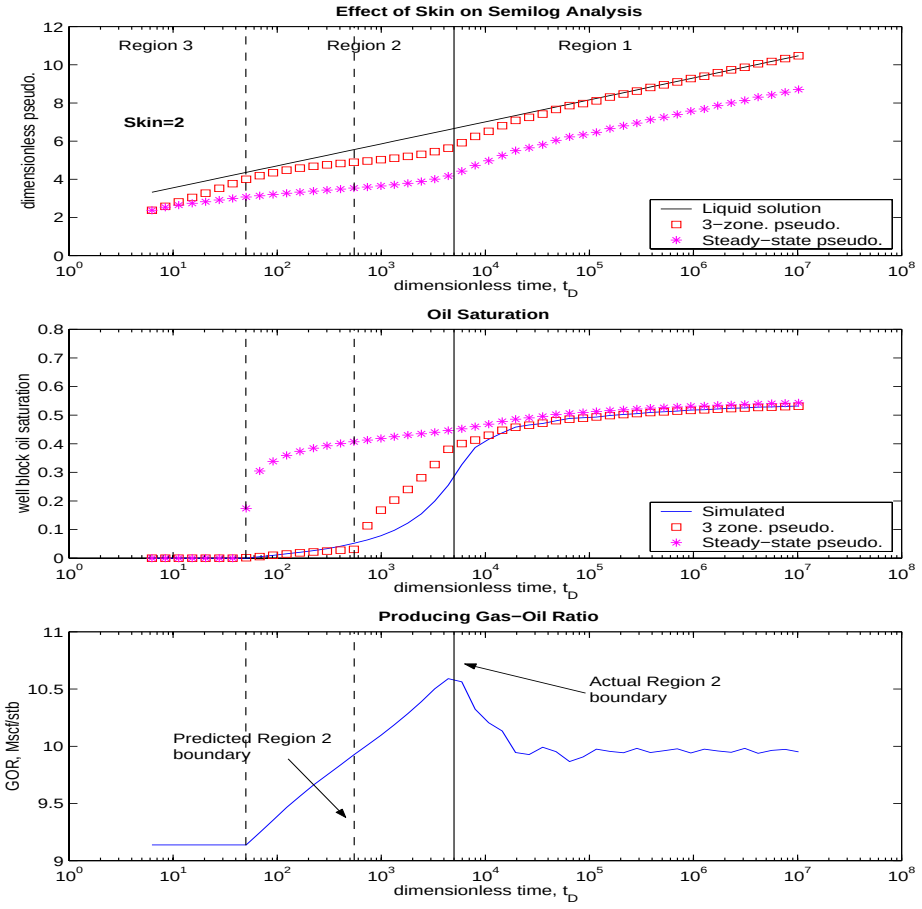

Figure 4.6: Effect of Skin on the Pseudopressures (Case Shown: R21112, skin=2)

value of the gas-oil ratio. The results of the sensitivity to skin are summarized using bar charts in Figure 4.8. The plots on the left column show kh^*/kh, the ratio of the estimated flow capacity to the true capacity, a value of 1 means that the method is very accurate, a value greater than 1 means that kh^* overestimates the true kh, a value lesser than 1 means that the flow capacity is underestimated. The plots on the right columns display the difference $\Delta skin$ between the estimated skin s^* and the true skin s. The steady-state method tends to overestimate the flow capacity and underestimate the skin and is less accurate than the three-zone method for the cases shown in Figure 4.8. The skin is estimated less accurately as the true skin gets

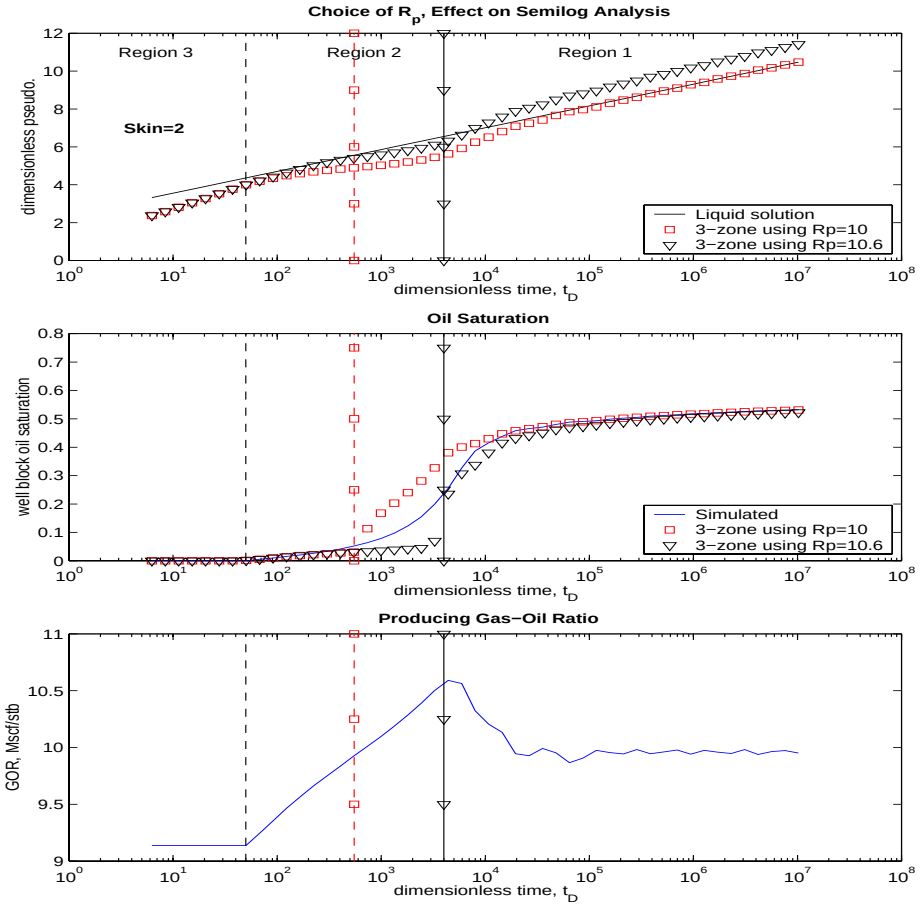

Figure 4.7: Three-Zone Method, Effect on the Input Parameter R_p

bigger. However there is no general trend for the estimation of kh as the skin gets bigger. For instance, for MIX3 (lower row of plots) kh is less accurate for $skin = 4.6$ than for $skin = 0$ or 2, but if we consider the mixture MIX2 (upper row of plots) this conclusion does not hold.

4.2.3 Fluid Effect

The effect of the mixture richness in condensate is considered in this section. The semilog analysis of the leaner mixture (MIX1) and of the richer mixture (MIX4) is

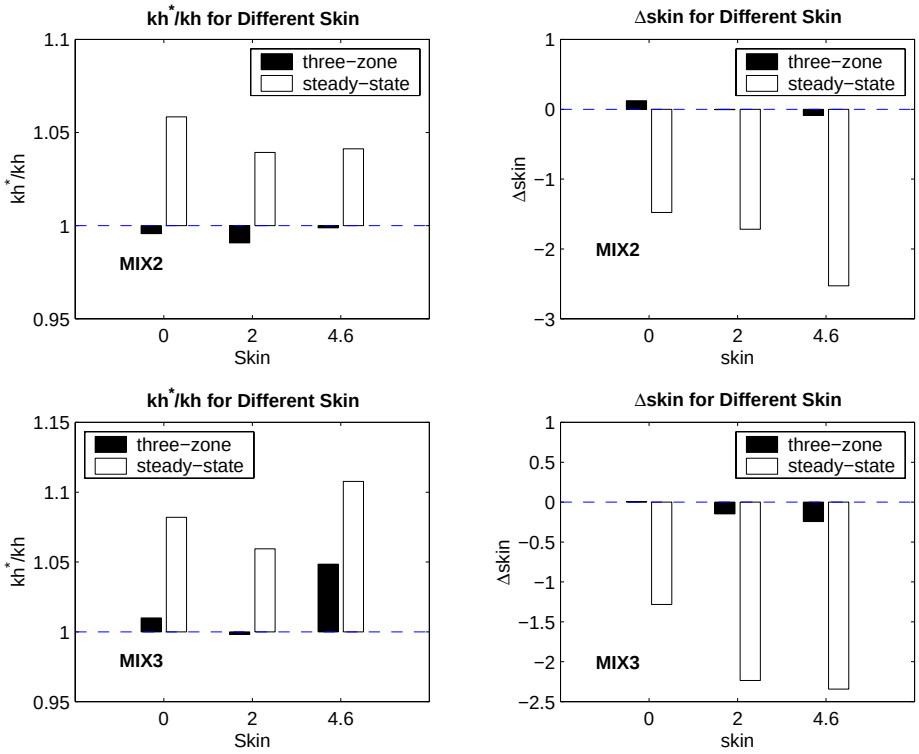

Figure 4.8: Sensitivity on the Skin

represented in Figure 4.9.

Figure 4.10 shows bar charts of the ratio kh^*/kh and the difference $\Delta skin$ for different mixtures for $skin = 2$ (cases with $skin = 0$ or $skin = 4.6$ show similar results trend). The steady-state method is less accurate for richer mixture. For the steady-state method, the flow capacity kh tends to be more greatly overestimated and the skin more greatly underestimated as the considered mixture is richer in condensate. The three-zone method is less sensitive to the considered mixture, and the errors are less than 10% for kh and 0.6 unit for the skin.

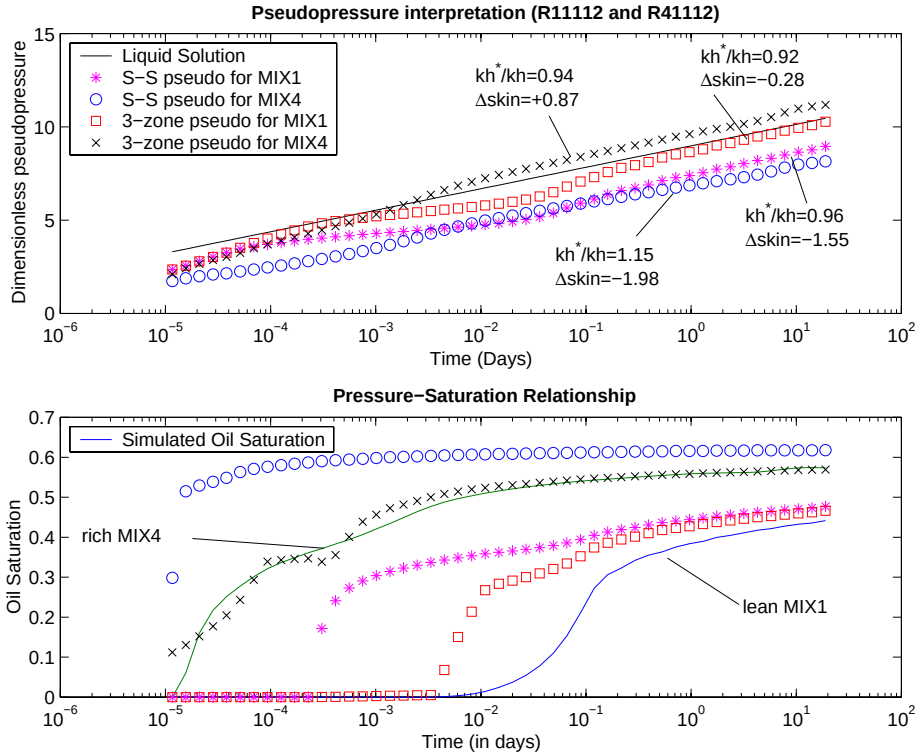

Figure 4.9: Drawdown Interpretations for Two Different Fluids (MIX1 and MIX2 with skin=2, cases R11112 and R41112)

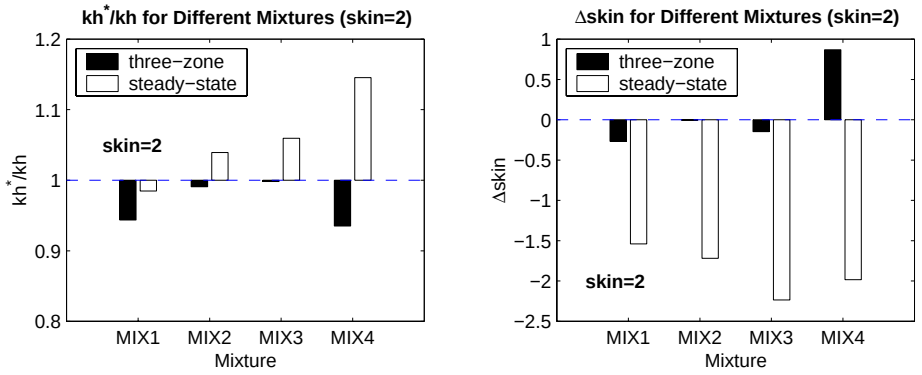

Figure 4.10: Sensitivity on the Fluid Richness: Results from the Four Mixtures

4.2.4 Effect of Relative Permeability

Only $k_{rg} = f(\frac{k_{rg}}{k_{ro}})$ is important: When computing the two-phase pseudopressures (either using steady-state or three-zone method), a pressure-saturation is needed. The pressure-saturation relationship is determined by relating the ratio $\frac{k_{rg}}{k_{ro}}$ with functions of pressure only, hence this ratio can be written as $\frac{k_{rg}}{k_{ro}}(p)$.

The two-phase pseudopressure is given by:

$$m_D(p) = \frac{2\pi C_1 kh}{q_t} \int_{p_i}^{p} \frac{\rho_g k_{rg}}{\mu_g} + \frac{\rho_o k_{ro}}{\mu_o} dp' \tag{4.1}$$

Recalling that in the two-phase pseudopressure integral Eq. 4.1, only the gas term has a significant contribution $\frac{\rho_g k_{rg}}{\mu_g}$; the value of the integral will then only depend on the relationship $k_{rg} = f(\frac{k_{rg}}{k_{ro}}(p))$. Therefore, sensitivities on relative permeabilities should be evaluated on different sets of curves that have different relationship $k_{rg} = f(\frac{k_{rg}}{k_{ro}})$ as Fevang (1995) advised.

As a proof, the relative permeability sets 1 and 4 shown in Figure 4.11 are considered, they have completely different $k_r(S_w)$ but share the same relationship $k_{rg} = f(k_{rg}/k_{ro})$. Two simulations are made each using one of the relative permeability curve sets, those simulations are then interpreted using the steady-state and the three-zone method. Figure 4.12 shows the results of the two simulations together with the pseudopressures. The well bottom hole pressures (upper left corner plot) are almost the same, the well block oil saturation (upper right corner plot) and the gas-oil ratio (lower left corner plot) are greater when using the relative permeability curve set 1 (because Set 1 leads to higher mobility of the gas phase than Set 4). Most importantly, the pseudopressures (steady-state and three-zone) are exactly the same for the two simulations proving the previously stated result that only the $k_{rg} = f(k_{rg}/k_{ro})$ relationship is important for the pseudopressure computation.

Considering the remarks made earlier, three sets of relative permeability curves, that have a different $k_{rg} = f(k_{rg}/k_{ro})$, were used to test the sensitivity to k_r (the k_r curves

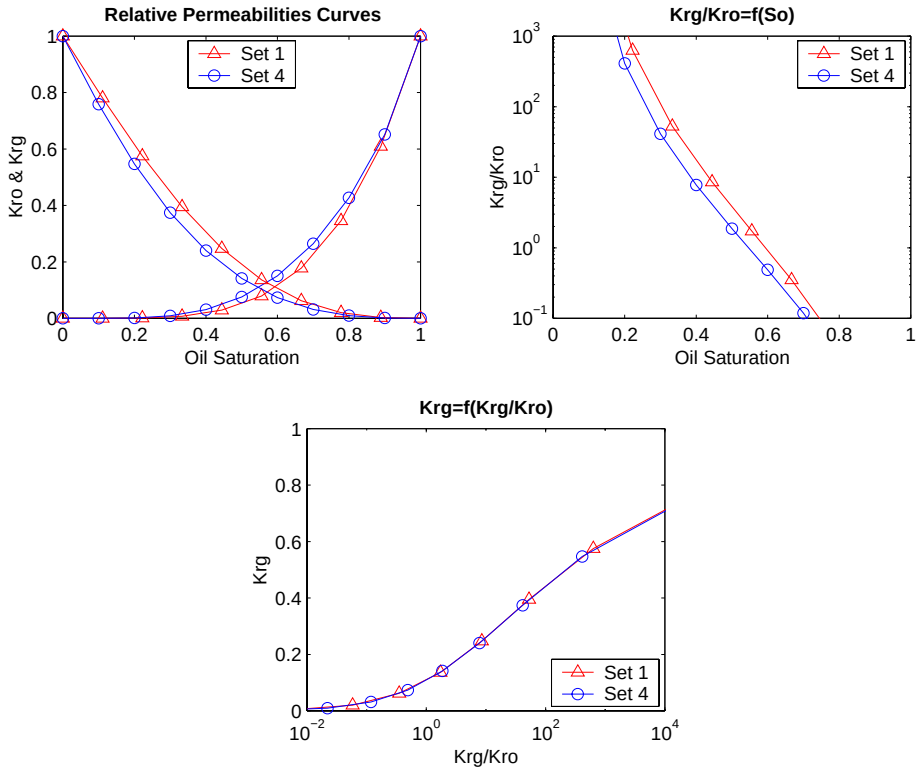

Figure 4.11: Two Sets of Gas-Oil Relative Permeability Curves that have Identical k_{rg}=f(k_{rg}/k_{ro}) Relationship

are shown in Figure 4.5). Semilog interpretation using both steady-state and three-zone method for cases using each of the three Sets are shown in Figure 4.13. The errors made on the kh and on the skin estimation are shown in Figure 4.14 for the case of MIX2 with $s = 2$. Additional cases were considered and the results are given in Appendix D. The two methods are not very sensitive to the relative permeability curves used and the errors on the estimation of the flow capacity kh are less than 10% in all the cases considered here.

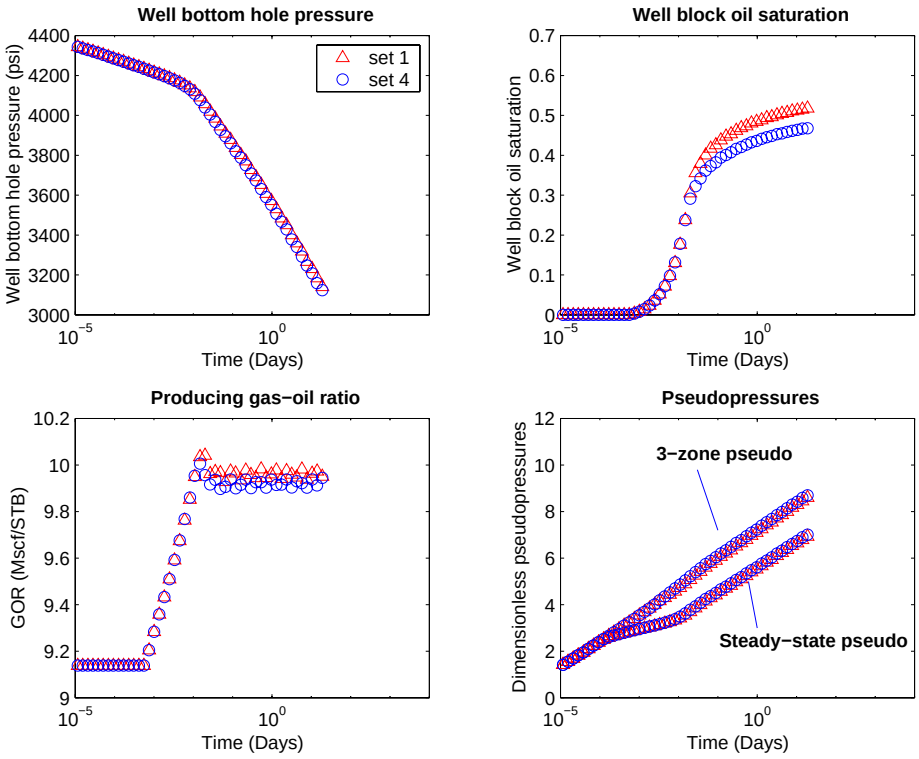

Figure 4.12: Two Simulations using Relative Permeability Curves having the Same $k_{rg} = f(\frac{k_{rg}}{k_{ro}})$

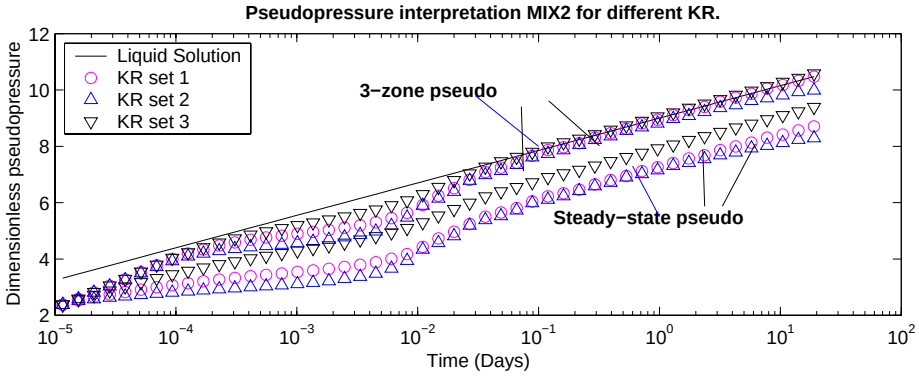

Figure 4.13: Drawdown Interpretations for Cases using Different Relative Permeability Curves (MIX2 with skin=2, cases R21112, R22112 and R23112)

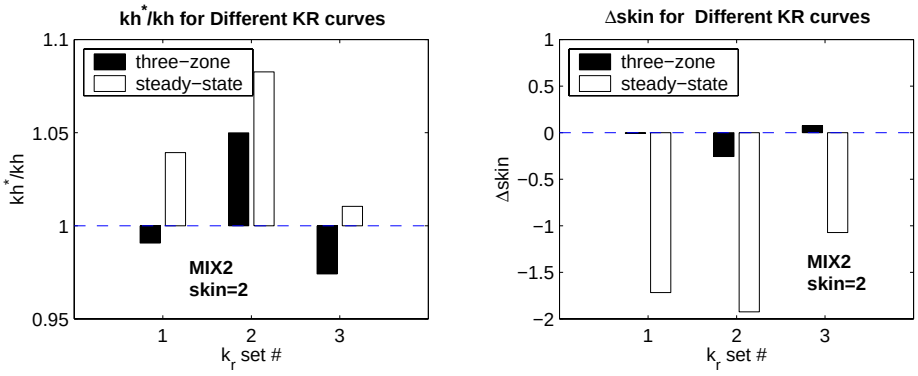

Figure 4.14: Sensitivity on the Relative Permeability Curves

4.2.5 Effect of Total Molar Flow Rate

A constant total molar flow rate is used instead of volumetric flow rate for the drawdown. Figure 4.15 shows the interpretation using the two-phase pseudopressures of three cases with three different total molar flow rate, 5000, 7000 and 10000 $lb-M/day$. The cases shown in Figure 4.15 uses the mixture MIX2 and a skin of 2. Cases using the richer mixture MIX4 are also interpreted, Figure 4.16 presents the results for MIX4, the results for MIX2 are similar. The two methods (three-zone and steady-state) are found more accurate for higher flow rate.

4.2.6 Effect of the Initial Pressure Difference $p_i - p_{dew}$

For a given fluid, the difference between the initial pressure and the dewpoint pressure $(p_i - p_{dew})$ is the dominant parameter that effects the size of Region 2. Hence the steady-state method, which does not account for Region 2, is more sensitive to the initial pressure p_i than the three-zone method. Figure 4.17 and Figure 4.18 demonstrate the influence of the initial pressure difference, $(p_i - p_{dew})$ on the accuracy of the estimated flow capacity and skin for different mixture and skin condition. The smaller the difference, the less accurate the interpretation of skin, however the interpretation of the flow capacity remains accurate. The steady-state is less accurate than the three-zone method for the cases shown in Figure 4.17 and Figure 4.18.

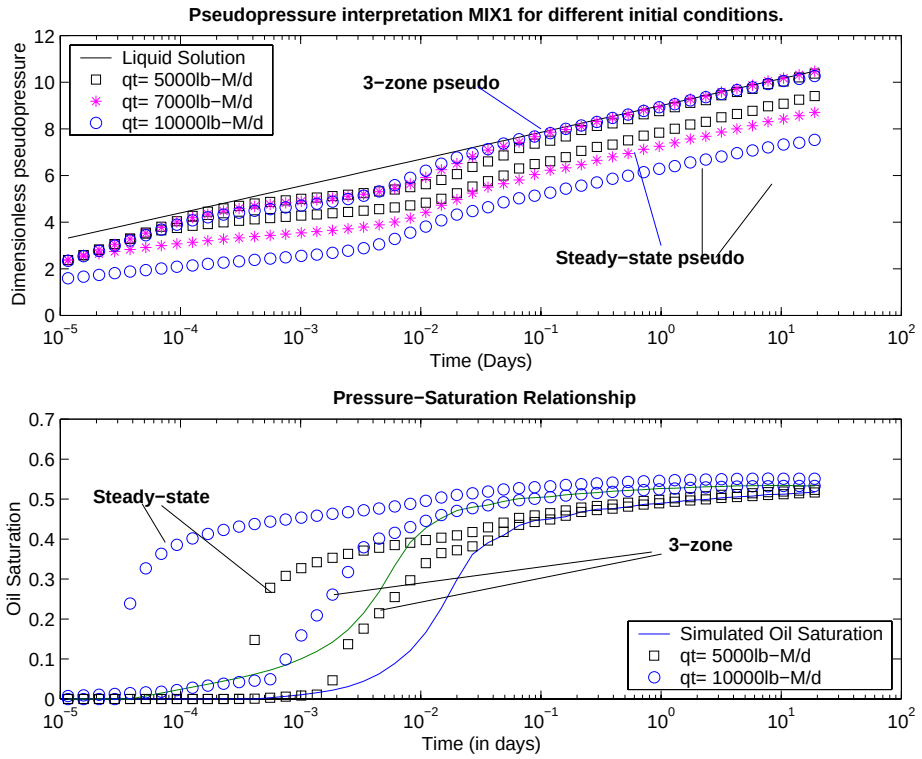

Figure 4.15: Drawdown Interpretations of Cases with Different Specified Total Molar Flow Rate q_t (cases shown: MIX2, skin=2: R21112, R21212 and R21312)

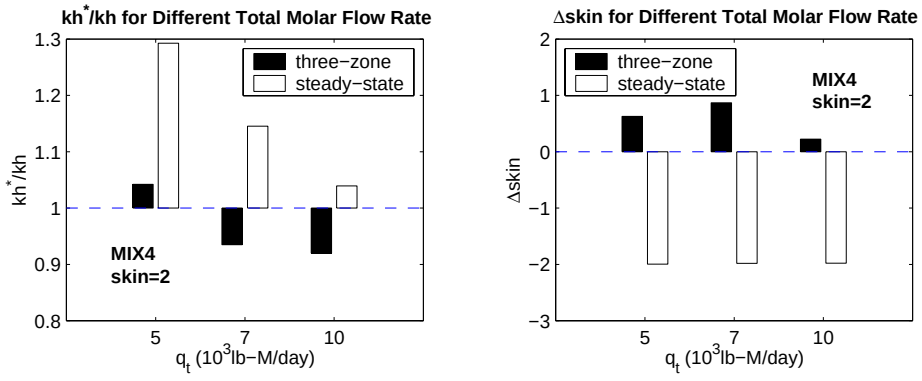

Figure 4.16: Sensitivity on the Specified Total Molar Flow Rate q_t

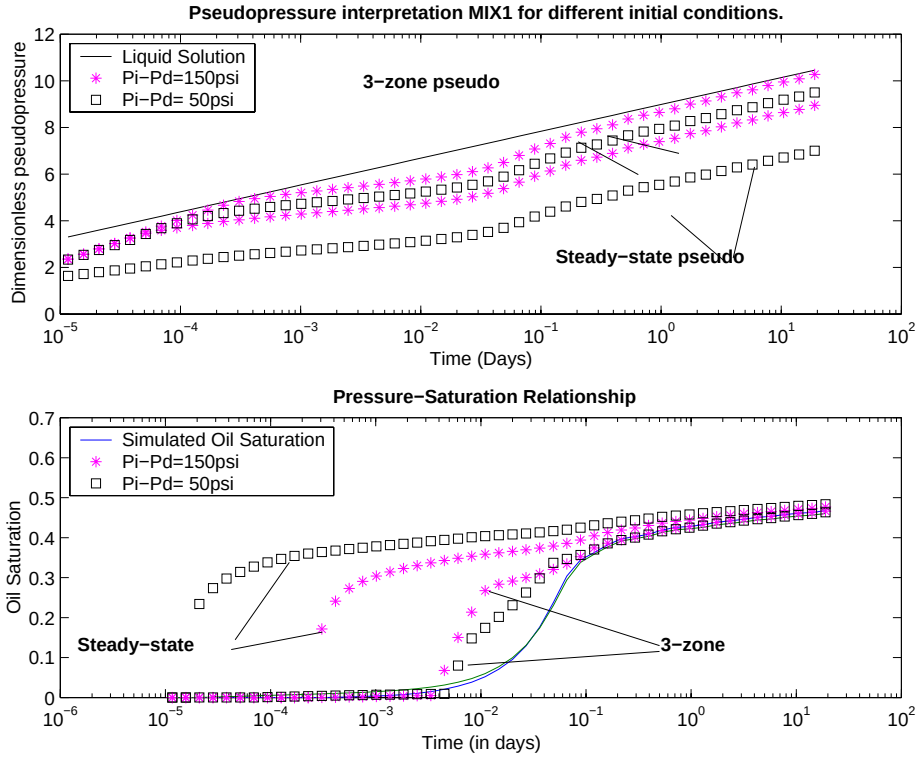

Figure 4.17: Drawdown Interpretations of Cases with Different Initial Pressure Conditions (cases shown: MIX1 with skin=2, R11112 and R11132)

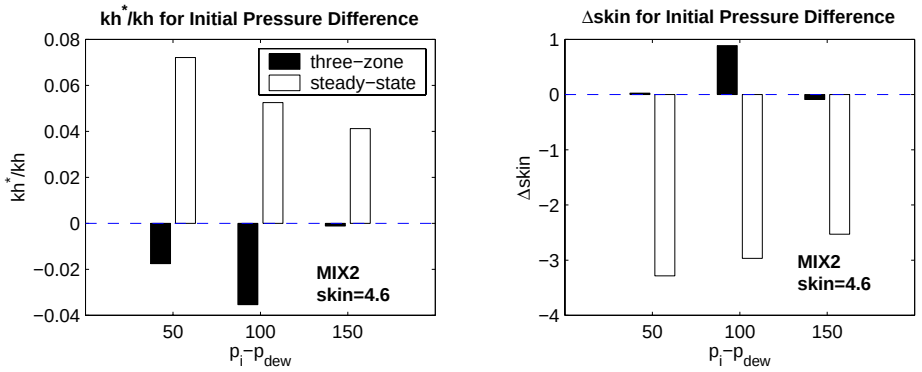

Figure 4.18: Sensitivity on the Initial Pressure Difference ($p_i - p_{dew}$)

4.2.7 Conclusions

A large range of cases was considered (67 cases) in order to test the accuracy of the three-zone and the steady-state method in interpreting well tests. For each of these cases, the flow capacity and the skin has been estimated and are given in Appendix D. The ratio kh^*/kh and the difference $\Delta skin = s^* - s$ of all the 67 cases have been plotted on the histograms in Figure 4.19 (the asterisk * refers to the estimated value, no asterisk refers to the true value). The three-zone method evaluates both kh and the skin reasonably accurately although with slightly overestimated values. The steady-state method slightly overestimates kh and dramatically underestimates the skin. Most of the deviation from the correct estimation ($kh^*/kh = 1$ and $\Delta skin = 0$) is due to the cases with nonzero skin. Figure 4.20 shows the histograms of the 42 cases with nonzero skin only. Considering only those 42 cases the same conclusions about the efficiency of the methods can be made.

The interpretation of the 67 drawdown cases using both the steady-state and the three-zone method leads to the following conclusions:

- The three-zone method predicts an accurate flow capacity kh^* and an accurate skin provided that the test lasts long enough such that Region 1 develops at the well.
- The steady-state method ignores the existence of Region 2 and underestimates the skin, the flow capacity being slightly overestimated.
- The presence of a nonzero skin delays the stabilization of the pseudopressures.
- The performances of the three-zone and steady-state methods are not sensitive to any of the studied parameters, except for the pressure difference $(p_i - p_{dew})$.
- The closer the initial reservoir pressure is to the dew point, the less accurate the interpretation. The accuracy of the three-zone method is less affected by this parameter than that of the steady-state method.

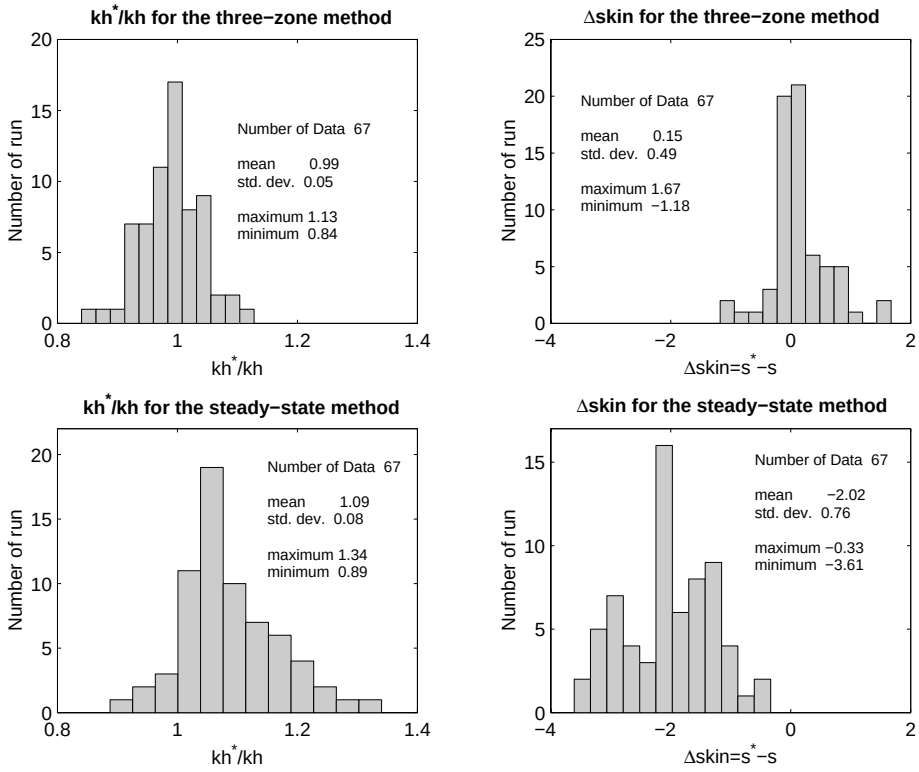

Figure 4.19: Results of the Sensitivity Cases in Drawdown, all 67 Cases

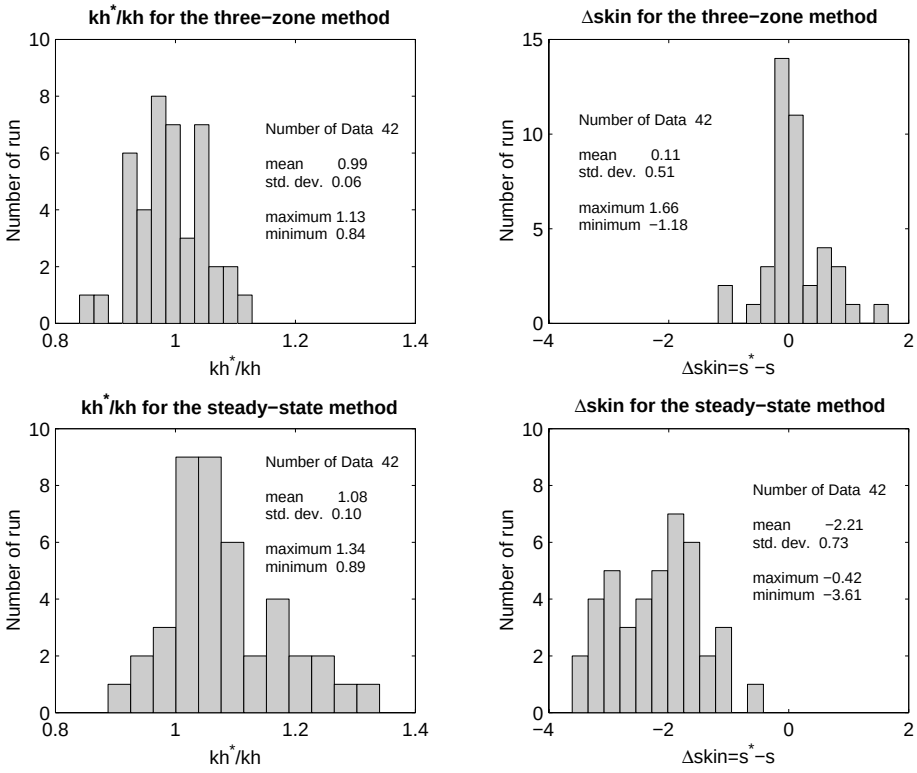

Figure 4.20: Results of the Sensitivity Cases in Drawdown, only the 43 Nonzero Skin Cases

4.3 Robustness of the Two-Phase Pseudopressure

Up to this point, the relative permeability, the measured gas-oil ratio and the fluid characterization were assumed known and representative at the reservoir scale. However, the relative permeability measured on core plugs may not be representative at the reservoir scale. Producing gas-oil ratio, difficult to measure, is uncertain. The fluid sampling can be very difficult, specially if the initial pressure of the reservoir is close to the dew point pressure. In the present section, the effects of those uncertainty and measurements errors on the accuracy of the interpretation using the two-phase pseudopressure are considered.

4.3.1 To the Relative Permeability Curves

The simulation uses a given set of relative permeability curves, however a different set is used for the calculation of the pseudopressures. As shown previously in Section 4.2.4, for a given pressure-saturation relationship, only the function $k_{rg} = f(\frac{k_{rg}}{k_{ro}})$ has an effect on the pseudopressure. Hence the set of relative permeability curves to be used for the interpretation has a different function $k_{rg} = f(\frac{k_{rg}}{k_{ro}})$ than the curves used in the simulation. Two alternative relative permeability sets, shown in Figure 4.21 are considered; they share the same k_{ro} curve as the "true" relative permeability, but have different k_{rg} curve, referred as to k_{rg}^{+} and k_{rg}^{-}. k_{rg}^{+} leads to higher gas mobility than the true k_{rg}, k_{rg}^{-} to lower gas mobility. The two relative permeability sets, k_{rg}^{+} and k_{rg}^{-} have a different $k_{rg} = f(\frac{k_{rg}}{k_{ro}})$ relationships than the true k_r.

Figure 4.22 shows that the accuracy of the method are very sensitive to errors in the relative permeability curves. The flow capacity is estimated with more than 20% error when the representative relative permeability are not known. Consequently, the skin is evaluated badly as well.

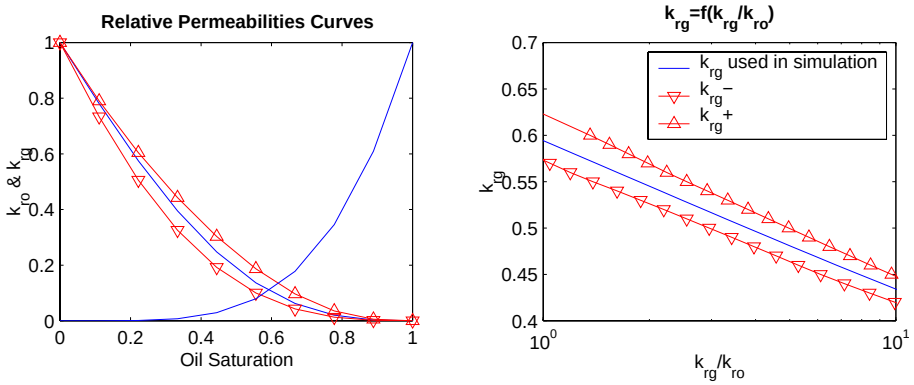

Figure 4.21: Different Relative Permeability Curves Used for Simulation and its Interpretation

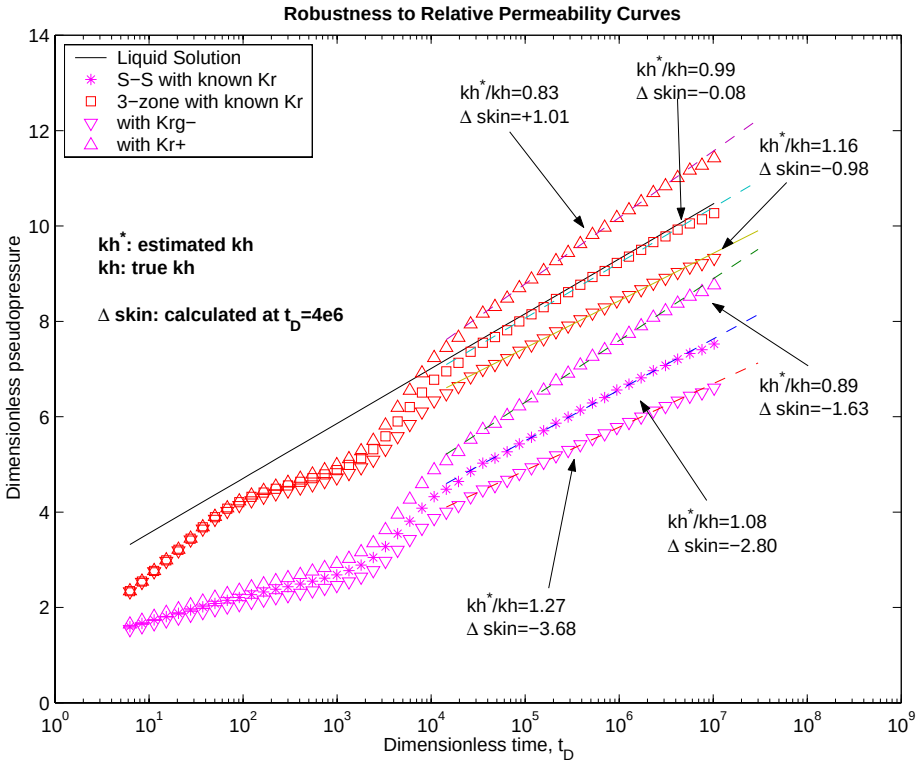

Figure 4.22: Drawdown Interpretations, Robustness to Error in the Relative Permeability Curves

4.3.2 To the Measured Producing Gas Oil Ratio (GOR)

The producing gas-oil ratio is often subject to large measurement errors and consequently is not known accurately. In Section 3.4.5, it has been shown that R_p should be set equal to the value of the gas-oil ratio at late time, in this section, different values for R_p are considered in order to quantify the impact of error in the gas-oil ratio to the accuracy of the three-zone method.

Figure 4.23 shows the "true" producing gas-oil ratio that is observed during the numerical simulation of case R11132 (MIX1, skin=2, $\Delta p = 100psi$). Since the skin is nonzero, the gas-oil ratio shows a maximum as has been discussed in Section 2.2.4 and Section 4.2.2. Figure 4.24 shows the interpretation of the case R11132 using the three-zone pseudopressure computed with different values for R_p. As has been shown in Section 3.4.5, if the stabilized GOR value (32.5 Mscf/stb) is used for R_p, the pseudopressure is a correct liquid analog and both the flow capacity and the skin are estimated accurately. However, if other values are used for R_p, the three-zone pseudopressure does not follow the liquid solution any more. If a higher value of R_p is retained (that is overestimating the gas-oil ratio), the flow capacity kh would be underestimated. The gas-oil ratio cannot be underestimated more than its initial value (29 Mscf/stb in this case), since it has to agree with the fluid characterization. Figure 4.25 and Figure 4.26 show the gas-oil ratio and the interpretation for the mixture MIX2 with a skin of 4.6, the same conclusions can be made.

The input parameter R_p can be seen as a parameter that controls how much of the fluid effects (viscosity, density and relative permeability) are integrated in the pseudopressure. If R_p is too low in comparison with the stabilized GOR value, the three-zone pseudopressure will integrate more fluid effect than in reality. If R_p is too high, then too little fluid effect is integrated in the pseudopressure. At the limits, if R_p equals the initial GOR value, the three-zone pseudopressure equals the steady-state pseudopressure, if R_p is very large, the three-zone pseudopressure equals the real gas pseudopressure as shown in Figure 4.27.

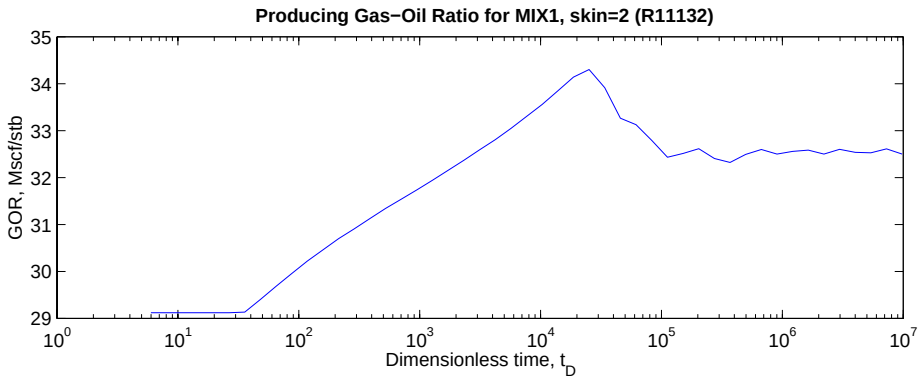

Figure 4.23: Producing Gas-Oil Ratio Observed in the Case Shown in Figure 4.24

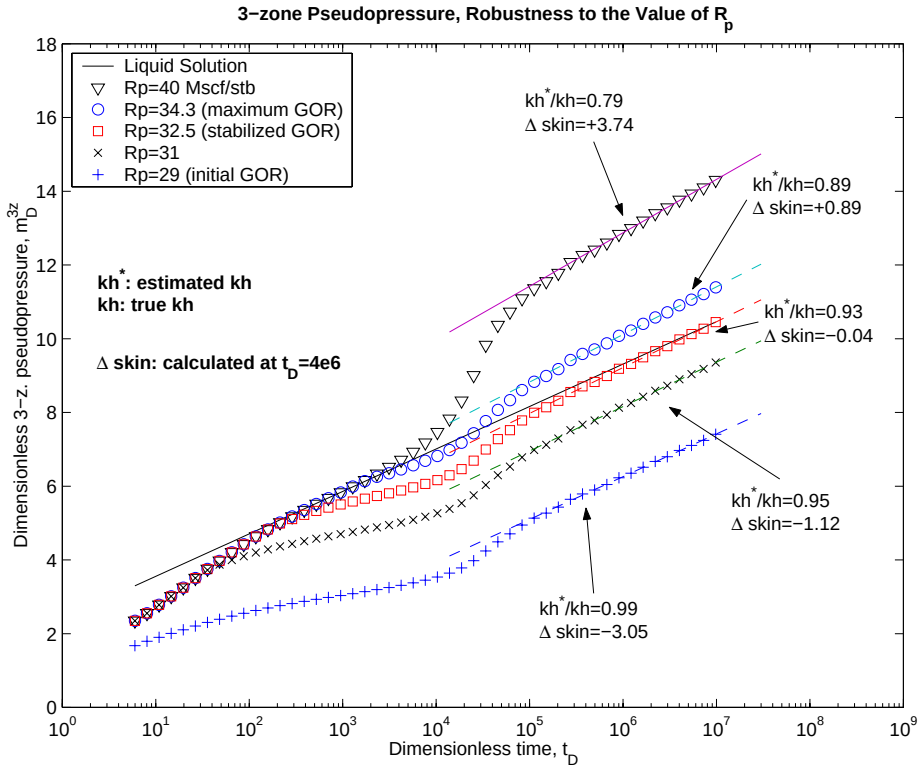

Figure 4.24: Drawdown Interpretations for the Lean Mixture MIX1 with skin=2, Robustness to Measurements Errors in the Gas-Oil Ratio (Case Shown R11132)

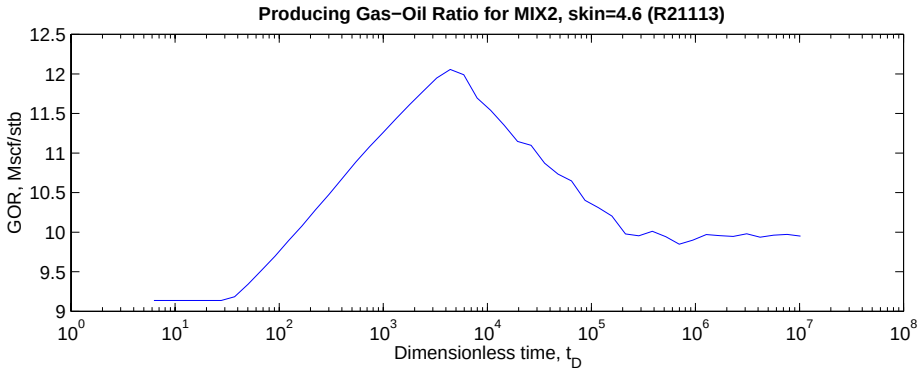

Figure 4.25: Producing Gas-Oil Ratio Observed in the Case Shown in Figure 4.24

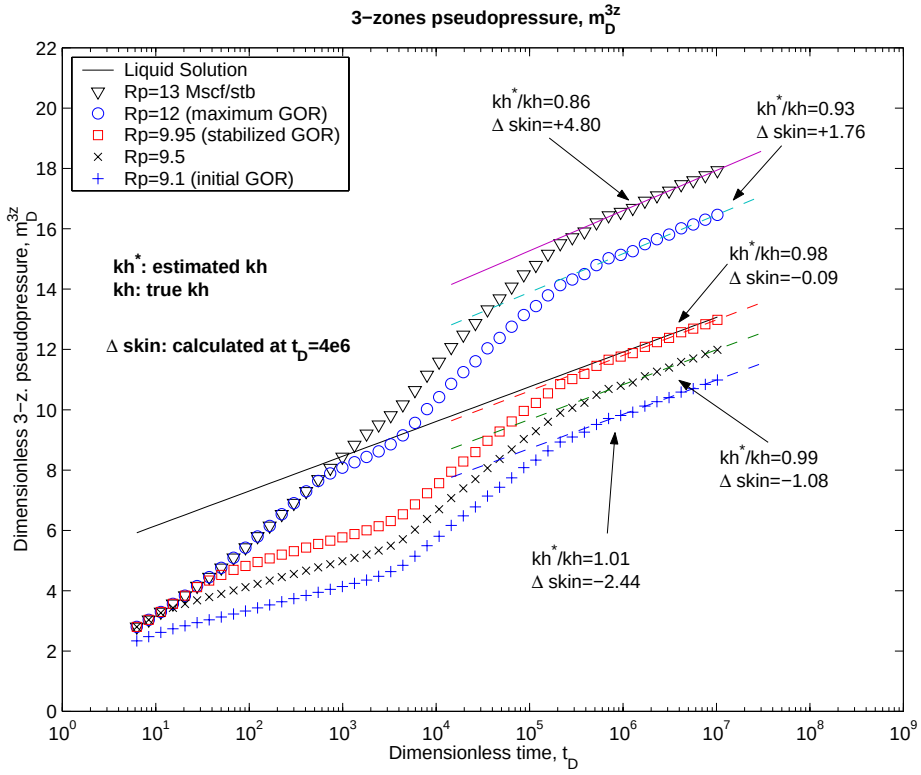

Figure 4.26: Drawdown Interpretations for the Mixture MIX2 with skin=4.6, Robustness to Measurements Errors in the Gas-Oil Ratio (case shown R21113)

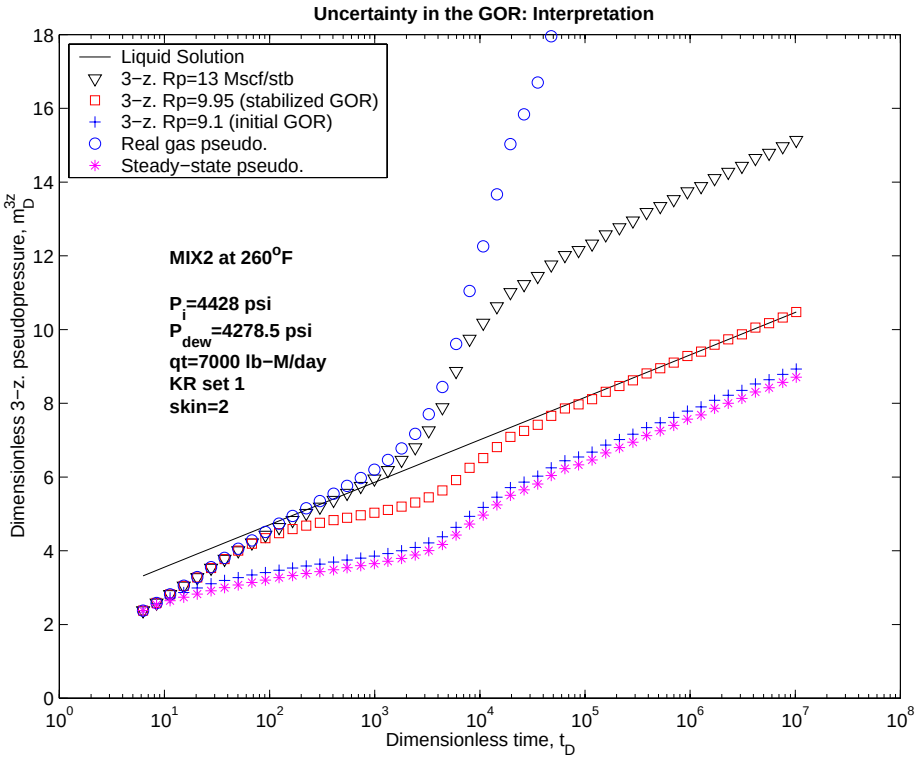

Figure 4.27: Interpretation of the input Parameter R_p for the Three-Zone Method (case shown R21112)

4.3.3 To the Fluid Sampling and Characterization

The sampling of gas condensate may lead, in some cases, to bad estimates of the original in situ reservoir oil and gas composition. In this section, the error in the original fluid characterization is considered. Fluid samples are usually taken in the wellbore early in the production, if the initial pressure is far above the dew-point the sample mixture will be the original in situ reservoir fluid. However, if the initial pressure is near the dew point pressure or if the sampling is done after some time of production, the sample may not be representative of the original mixture. Figure 4.28 shows how the producing wellstream mixture changes during a drawdown test.

The same drawdown test has been interpreted using two-phase pseudopressure, however, the fluid properties (viscosity, density) are taken from the late time producing wellstream mixture instead of the original reservoir mixture. Figure 4.29 shows the resulting steady-state pseudopressure and three-zone pseudopressure. As seen in Section 3.4.5, the pressure-saturation relationship is computed in Region 1 using Eq. 4.2.

$$\frac{k_{rg}}{k_{ro}}(p) = (\frac{R_p - R_s}{1 - r_s R_p})\frac{\mu_g B_{gd}}{\mu_o B_o} \tag{4.2}$$

It has also been shown that Equation 4.2, used for the computation of the three-zone pseudopressure, leads to the same pressure-saturation relationship as Equation 4.3 when using the later wellstream mixture composition.

$$\frac{k_{ro}}{k_{rg}} = \frac{\rho_g L \mu_o}{\rho_o V \mu_g} \tag{4.3}$$

The steady-state method uses the Equation 4.3, however the considered mixture is usually the original in situ reservoir mixture. Therefore, as the later wellstream mixture is now considered instead of the original mixture, the steady-state method will predict exactly the same pressure-saturation relationship as the three-zone method in Region 1. Hence, the only difference between the steady-state pseudopressure using the later composition and the three-zone method using the original mixture is the contribution of Region 2 in the pseudopressure, which is not accounted for in the steady-state method. However, as has been discussed in Section 3.4.7 the contribution of Region 2 in the integral is negligible. Finally, the steady-state pseudopressure,

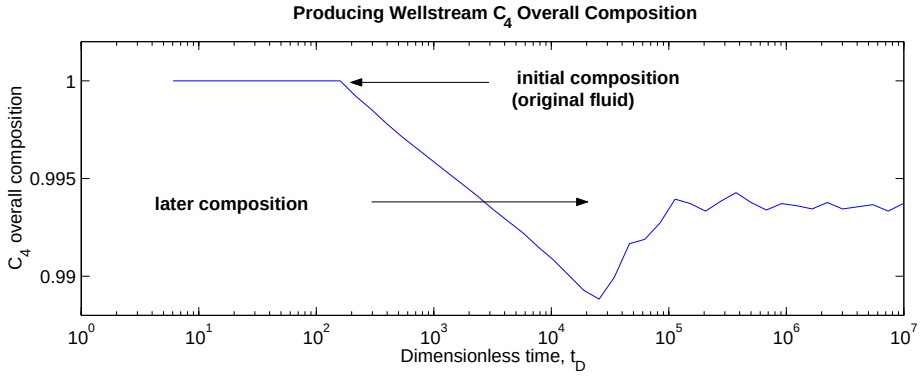

Figure 4.28: Overall Producing Wellstream Composition (case shown: R11112)

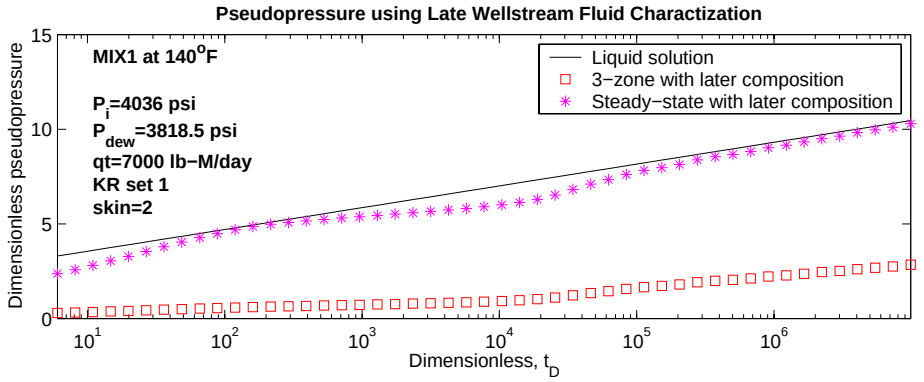

Figure 4.29: Drawdown Interpretations Using the Late Wellstream Fluid Characterization Instead of the Original Fluid (Case Shown: R11112)

computed using the later wellstream mixture composition, is almost identical to the three-zone pseudopressure using the original mixture composition and therefore it is very close to the liquid solution as shown in Figure 4.29. On the other hand, the three-zone pseudopressure, if computed using the late wellstream mixture composition deviates significantly from the liquid solution as it will have corrected twice for composition change.

4.3.4 Conclusions

The steady-state and the three-zone methods are shown not to be robust to errors in the relative permeability, gas-oil ratio measurements and fluid characterization. Small errors in the relative permeability curves (due to nonrepresentativity of the relative permeability for example) yield to large errors in the estimated flow capacity and skin.

For the three-zone method, the input parameter R_p should be set to the producing gas-oil ratio value after stabilization in Region 1, GOR_1. As the gas-oil ratio is being overestimated ($R_p > GOR_1$), the flow capacity is being underestimated. The parameter R_p is a measure of the amount of fluid effects being integrated in the three-zone method, if R_p is set to the initial gas-oil ratio (corresponding to the original reservoir mixture) the three-zone pseudopressure equals the steady-state pseudopressure and too much fluid effect is integrated leading to an overestimated flow capacity and an underestimated skin. On the other hand, if R_p is very large, the three-zone pseudopressure equals the real gas pseudopressure, which integrates too few fluid effects, the flow capacity is then underestimated and the skin overestimated.

The three-zone method accounts for the wellstream composition change during Region 2, therefore the original mixture composition should be used when computing the pseudopressure. The steady-state method does not account for the composition change and gives less accurate results than the three-zone method when the original reservoir mixture composition is used. However, if the later wellstream composition is used, the steady-state method approximates the three-zone method (using the original mixture composition) and therefore gives accurate results.

Chapter 5

Conclusions

Gas condensate wells producing with a bottom hole pressure below the dewpoint develop up to three flow regions in the reservoir. Region 1 has a constant flowing composition (constant producing gas-oil ratio) where both gas and oil flow simultaneously. Most of the flow resistance that complicates the well test interpretation comes from the reduced gas mobility in Region 1. Region 2 is a zone of condensate accumulation with no mobility, the composition of the flowing mixture changes in this region. Region 3 is the outer region where the reservoir pressure is greater than the dewpoint and only gas is present.

Two methods to compute the two-phase pseudopressure were proposed. The "steady-state" method assumes that the relationship between the pressure and the saturation during the test can be approximated by the relationship observed during a hypothetical steady-state flow. The steady-state method tends to slightly overestimate the reservoir flow capacity kh but drastically underestimate the skin. The "three-zone" method uses a different pressure-saturation relationship for each of the three flow regions. Region 1 relationship is computed using the Evinger and Muskat (1942) approach, modified for gas condensate systems. Region 2 uses the saturation from the liquid dropout curve from a constant volume depletion experiment (CVD). Region 3 pseudopressure is the same as for single-phase gas. Because the three-zone method

accounts for the composition change in Region 2, the interpretation of the pseudopressure leads to correct estimation of both the flow capacity and the skin.

The two methods were tested over a large number of cases using different reservoir and fluid parameters (sensitivity to skin, fluid richness, relative permeability curves, flow rate and initial reservoir pressure were considered). For all the studied cases, the three-zone pseudopressure was found to be the right liquid analog, the steady-state pseudopressure agreed in the kh determination only.

However the steady-state and the three-zone multiphase pseudopressure are not robust to errors in the gas-oil ratio, the fluid sampling and the relative permeability. Even small errors in the gas-oil ratio lead to large error in the estimation of parameters when using the three-zone method (the steady-state method does not use the GOR information). When the fluid sampling can lead to the original gas composition the three-zone method should be used, however if only the producing wellstream composition is known the steady-state method should be used. Since the composition is initially not known, we cannot know exactly to which fluid the composition corresponds, and therefore which method to use for the well test interpretation. Finally, those methods are very sensitive to errors in relative permeability. The relative permeability curves are usually not unique and not precisely known at the reservoir scale, therefore the use of the two-phase pseudopressure methods may introduce more uncertainty for well tests interpretation than the more classical use of single-phase pseudopressure.

Even though the two-phase pseudopressures cannot be used efficiently for well test interpretation, they may be useful for well deliverability calculations and sensitivity analysis.

For the last decade, relative permeability behavior for gas condensate systems has been the subject of active research. The relative permeability curves have been proven to be dependent on the velocity and on the interfacial tension (IFT), effects that were

not considered in this report.

The relative permeability curves considered in this work included an oil critical saturation, below which the oil phase is immobile, but no residual gas saturation S_{gr} (corresponding to the trapped gas during the drawdown period). For future advanced research in gas condensate well test analysis, the relative permeabiliy curves should include a residual gas saturation, a critical oil saturation and be dependent on the velocity.

Bibliography

Al Hussainy, R. and Ramey, H.: 1966, Application of real gas flow theory to well testing and deliverability forecasting, *J. Pet. Tech.* **237**, 637–642.

Al Hussainy, R., Ramey, H. and Crawford, P.: 1966, The flow of real gases through porous media, *J. Pet. Tech.* **237**, 624–636.

Aziz, K.: 1999, *Fundamentals of Reservoir Simulation Class Notes*, Stanford Univ.

Boe, A., Skjaeveland, S. M. and Whitson, C. H.: 1981, Two-phase pressure test analysis, *SPE paper 10224* .

Chopra, A. and Carter, R.: 1985, Proof of the two-phase steady-state theory for flow through porous media, *SPE paper 14472* .

Coats, K. H.: 1988, Simulation of gas condensate reservoir performance, *JPT* pp. 1870–1886.

Evinger, H. H. and Muskat, M.: 1942, Calculation of theorical productivity factor, *SPE Form. Eval.* **146**, 126–139.

Fetkovich, M. D., Guerrero, E. T., Fetkovich, M. J. and Thomas, L. K.: 1986, Oil and gas relative permeabilities determined from rate-time performance data., *SPE paper 15431* .

Fevang, O.: 1995, *Gas Condensate Flow Behavior and Sampling*, PhD thesis, Norges Tekniske Hogskole.

Fussel, D. D.: 1973, Single well performance for gas condensate reservoirs, *J. Pet. Tech.* **255**, 860–870.

Gravier, J. F.: 1986, *Proprietes des Fluides de Gisements*, Editions Technip.

Hawkins, M. F. J.: 1966, A note on the skin effects, *Trans.* **207**.

Horne, R. N.: 1995, *Modern Well Test Analysis*, Petroway Inc.

Jatmiko, W., Daltaban, T. and Archer, J.: 1997, Multiphase transient well testing for gas condensate reservoirs, *paper SPE 38646 presented at the 1997 SPE Annual Technical Conference and Exhibition.*

Jones, J. R.: 1985, *Computation and Analysis of Single Well Responses for Gas Condensate Systems*, PhD thesis, University of Tulsa, OK.

Jones, J. R. and Raghavan, R.: 1988, Interpretation of flowing well response in gas-condensate wells, *SPE paper 14204* .

Jones, J. R.and Vo, D. T. and Raghavan, R.: 1989, Interpretation of pressure-buildup responses in gas condensate wells, *SPE paper 15535* .

Lohrenz, J., Bray, B. and Clark, C.: 1964, Calculating viscosity of reservoir fluids from their composition, *J. Pet. Tech.* **231**.

Moses, P. L. and Donohoe, C. W.: 1962, Gas condensate reservoirs, *Petroleum Engineering handbook*, SPE, pp. 39:1–39:28.

O'Dell, H. G. and Miller, R. N.: 1967, Successfully cycling a low-permeability high-yield gas condensate reservoir., *J. Pet. Tech.* pp. 41–47.

Raghavan, R., Chu, W.-C. and Jones, J. R.: 1995, Practical considerations in the analysis of gas-condensate well tests, *SPE paper 30576* .

Thompson, L., Niu, J.-G. and Reynolds, A.: 1993, Well testing for gas condensate reservoirs, *SPE paper 25371* .

Wall, C. G.: 1982, Characteristics of gas condensate reservoirs and traditional production methods, *North Sea Gas Condensate Reservoirs and their Development 1982*, Oyez scientific and technical service, pp. 1–12.

Whitson, C. H. and Torp, S. B.: 1983, Evaluating constant volume depletion data, *J. Pet. Tech.* pp. 610–620.

Xu, S. and Lee, J. W.: 1999a, Gas condensate well test analysis using a single-phase analogy, *SPE paper 55992* .

Xu, S. and Lee, J. W.: 1999b, Two-phase well test analysis of gas condensate reservoirs, *SPE paper 56483* .

Yadavalli, S. and Jones, J.: 1996, Interpretation of pressure transient data from hydraulically fractured gas condensate wells, *paper SPE 36556 presented at the 1996 SPE Annual Technical Conference and Exhibition*.

Nomenclature

B_{gd}	dry gas Formation Volume Factor (FVF), RB/scf
B_o	oil FVF, RB/STB
C_1	conversion constant, 0.00633 ft^3/ft
c_t	total compressibility, psi^{-1}
h	reservoir thickness, ft
H	Horner time
k	absolute permeability, md
k_s	altered zone permeability, md
k_{rg}	gas relative permeability
k_{ro}	oil relative permeability
kh	flow capacity
L	molar liquid fraction
kh^*	estimated flow capacity
$m(p)$	pseudopressure function
$m^{gas}(p)$	real gas pseudopressure, $psi.lb - M/(cP.ft^3)$
$m_D^{gas}(p)$	real gas dimensionless pseudopressure
R_p	producing gas-oil ratio, input parameter for the three-zone method, MCF/stb
p_{dew}	original reservoir gas dew point pressure, psi
p_i	initial reservoir pressure, psi
p^*	pressure at the boundary between Region 1 and Region 2, psi
p_r	reservoir pressure, psi
p_{ws}	well shut pressure, psi

p_{wf}	well flowing pressure, psi
q_t	total molar rate or wet gas rate $lb-M/days$
r	radius, ft
R	gas constant, 10.735 $psi.ft^3/lb-M.^{o}$R
r_{dew}	radius at which the pressure equals the dew point pressure, ft
r_s	solution condensate-gas ratio, stb/MCF
r_{skin}	extend of the altered permeability zone, ft
r_w	well radius, ft
R_s	solution gas-oil ratio, MCF/stb
s	skin
s_t	total skin
s_m	mechanical skin
s_{2p}	skin due to the two-phase region or condensate bank
s^*	estimated skin
$\Delta skin$	Difference between estimated skin and true skin: $\Delta skin$=$s^* - s$
S_o	oil saturation
S_{oc}	critical oil saturation
S_{oCVD}	oil saturation in lab CVD
S_{wi}	irreducible water saturation
T	reservoir temperature, °R or °F
t	time, $days$ or $hours$
t_D	dimensionless time
t_p	producing time, $days$ or $hours$
v	molar volume, $ft^3/lb-M$
V	vapor molar fraction
Z	Z factor
z_g	gas z factor
z_o	oil z factor

Abbreviations

$BHFP$	bottom hole flowing pressure, psi
CCE	constant composition expansion
CVD	constant volume depletion
GOR	gas-oil ratio, MCF/stb
OGR	condensate-gas ratio, stb/MCF

Superscripts

gas	refers to the real gas pseudopressure
$3Z$	refers to the three-zone method
SS	refers to the steady-state method

Subscripts

D	dimensionless
g	refers to the gas phase
i	initial
o	refers to the oil phase
wf	well flowing
ws	well shut-in
wf, s	well flowing at the moment of shut-in

Symbols

η	hydraulic diffusivity ($\eta = \frac{k}{\phi \mu c_t}$)
λ	Corey pore size distribution factor
μ_g	gas viscosity, cP
μ_o	oil viscosity, cP
ρ_g	gas molar density, $lb - M/ft^3$
ρ_o	oil molar density, $lb - M/ft^3$
ϕ	porosity

Appendix A

Simulation of Laboratory Experiments

A.1 Constant Composition Expansion

A sample of the reservoir fluid is placed in a laboratory cell. The pressure is adjusted to a value equal to or greater than the initial reservoir pressure and the temperature is set to the reservoir temperature. The pressure is then reduced by increasing the volume of the cell in increments. No gas or liquid is removed from the cell such that the overall composition of the fluid remains equal to the initial composition. At each step, the pressure, total volume of the reservoir fluid (oil and gas) and the separated phase volume are measured. The procedure is also called flash vaporization, flash liberation, flash expansion or constant mass expansion. The CCE experiment can be simulated using a tuned equation of state, the viscosity being computed from the composition (Lohrenz et al., 1964, method was used here).

A.2 Constant Volume Depletion

This procedure is usually performed for a gas condensate to simulate the conditions encountered in the reservoir. The sample of reservoir gas in the laboratory cell is

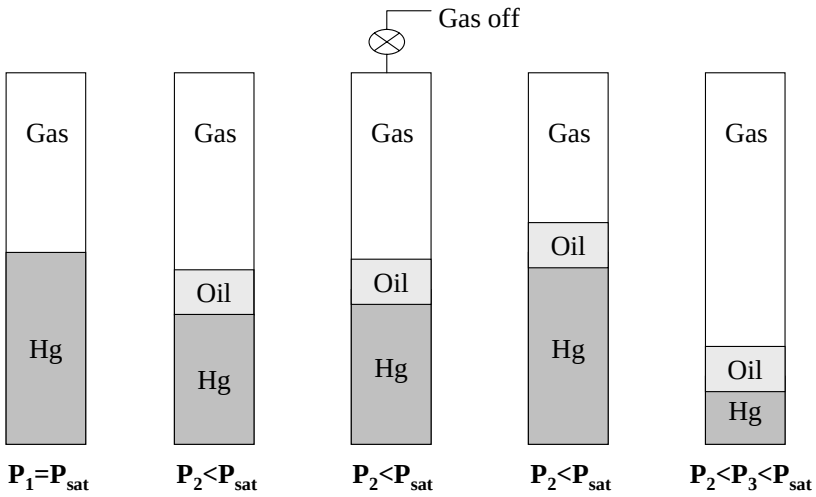

Figure A.1: Schematic Constant Volume Depletion Experiment

brought to the dew-point pressure, and the temperature is set to the reservoir temperature. The pressure is reduced by increasing the cell volume. Part of the gas is expelled from the cell until the volume of the cell equals the volume at the dew-point. The gas collected is sent to a multistage separator. The process is repeated for several pressure steps. A schematic of the constant volume depletion process is shown in Figure A.1. The paper of Whitson and Torp (1983) gives more explanation about this experiment and how to interpret the data.

A.3 Black-Oil Properties

The black-oil approximation assumes that PVT behavior of reservoir oil can be modeled by "two components" denoted "oil" and "gas", furthermore, the reservoir gas is modeled by the same "two components" oil and gas assuming that they have the same properties. These components correspond to fluids that end up at surface conditions in the liquid and vapor stock tanks. By definition, it is assumed that they are of fixed composition with constant mass and density. The properties of the fluid in the reservoir are then described by functions that are assumed to be dependent on pressure (and saturation) only (Aziz, 1999).

There are two classical techniques due to Whitson and Torp (1983) and to Coats (1988). For this study, the Whitson and Torp (1983) method has been used. Both methods are essentially the same: the reservoir fluid is subjected to a depletion process (CVD for gas condensate), from which reservoir properties of the fluid can be evaluated. The reservoir liquid and vapor streams are then taken to stock tank conditions via a separator network. The reservoir fluid is potentially described by six variables being:

- solution gas-oil ratio R_s
- solution condensate-gas ratio r_s
- formation volume factor B_g (for gas) and B_o (for oil)
- viscosity

This procedure is generally performed to obtain PVT data for black oil simulation. Although black oil instead fully compositional simulation is not adequate for gas condensate flow representation (Section 4.1.1), the black oil properties are useful to compute the three-zone pseudopressure (Section 3.4.5).

Appendix B

Descriptions of the Cases Used

B.1 Identification of the Cases

Sensitivities to various parameters have been studied, for identification purposes, each of the studied case were given a identifier name composed by the letter "R" (for "run")followed by 5 integers, each of the integer representing a pre-set value of a property or characteristic that may be changed, Figure B.1 illustrate the construction of the names. The pre-set values corresponding to each field are tabulated in the Tables B.1 to B.5. The following Section B.3 and Section B.4 present the relative permeability curves and mixtures in more detail.

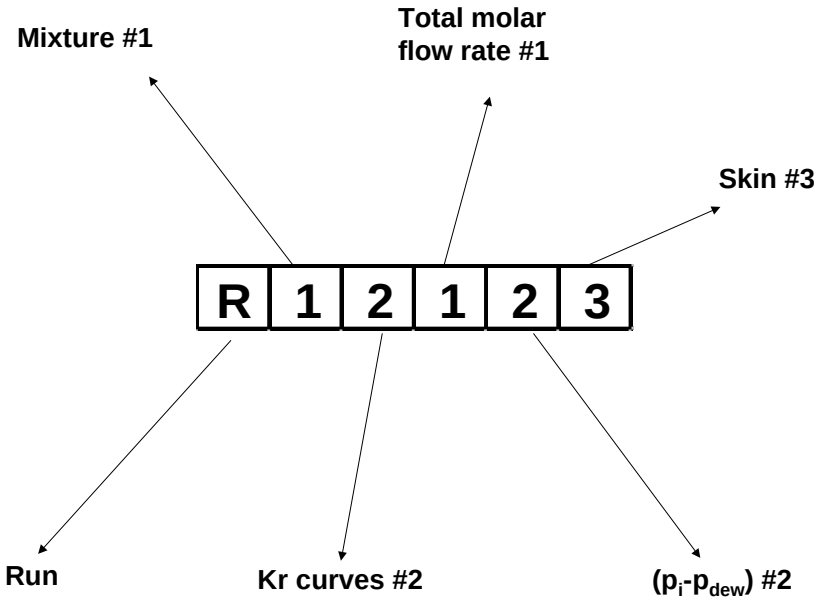

Figure B.1: Identifier Specification of the Studied Cases

Table B.1: Mixture Identifier

Mixture Identifier #	Mixture Name	Maximum CCE drop-out (%)	Initial r_s (stb/MMscf)
1	MIX1	6.0	34.35
2	MIX2	14.1	109.45
3	MIX3	24.9	143.93
4	MIX4	35.3	180.01

Table B.2: Total Molar Flow Rate Identifier

k_r	k_r set #	Comments
1	1	base k_r
2	2	more favorable to gas
3	3	less favorable to gas
4	4	same function $k_{rg} = f(k_{rg}/k_{ro})$ as base case

Table B.3: Total Molar Flow Rate Identifier

Total Molar Flow Rate Identifier	q_t lb-M/days
1	7000
2	5000
3	10000

Table B.4: Initial Pressure Identifier

Initial Pressure Identifier	$(p_i - p_{dew})$ psi
1	150
2	400
3	100
4	50

Table B.5: Skin Factor Identifier

Skin Factor Identifier	skin	Extend of the skin zone, feet	Ratio of Permeability $k_{altered}/k$
1	0	0.0	1.0
2	2	1.9	0.5
3	4.6	4.3	0.5

B.2 Reservoir Characteristics

The same radial homogeneous reservoir model has been used for all the studied cases. A single well, fully perforated is located at the center of the reservoir, which can be considered infinite over the drawdown and buildup duration. The principal characteristics of the reservoir model are given in Table B.6. The numerical stability of the simulation is greatly affected by the radial distribution of the grid cells that has to be chosen carefully (see Section 4.1.2). The same grid size distribution, given in Table B.7 was used for all the cases.

Table B.6: Reservoir Properties Used in Simulations

Porosity ϕ, %	20
Absolute (horizontal) Permeability k, md	5
Reservoir Height h, ft	30
Irreducible Water Saturation, %	0
Reservoir Area, acres	1950
Rock Compressibility, psi^{-1}	4.10^{-6}

Table B.7: Grid Size Distribution

Number of Grid Cell	30
Inner Most Grid Radius, ft	0.25
Grid Cell Size, ft	0.53 0.4429 0.6539 0.9655 1.4255 2.1046 3.1072 4.5876 6.7732 10 10 10 10 35 40 47 68 100 150 200 200 300 500 500 500 500 500 500 500 500

B.3 Relative Permeabilities Curves

Six different sets of relative permeability curve were used to test the sensitivity and the robustness of the methods. kr Set 1 is Corey-type ($S_{wi} = 0$, $k_r(S_{wi}) = 1$, $\lambda = 2$,

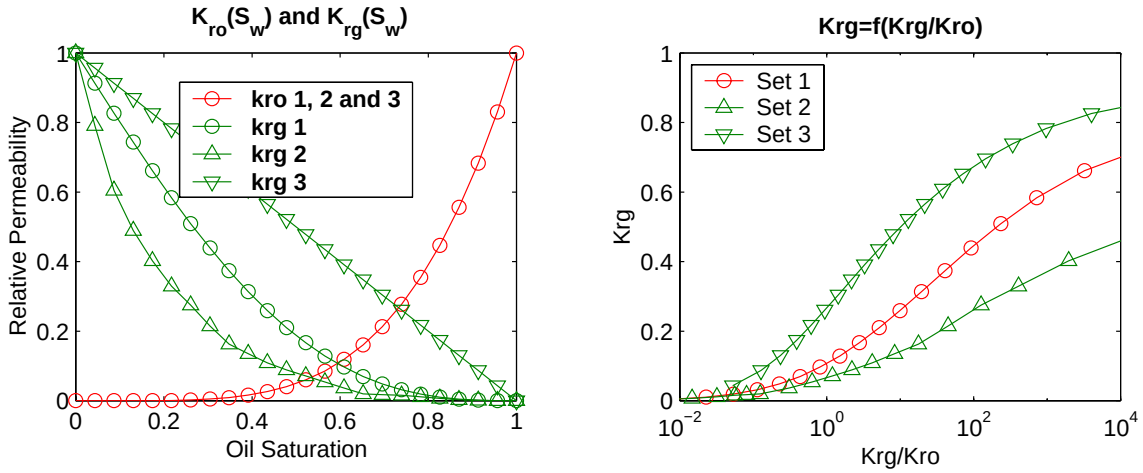

Figure B.2: Relative Permeability Curves 1, 2 and 3

and $S_{oc} = 0.1$) curves which are described by the following equations:

$$k_{ro} = k_r(S_{wi})(S_o^*)^2\left(\frac{S_o}{1 - S_{wi}}\right)^{(2+\lambda)/\lambda}$$
$$k_{rg} = k_r(S_{wi})(S_g^*)^2[1 - (1 - S_g^*)^{(2+\lambda)/\lambda}] \tag{B.1}$$

where

$$S_o^* = \frac{S_o - S_{oc}}{1 - S_{wi} - S_{oc}} \quad \text{and} \quad S_g^* = \frac{S_g}{1 - S_{wi}} \tag{B.2}$$

kr Sets 2 and 3 share the same relative permeability to oil (k_{ro}) as kr Set 1, the relative permeability to gas is less favorable to gas for kr Set 2 and more favorable for kr Set 3. The relative permeability curves are shown in Figure B.2, notice that they are all different on the k_{rg} vs. k_{rg}/k_{ro} plot.

A fourth set of relative permeability curves was considered to show that only the function $k_{rg} = f(k_{rg}/k_{ro})$ matters for pseudopressure computation. This kr Set 4 is different from kr Set 1 in terms of $k_{rg}(S)$ and $k_{ro}(S)$, but shares the same $k_{rg} = f(k_{rg}/k_{ro})$ as shown in Figure B.3.

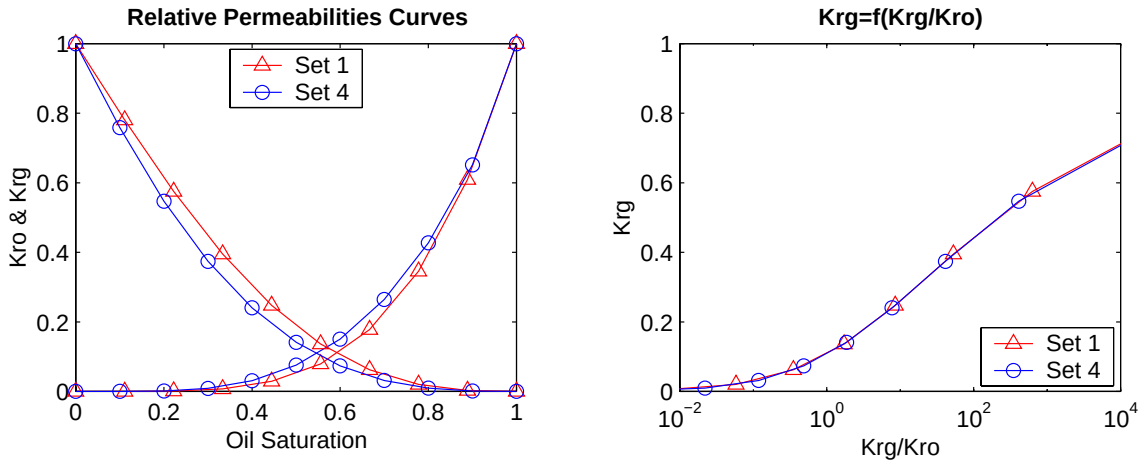

Figure B.3: Relative Permeability Curves Set 1 and 4, that shares the Same $k_{rg} = f(k_{rg}/k_{ro})$ Relationship

B.4 Mixture Description

We chose simple mixtures to represent different gas condensate systems. The various compositions we considered enabled us to incorporate all important features (relevant to phase behavior) of the problem (well productivity, deliverability prediction, well test analysis). The conclusions on the method being used remain the same for more complex mixtures. Mixtures MIX1, MIX2, MIX3 and MIX4 are simple mixtures of three hydrocarbon components: methane (C_1), butane (C_4) and decane (C_{10}).

The fluid behavior was simulated using the Peng-Robinson equation of state (EOS) with volume correction. We used an EOS to simulate laboratory experiments such as constant composition expansion (CCE) and constant volume depletion (CVD) and to generate black oil data of the mixtures (using the Whitson and Torp, 1983, method). Viscosities (in both numerical flow simulator and CCE-CVD simulation) were computed with the procedure described by Lohrenz et al. (1964) for both liquid and vapor phases.

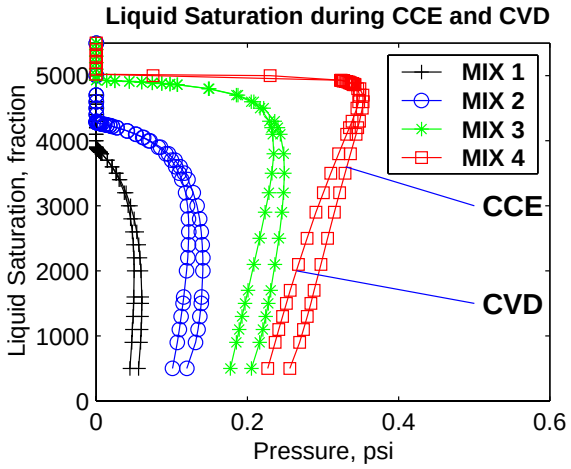

Figure B.4: Oil Saturation in Lab CCE and CVD

The mixture compositions are shown in Table B.8. The dissolution condensate gas ratio r_s is given at the dew point pressure of the mixture where it is constant and maximum. L_{max}^{CCE} represents the maximum liquid dropout during a CCE experiment.

Table B.8: Mixture Compositions

Mixture	1	2	3	4
T (°F)	140	260	220	220
p_{dew} (psi)	3886.3	4278.5	4930.8	4930.5
L_{max}^{CCE}	6	14.1	24.9	35.3
r_s **at** p_{dew} (STB/MMSCF)	34.35	109.45	143.93	180.01
$\mathbf{C_1}$	0.9561	0.89628	0.89	0.87
$\mathbf{C_4}$	0.018	0.02998	0.0155	0.015
$\mathbf{C_{10}}$	0.0259	0.07374	0.0945	0.115

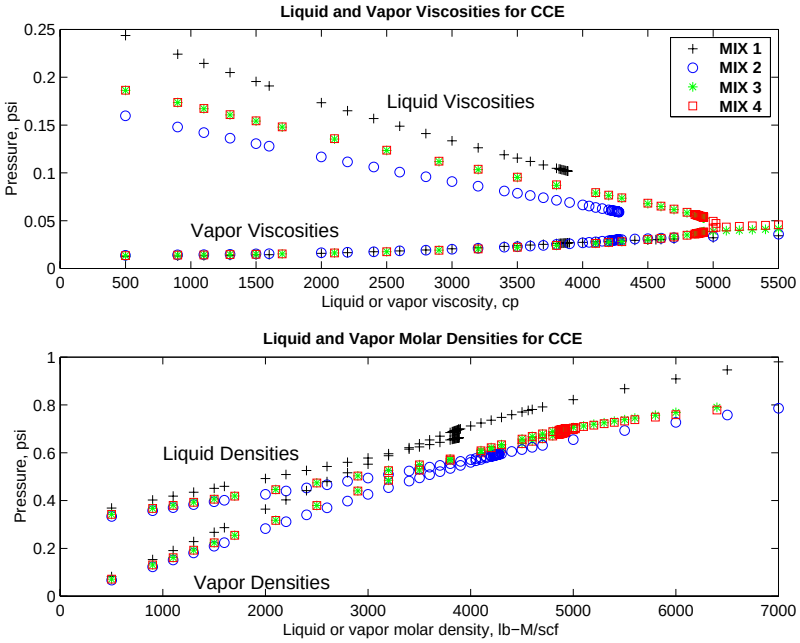

Figure B.5: Viscosity and Molar Densities of the Mixtures

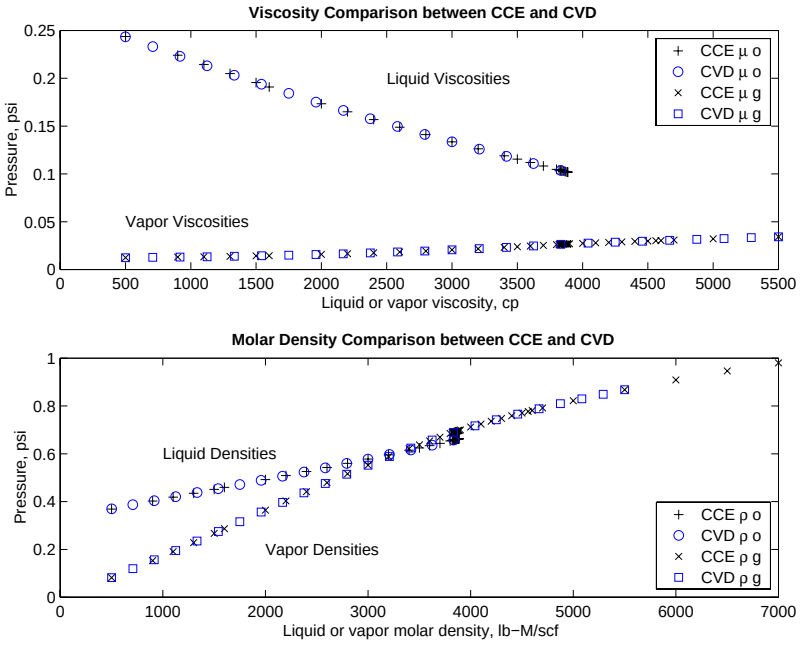

Figure B.6: Comparison of Viscosity and Molar Densities from CCE and CVD (MIX1)

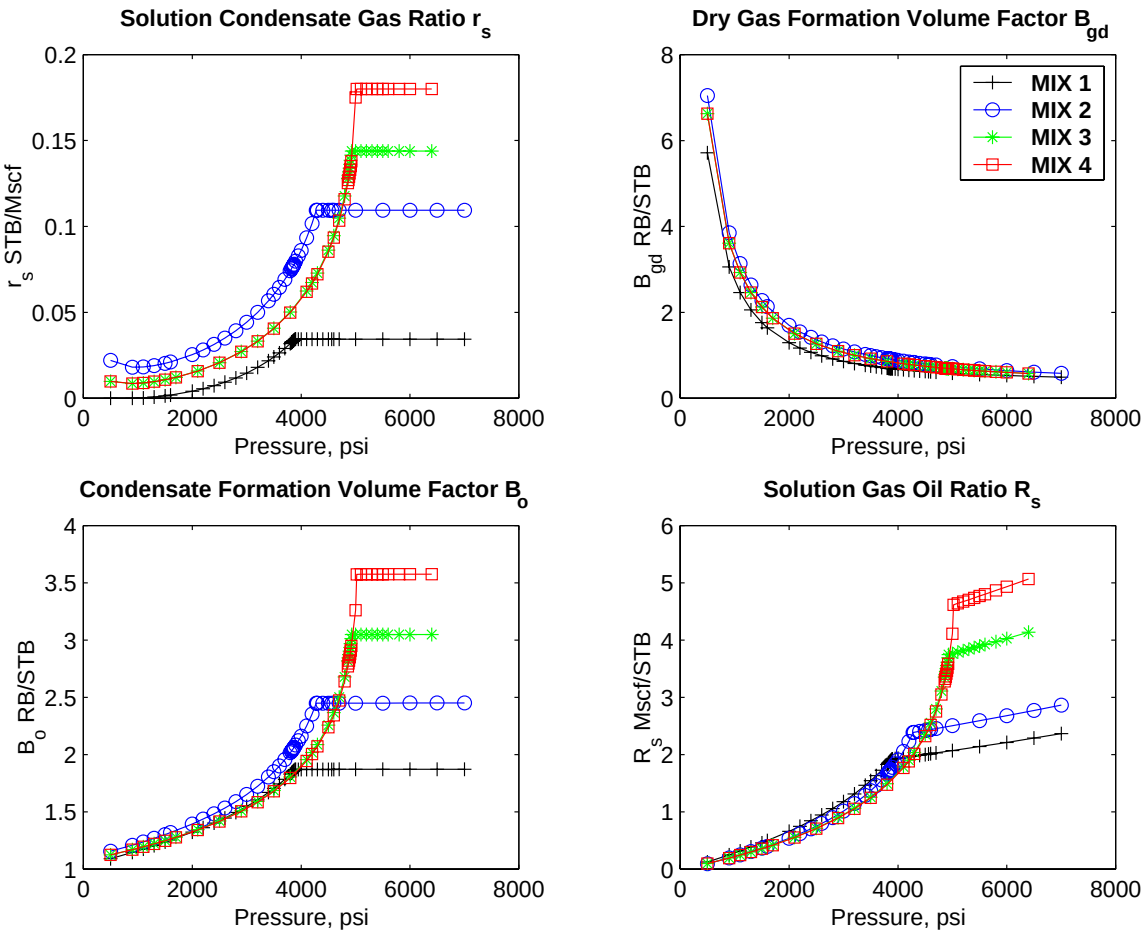

Figure B.7: Black Oil Data for MIX1, MIX2, MIX3 and MIX4

Appendix C

Eclipse Data Set

```
-- ================================================================================
-- Study      : Gas Condensate Well Test
-- AUTHOR     : B. Roussennac
-- SIMULATOR  : Eclipse 300
-- DATE       : Fri Apr  7 11:48:38 PDT 2000
-- ================================================================================
-->MIX1
-- pdew2=3886.3 psia,  TEMP=140 F
-- skin=4.6: RS=6 K=5 md KS=2 md
-- pi=4036 psi, pi-pdew=150 psi, qt=7000 lb-mole/day
-- ================================================================================
RUNSPEC
-- ================================================================================
FIELD
RADIAL
AIM
--3 components in study
COMPS
3 /
--Peng-Robinson equation of state to be used
```

```
EOS
PR/
DIMENS
-- NR NTHETA NZ
   30  1    1 /
TABDIMS
      1     1     80     1*    1    1*    1*     1*  /
WELLDIMS
     1       1       1       1    /
-- Single phase fluis is a gas:
ISGAS
MULTSAVE
1 /
FMTOUT
UNIFOUT
-- =================================================================
GRID
-- =================================================================
INIT
INRAD
.25 /
DR
0.53000 0.4429 0.6539 0.9655 1.4255 2.1046 3.1072 4.5876  6.7732 10  10  10
10      35     40     47     68     100    150    200     200    300 500 500
500     500    500    500    500    500/
EQUALS
DTHETA
360 /
DZ
30 /
TOPS
```

```
7000/
PORO
 0.20 /
PERMTHT
30*5 //
PERMR
6*2 24*5 /
-- ================================================================================
PROPS
-- ================================================================================
-- Include File with Fluid Description
INCLUDE
'incfiles/FLUIDRAGPG.INC'/
-- degree F
RTEMP
140/
-- Include KR tables to be used
INCLUDE
'incfiles/KRSET1.INC'/
--Rock and water pressure data
ROCK
4036 0.000004 /
PVTW
4036 1.0 0.000003 0.31 0.0 /
--Surface density of water
DENSITY
1* 63.0 1* /
-- ================================================================================
SOLUTION
-- ================================================================================
EQUALS
```

```
PRESSURE
4036 /
SWAT
0 /
SGAS
1 //
ZMF
30*.9561
30*.018
30*.0259/
OUTSOL
PRES SOIL XMF YMF VMF VOIL VGAS BOIL BGAS DENO DENG KRG KRO ZMF /
RPTPRINT
13*0/
-- ================================================================================
SUMMARY
-- ================================================================================
RUNSUM
RPTONLY
-- Properties to be output
INCLUDE
'incfiles/SUMMARY.INC'/
-- ================================================================================
SCHEDULE
-- ================================================================================
-- DO NOT USE PSEUPRES KEYWORD HERE, IT GAVES "BAD" RESULTS:
-- TM was specified to be 7000 lb-M/day, however
-- the simulator oscillated
--PSEUPRES
--PICOND
--3*/
```

```
SEPCOND
SEP FIELD 1 60 14.7 //
WELLSPEC
P FIELD 1 1 1*  SEP//
COMPDAT
--name i j k1 k2 flag sat.tab trans id kh skin D dir
   P   1 1 1  1 'OPEN' 1*     1*   .5 1*  0   1* 'Z'//
--Well P set to target total molar rate of 7000lb-mole/d,
--with min bhp of 500 psi
WELLPROD
P TM 4* 500 5* 7000 //
TUNING
1.1574E-6  1.1574E-1  1.1574E-7  1*  1.1  0.5   ///
TSTEP
3*3.8581E-6   4.0205610e-06 5.4171651e-06 7.2989013e-06 9.8342877e-06/
TSTEP
1.3250380e-05 1.7853104e-05 2.4054656e-05 3.2410414e-05 4.3668673e-05
5.8837662e-05 7.9275835e-05 1.0681352e-04 1.4391685e-04 1.9390860e-04
2.6126576e-04 3.5202046e-04 4.7430022e-04 6.3905574e-04 8.6104165e-04
1.1601378e-03 1.5631296e-03 2.1061069e-03 2.8376957e-03 3.8234133e-03
5.1515350e-03 6.9410005e-03 9.3520645e-03 1.2600649e-02 1.6977679e-02
2.2875139e-02 3.0821173e-02 4.1527384e-02 5.5952564e-02 7.5388553e-02
1.0157593e-01 1.3685991e-01 1.8440032e-01 2.4845462e-01 3.3475918e-01
4.5104296e-01 6.0771971e-01 8.1882057e-01 1.1032506e+00 1.4864817e+00
2.0028342e+00 2.6985496e+00 3.6359326e+00 4.8989301e+00/
END
```

Appendix D

Table of Results of All the Studied Cases

More than 60 cases were simulated and interpreted using both the steady-state two-phase pseudopressure and the three-zone two-phase pseudopressure, some of those cases are documented in the report. Table D.1 summarizes the results of the interpretation of all the studied cases. The name identifier described in Appendix B.1 is used here, please refer to Figure B.1.

Table D.1: Results of the Sensitivity for All Studied Cases

	Three-zone method		**Steady-state method**	
Identifier	kh^*/kh	$\Delta skin = s^* - s$	kh^*/kh	$\Delta skin = s^* - s$
Effect of the Fluid and Skin				
R11111	0.99	-0.06	1.05	-1.27
R11112	0.94	-0.27	0.98	-1.54
R11113	0.85	-0.38	0.88	-1.72
R21111	1.00	0.12	1.06	-1.48
R21112	0.99	-0.00	1.04	-1.72
R21113	1.00	-0.09	1.04	-2.53
R31111	1.03	0.02	1.10	-1.28
R31112	1.06	-0.12	1.13	-2.20
R31113	1.09	-0.21	1.16	-2.32
R41111	0.91	0.80	1.14	-2.13
R41112	0.93	0.87	1.15	-1.98
R41113	1.01	1.15	1.24	-2.09
Effect of the k_r				
R22111	1.04	0.04	1.07	-1.54
R22112	1.25	-0.19	1.29	-1.86
R23111	0.99	0.12	1.04	-0.93
R23112	0.97	0.08	1.01	-1.07
R32111	0.97	-0.17	1.02	-1.18
R32112	1.09	-0.51	1.14	-2.40
R33111	1.00	0.07	1.06	-0.83
R33112	1.00	0.07	1.06	-1.38
R42111	1.01	-0.16	1.20	-1.89
R42112	1.13	0.21	1.34	-1.45
R43111	0.97	0.37	1.09	-1.25
R43112	0.97	0.33	1.08	-1.21

Table D.2: Results of the Sensitivity for All Studied Cases (Cont'd)

	Three-zone method		**Steady-state method**	
Identifier	kh^*/kh	$\Delta skin = s^* - s$	kh^*/kh	$\Delta skin = s^* - s$
k_r having the same $k_{rg} = f(k_{rg}/k_{ro})$ than k_r set # 1				
R14111	0.99	0.11	1.04	-1.65
R14112	0.99	0.03	1.03	-2.46
R14113	0.99	0.15	1.06	-1.19
R24111	1.02	0.00	1.08	-2.12
R24112	1.07	-0.13	1.13	-2.22
R24113	0.95	0.24	1.16	-1.94
R34111	0.95	0.28	1.16	-1.79
R34112	1.06	0.55	1.23	-1.92
R34113	0.97	-0.07	1.06	-2.23
R44111	0.96	0.07	1.04	-2.01
R44112	0.93	0.03	1.03	-3.33
R44113	0.93	0.03	1.03	-3.33
Effect of the Total Molar Flow Rate q_t				
R21211	1.05	0.15	1.15	-1.98
R21212	1.10	-0.07	1.19	-2.73
R21311	0.98	-0.04	1.01	-0.91
R21312	0.93	-0.19	0.96	-1.12
R41211	0.94	0.28	1.17	-2.12
R41212	1.04	0.63	1.29	-2.00
R41311	0.93	0.46	1.07	-2.01
R41312	0.92	0.22	1.04	-1.98
R41411	0.99	1.67	1.03	-0.33
R41412	1.00	1.66	1.03	-0.42

Table D.3: Results of the Sensitivity for All Studied Cases (Cont'd)

	Three-zone method		**Steady-state method**	
Identifier	kh^*/kh	$\Delta skin = s^* - s$	kh^*/kh	$\Delta skin = s^* - s$
Effect of $(\mathbf{p_i - p_{dew}})$				
R11131	0.99	0.10	1.10	-2.10
R11132	0.93	-0.09	1.00	-2.92
R11133	0.84	-0.19	0.89	-3.20
R11141	1.03	-0.74	1.14	-3.16
R11142	0.96	-1.00	1.03	-3.42
R11143	0.88	-1.18	0.93	-3.61
R21131	0.96	0.94	1.10	-2.19
R21132	0.95	0.87	1.06	-2.84
R21133	0.96	0.89	1.05	-2.97
R21141	0.99	0.22	1.13	-3.05
R21142	0.98	0.07	1.08	-3.14
R21143	0.98	0.03	1.07	-3.28
R31131	1.03	0.19	1.15	-2.04
R31132	1.05	0.00	1.16	-2.61
R31133	1.09	0.00	1.19	-2.69
R31141	1.01	0.57	1.21	-2.83
R31142	1.03	0.52	1.21	-2.84
R31143	1.06	0.65	1.22	-2.98
Other Cases				
R13242	0.98	0.04	1.05	-1.22
R13342	0.92	-0.16	0.97	-1.49
R11342	0.98	-0.09	1.01	-1.52